



universität  
wien

# DISSERTATION

Titel der Dissertation

## Molecular Mechanism of Draxin Signaling in Axonal Guidance

Verfasserin

Rajeshwari Meli

angestrebter akademischer Grad

Doctor of Philosophy (PhD)

Wien, 2014

Studienkennzahl lt. Studienblatt: A 091 490

Dissertationsgebiet Studienblatt: Dr.-Studium der Naturwissenschaften UniStG Molekulare Biologie

Betreuerin / Betreuer: Univ.-Prof. Dr. Friedrich Propst

*Dedicated to my parents  
and  
my beloved husband.....*

*Courage doesn't always ROAR. Sometimes courage is the quite  
voice at the end of the day saying  
"I WILL TRY AGAIN TOMORROW".*

*-Mary Anne Radmacher*

## **Table of contents.**

<b>Acknowledgements</b>	<b>I</b>
<b>Zusammenfassung</b>	<b>III</b>
<b>Summary</b>	<b>VI</b>
<b>Abbreviations</b>	<b>VIII</b>
<b>Publications</b>	<b>X</b>
<b>1. Introduction</b>	<b>1</b>
1.1. Nervous system	1
1.1.1. Mouse cerebral cortex	2
1.1.2. Neuronal development	4
1.2. Axonal guidance	5
1.2.1. Netrin	7
1.2.2. Semaphorins	8
1.2.3. Draxin	11
1.2.4. Slits	13
1.3. The growth cone	14
1.4. Growth cone cytoskeleton elements	15
1.5. Microtubule dynamics	18
1.6. MAP1 proteins	19
1.7. MAP1B	20
1.7.1. MAP1B phosphorylation	22
1.8. Growth cone signaling	24
1.8.1. DCC and UNC5 receptor	24
1.8.2. GSK3kinase	26
1.8.3. PI3 kinase	27
1.8.4. PKB/Akt kinase	28
1.8.5. PTEN	29

<b>2. Results</b>	<b>30</b>
2.1. Draxin-dependent neurite inhibition is suppressed in MAP1B <sup>-/-</sup> neurons	30
2.1.1. Draxin inhibits neurite outgrowth in cortical explants	30
2.1.2. No inhibition of neurite outgrowth by draxin in MAP1B <sup>-/-</sup> cortical explants culture.	33
2.2. Draxin induced inhibition of neurite outgrowth are MAP1B dependent	34
2.3. Draxin inhibits neurite outgrowth in dissociated cortical neurons	35
2.4. Establishment of growth cone collapse Assay	37
2.5. Draxin-induced growth cone collapse are suppressed in MAP1B-deficient neurons.	39
2.6. Draxin increases MAP1B phosphorylation at a GSK-3 $\beta$ -dependent phosphorylation site	41
2.7. Draxin signaling involves activation of GSK-3 $\beta$ and inhibition of Akt	42
2.8. Involvement of GSK-3 $\beta$ and Akt pathway in draxin-induced growth cone collapse.	45
2.9. Draxin-induced growth cone collapse is dependent on activation of GSK-3 $\beta$ and inhibition of Akt	48
2.10. Draxin-induced growth cone collapse is mediated by DCC receptor	51
<b>3. Discussion</b>	<b>52</b>
3.1. Model of draxin signaling mechanism.	57
<b>4. Introduction</b>	<b>58</b>
4.1. Nitric oxide and its signaling	58
4.1.1. Rho kinase	59
<b>5. Results</b>	<b>60</b>
5.1. Nitric oxide induced myosin activation is ROCK dependent	60
<b>6. Discussion</b>	<b>64</b>
<b>7. Materials and methods</b>	<b>66</b>
7.1. Animals	66
7.2. Cortical explants preparation and primary cortical neuronal culture	66
7.2.1. Dissection of mouse cerebral cortex	66
7.2.1.1. Materials required	66

7.2.1.2.	Dissection of the brain	67
7.2.1.3.	Cortical explant culture	68
7.2.1.4.	Neurite outgrowth assay	69
7.2.1.4.1.	Using draxin condition medium	69
7.2.1.4.2.	Using recombinant draxin	69
7.2.2.	Preparation of cortical primary neuronal cell culture	70
7.2.2.1.	Materials required	70
7.2.2.2.	Protocol	70
7.2.2.2.1.	Growth cone collapse assay	71
7.3.	Neuronal treatments	72
7.4.	Plasmids and Nucleofection	72
7.5.	Inhibitors and blockers	73
7.6.	Cell culture methods	73
7.6.1.	Materials required	73
7.6.2.	Procedure for Passaging/ splitting Cells	74
7.6.3.	Thawing cells	75
7.6.4.	Treatment of N2a cells for NO-induced axon retraction experiment	75
7.6.5.	Transfection of cell lines	77
7.7.	Immunocytochemistry	78
7.8.	Preparation of protein extracts and their separation.	78
7.9.	Statistical analysis methods	80
<b>8.</b>	<b>Reagents and chemicals</b>	<b>80</b>
8.1.	Buffers and solutions	80
8.2.	Common reagents	82
8.3.	Inhibitors and guidance molecules	84
8.4.	Cell Culture Reagents	85
8.5.	Primary antibodies	86
<b>9.</b>	<b>References</b>	<b>87</b>
<b>10.</b>	<b>Curriculum vitae</b>	<b>104</b>

## ACKNOWLEDGEMENTS

I would like to thank to my PhD supervisor, **Prof. Friedrich Propst**, for his guidance and support and for allowing me to work in his lab. I would like to express my sincere gratitude towards **Dr. Petronela Weisová** for her scientific advice and insightful discussions. I really appreciate all her contributions both scientific and non-scientific.

I extend my sincere gratitude to my committee **Prof. Manuela Baccarini** and **Prof. Johannes Nimpf** for their timely suggestions and for consistently keeping me on track.

It is a great pleasure to thank my previous lab members **Anton, Waltraud** and **Zuszi** for their friendship and great working environment.

I will forever be appreciative to **Ilona, Prabha, Mamta & Silpi** for the huge moral support and helping me to correct my thesis.

I gratefully acknowledge our international program “**Molecular mechanism of cell signaling**” for the scientific and financial support that made my PhD work possible. I thank our program managers **Dr. Elisabeth Froschauer** and **Dr. Elena Rodionova** for helping me with paper works including visa permits and University contracts. I thank **Austrian Science fund (FWF)** for funding my studies in Vienna.

Life’s greatest blessing is the love of the family. I am grateful to my parents for the way they raised me up and their struggle in life always been my inspiration to achieve better.

I am grateful to my husband **Vaibhav Jadhav** for being my best friend and a great companion through all good and bad times. His unconditional love and support has been instrumental to pursue my Doctoral studies.

It is a great pleasure to thank my brother **Vijay** and his wife **Bhumika Meli** for their guidance during my early struggling days. I thank my sister **Poornima Belludi** for being my greatest advisers for life. Their love has been my strengths.

I thank **Sheila** and **Dalipsingh shokeen** and my in-laws **Rajeshri** and **Manikrao Jadhav** for their encouragement during my PhD studies.

Last but not the least I thank all my friends and family for their good wishes which made this work possible.



## Zusammenfassung

Während der neuronalen Entwicklung reagieren Axone auf eine Bandbreite an Signalen um zu ihren Zielen zu gelangen. Wachstumskegel an der Spitze der Axone wählen ihren Pfad mit Hilfe von extrazellulären Signalen den Steuerungssignalen. Diese bestehen aus fingerähnlichen Ausbuchtungen, Filopodien und schleierartigen Strukturen, die als Lamellopodien bezeichnet werden. Signale können Wachstumskegel entweder anziehen oder abstoßen. Extrazelluläre Signale sind Moleküle die von Zellen entlang des axonalen Weges segregiert werden oder auf der Zelloberfläche präsentiert werden. Sie beinhalten Netrin, Semaphorine und Ephrine. Diese Steuerungssignale regulieren das Vorandringen der Wachstumskegel sowie Richtung und Verzweigung während Neuausrichtungen des Zytoskeletts.

Die Dynamik von Wachstumskegeln wird durch zwei Komponenten des Zytoskeletts reguliert, Aktin und Mikrotubuli. Mikrotubuli sind extrem dynamische Strukturen, involviert in Neuritenextension, -repulsion und -polarität. Die Dynamik von Mikrotubuli wird reguliert durch MAP1Bs (*microtubule associated protein 1B*), eine Klasse von Proteinen die entlang der Mikrotubuli binden und deren Funktion in Wachstum und Steuerung regulieren. MAP1B *knockout* (KO) Mäuse zeigen verschiedene Defekte, unter anderem Agenesie des Corpus Callosum und fehlgeleitete Kommissuren welche Probst-Bündel bilden.

Seit kurzem ist das Steuerungssignal Draxin als ein wichtiges repulsives Axon-Steuerungssignal bekannt. Es ist essentiell für die Bildung von Kommissuren des Rückenmarks und des Vorderhirns; eingeschlossen das Corpus Callosum. Draxin wird in verschiedenen Hirnregionen exprimiert: Cortex, Riechkolben, Mittelhirn und Cerebellum. Es inhibiert das Herauswachsen von Neuriten aus dem dorsalen

Rückenmark, Riechkolben und corticalen Explantaten *in vitro*. Draxin vermittelt die Inhibition durch verschiedene Rezeptoren: DCC (*deleted in colorectal cancer*), Neogenin, UNC5s (H1, H2, H3) und DSCAM (*Down's syndrome cell adhesion molecule*). Die molekularen Details der Draxin Wirkungsweise sind unbekannt.

Im ersten Teil meiner Arbeit habe ich untersucht wie MAP1B in Draxin und Semaphorin3A (Sema3A) induzierter Inhibition des Neuritenauswuchses sowie dem Zusammenbruch von Wachstumskegeln involviert ist. Zur Beantwortung dieser Fragen habe ich zwei Versuchsansätze etabliert. Zur Untersuchung des Neuritenauswuchses wurden zerebrale kortikale Explantate verwendet. Der Zusammenbruch von Wachstumskegeln wurde mittels dissoziierter kortikaler Neuronen untersucht. Die Versuche deuteten darauf hin das Draxin und Sema3A Signalwege von MAP1B abhängen. Mit Hilfe von genetischen und pharmakologischen Experimenten habe ich herausgefunden das Draxin induzierter Zusammenbruch von Wachstumskegeln stark von Draxinrezeptoren abhängt (DCC), sowie abhängig ist von der Proteinkinase Akt und Aktivierung von GSK-3 $\beta$  (Glykogen Synthase Kinase-3  $\beta$ ). Diese wiederum korreliert mit erhöhter Phosphorylierung von MAP1B. Die vorliegende Arbeit zeigt zum ersten Mal die molekularen Mechanismen welche der Draxin Repulsion zugrunde liegen. Sie stellt den Zusammenhang her zwischen Draxin und DCC mit MAP1B und beinhaltet die Identifizierung eines neuen GSK-3 $\beta$  Signalweges, welcher essentiell ist für repulsive Axonsteuerung. Zusätzlich habe ich den Effekt von Draxin auf die Polarisierung von dissoziierten kortikalen Neuronen und den Effekt von Sema3A auf die Verzweigung von pyramidalen Neuronen untersucht.

Im zweiten Teil meiner Arbeit habe ich mir die Rolle von Myosin in Stickoxid-induzierter Axon Repulsion in Mausneuroblastomazelllinien (N2a) angeschaut. Myosin ist ein Motor Protein welches in die Aktin-Myosin Kontraktion involviert ist.

Unter Verwendung von biochemischen Versuchen habe ich die Mono-Phosphorylierung der MRLC (*myosin regulatory light chain*) an Serin 19 als Indikator für Myosin Aktivität angesehen. N2a Zellen wurden mit SNAP, einem Stickoxid (NO) Donor, behandelt. Der Anstieg der Phosphorylierung wurde partiell inhibiert durch den ROCK Inhibitor Y27632. ROCK ist eine Rho-assozierte Kinase. Das Ergebnis deutet darauf hin das ROCK eine Schlüsselrolle zukommt in Myosinaktivierung als Reaktion auf die SNAP Behandlung. Zusammengefasst zeigen die Ergebnisse das Myosin wichtig ist für die Axon Repulsion induziert durch NO.

## Summary

During neuronal development axons respond to an array of signals to navigate to their targets. Growth cones at the tip of the axons choose their path with the aid of extracellular guidance cues. They are composed of finger like projections, filopodia and veil like structure called lamellipodia. Cues can either attract or repel growth cones. Extracellular cues are the molecules that are secreted or presented on the cell surface by cells along the axon path including netrin, semaphorins, slits and ephrins. These guidance cues regulate growth cone advance, turning, and branching behaviours of the growth through cytoskeleton rearrangements.

Growth cone dynamics is regulated by two cytoskeleton components, actins and microtubules (MTs). MTs are extremely dynamic structures, involved in neurite extension, retraction and polarity. The dynamics of microtubule is regulated by Microtubule associated protein 1B (MAP1B), a class of proteins which bind along the MTs and regulate their function in growth and guidance. MAP1B KO display various defects including agenesis of corpus callosum, misguided commissural forming probst bundles.

Recently known guidance cue draxin is an important repulsive axon guidance cue essential for the formation of spinal cord and forebrain commissures, including corpus callosum. Draxin is expressed in various brain regions including, cortex, olfactory bulb, midbrain and cerebellum. It inhibits the neurite outgrowth from dorsal spinal cord, olfactory bulb and cortical explants in vitro. Draxin induces neurite outgrowth inhibition through multiple netrin receptors: DCC (deleted in colorectal cancer), Neogenin, UNC5s (H1, H2, H3), and DSCAM (Down's syndrome cell adhesion molecule) but the molecular details of draxin signaling are unknown.

In the first part of my thesis I examined the involvement of MAP1B in draxin and Semaphorin3A (Sema3A) induced neurite outgrowth inhibition and growth cone collapse. In order to address these questions, I established two assays. For neurite outgrowth assay cerebral cortical explants were used whereas for growth cone collapse assay dissociated cortical neurons were used.

These assays suggested that draxin and Sema3A signaling is dependent on MAP1B. Using genetic and pharmacological approaches I found that draxin-induced growth cone collapse critically depends on draxin receptors (deleted in colorectal cancer, DCC), inhibition of protein kinase Akt and activation of GSK-3 $\beta$  (glycogen synthase kinase-3 $\beta$ ) which correlates with increased phosphorylation of MAP1B. This study, for the first time reveals molecular mechanisms involved in draxin repulsion, links draxin and DCC to MAP1B and identifies a novel MAP1B-dependent GSK-3 $\beta$  pathway essential for repulsive axon guidance. Additionally, I studied the effect of draxin on polarization of dissociated cortical neurons and the effect of Sema3A on branching of pyramidal neurons.

In the second part of my study I investigated the role of myosin in nitric oxide induced axon retraction in mouse neuroblastoma (N2a) cell lines. Myosin is motor protein involved in the acto-myosin contractility. Using biochemical assay I analyzed the monophosphorylation of the myosin regulatory light chain (MRLC) at Ser19 as an indicator of the myosin activity. N2a cells were treated with SNAP, a Nitric oxide (NO) donor. Treatment of SNAP enhanced the monophosphorylation of the MRLC. The increase in phosphorylation was partially inhibited by the rho-associated, coiled-coil-containing protein kinase (ROCK) inhibitor Y27632, suggesting that ROCK is the key to myosin activation in response to SNAP. These results demonstrated that myosin is important for the axon retraction induced by NO.

## Abbreviations

APC	Adenomatous polyposis coli protein
CAMs	Cell adhesion molecule
CNS	Central nervous system
CRMP2	Collapsing response mediating protein-2
CC	Corpus callosum
CDK5	Cyclin dependent kinase 5
DCC	Deleted in Colorectal Cancer
DMSO	Dimethylsulfoxid
DRG	Dorsal root ganglia
EB3	End binding protein 3
EHS	Engelbreth-Holm-Swarm
GW	Glial wedge
GSK-3	Glycogen synthase kinase 3 $\beta$
GDP	Guanosine-5'-diphosphate
IGG	Indusium griseum glia
kDa	Kilo Daltons
LC	Light chain
$\mu$ M	Micro Molar
$\mu$ g	Microgram
$\mu$ m	Micrometer
MT	Microtubule

MAP1B	Microtubule associated protein 1B
MZ	Midline zipper glia
MLC	Myosin light chain
NO	Nitric oxide
NOS	Nitric oxide synthase
PFA	Paraformaldehyde
PNS	Peripheral nervous system
PI3K	PI3 kinases
PLL	Poly-L-lysine
SDS	SDS polyacrylamide gel electrophoresis
Sema 3A	Semaphorin 3A
SNAP	S-nitrosothiol

## **Publications**

**1. Repulsive axon guidance by draxin is mediated by GSK-3 $\beta$  and Microtubule-associated protein MAP1B.**

**Meli Rajeshwari**, Weisova Petronela and Propst Friedrich

*(In communication JBC)*

**2. Nitric oxide-induced axon retraction involves simultaneous changes in microtubule and actin networks.**

Krupa Ewa, **Meli Rajeshwari**, Völk Thomas, Nothias Fatiha and Propst Friedrich.

*(In communication)*



# Part I

---

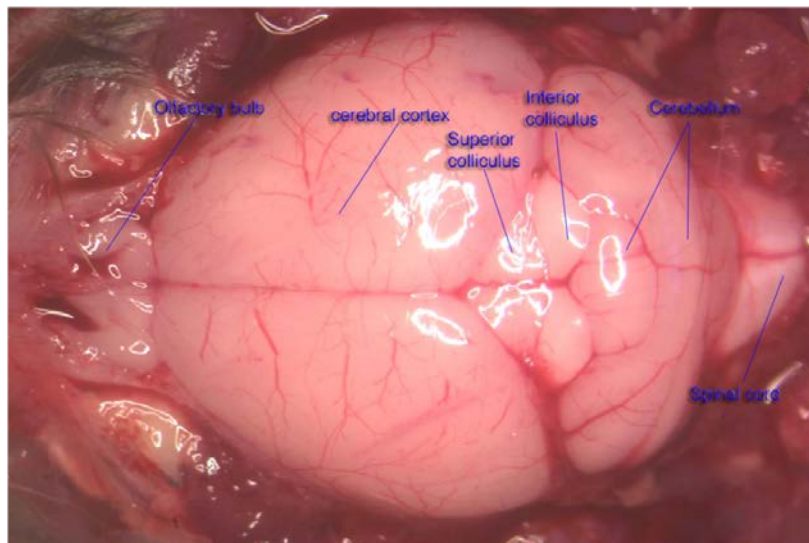
## Introduction

# 1. Introduction

## 1.1 Nervous system

The nervous system in mammals is composed of trillions of neurons, forming intricate connections with, on average, over a thousand other neurons. In mammals, the nervous system is composed of two components: the central nervous system (CNS) and the peripheral nervous system (PNS). The CNS consists of brain, cranial nerves and spinal cord. Nerves that exit from the spinal cord at various levels of the spinal column are the part of the PNS. Additionally, the PNS is composed of motor neurons and the autonomic nervous system, which is divided into the sympathetic and the parasympathetic nervous system. These two systems work mutually to collect information from inside the body and from the environment outside it. The system receives and process the collected information and then send out necessary instructions to the rest of the body, making it respond. The brain is the final destination for all the information gathered by the rest of the nervous system. Once information arrives, the brain recognizes and processes the information and sends out the necessary commands. The brain is subdivided into cerebrum and the brain stem. These parts function in storing and retrieving memory and making body movements smooth. Although the brain is the control center, its role would be incomplete without the spinal cord. Brain tissue contains two types of cells, namely neurons and glial cells. Neurons are the basic units of information transformation. Glial cells are supportive cells involved in many functions, including

protection of neurons, nutrient supply, modulation of neuronal impulses and insulation of neuronal axons and dendrites.



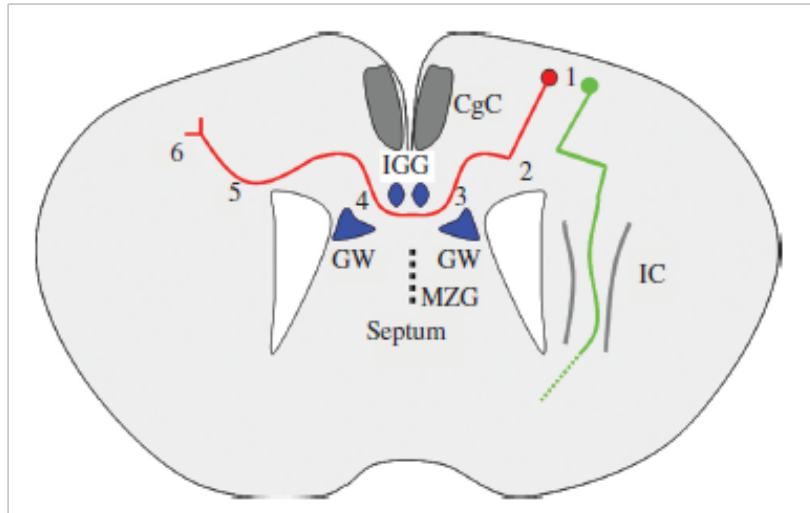
**Figure 1:** Image of a mouse brain *in situ*, after removal of cranial bones, depicting major parts of the brain including olfactory bulb, cerebral cortex, superior colliculus, inferior colliculus, cerebellum and spinal cord.

Image source: Mouse brain Library (MBL) <http://www.mbl.org/>

### 1.1.1 Mouse cerebral cortex

Mouse cerebral cortical hemispheres are connected through the large bundle of fibers within the cortex called the corpus callosum (CC). Neurons may choose to connect on the same side of the hemisphere (ipsilateral), or on the opposite side (contra lateral via corpus callosum). The cerebral cortex is composed of six layers and callosal axons originate from layers II, III and V of the cortex. Initially neurons from each layer send out an axon ventrally towards the intermediate zone (guide post number 1 in Fig. 2). Once these axons reach the intermediate zone they turn towards the midline. Further At position number two, callosal axons (red axon) are distinguished from subcortically

projecting axons (green axon), which turn laterally to project through the internal capsule (IC). Callosal axons then approach the midline by growing through the cingulate cortex (CgC). At this point the axons approach the midline in a sharp ventral trajectory and suddenly turn to cross the midline at the septal boundary (guide post number 3 in Fig. 2). At the septal boundary, the axons encounter the midline glial population known as the glial wedge and indusium griseum glia (IGG). As the axons turn to cross the midline they encounter another glial wedge (GW) in the opposite hemisphere, where the axons make another turn dorsally (guide post number 4 in Fig.2) to enter the contralateral cingulate cortex (position number 5 in Fig 2) and then the contralateral neocortex (guide post number 6 in Fig 2). Callosal axons follow the path laid down by the pioneers or sometimes in direct fasciculation with the pioneer cingulate axons during the midline. Hence cingulate pioneers are very critical in the formation of CC and in crossing the midline. These cell populations have been shown to express proteins (guidance cues) that help in the crossing of the axons to the contra lateral side. The importance of the midline glial structures in the development of the CC was first reported by Silver et al in 1982 (Silver, Lorenz et al. 1982). Studies show that the presence and correct orientation of GW is necessary to project the neurons towards the midline (Shu and Richards 2001). The MZ is hypothesized to be involved in midline fusion.



**Figure 2:** Development of corpus callosum. Formation of the corpus callosum is divided into six guide posts. Callosal axon is represented in red and subcortically projecting lateral axon is represented in green (Richards, Plachez et al. 2004).

### 1.1.2 Neuronal development

During development, neurons undergo many morphological changes from simple, symmetric cells to highly compartmentalized asymmetric cells. *In vitro* dissociated neuronal cultures are the best templates to study the neuronal development (Fig. 3).

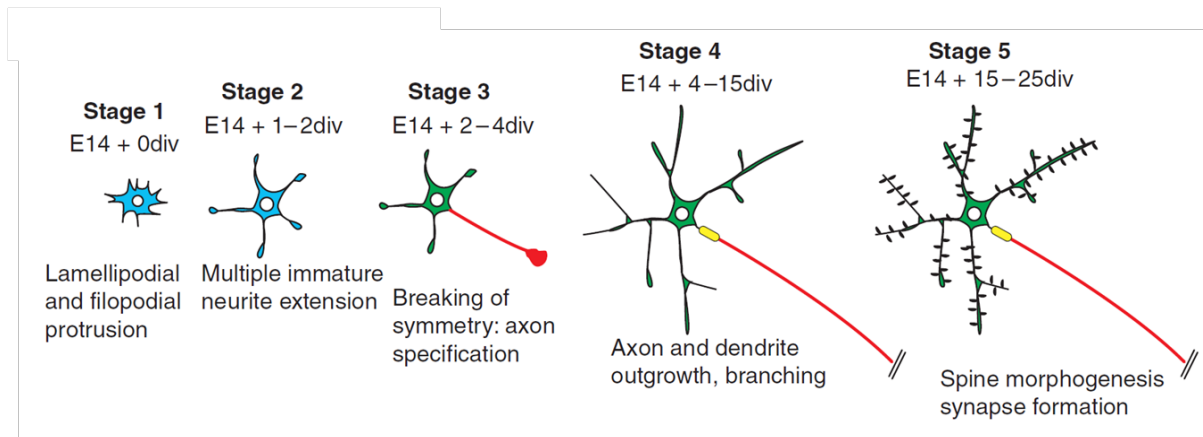


**Figure 3:** Developmental stages of cortical neurons *in vitro*. Dissociated cortical neurons show various stages during development. At stage 1, immature neurons show lamellipodial and filopodial protrusions (marked in blue). At stage 2, many immature neurites start to develop. Cells are still in symmetry. At stage 3, cells break the symmetry as one of the neurite grows rapidly and becomes axon (marked in red). Stage 4, this stage is characterized by the outgrowth and branching of axons and dendrites (marked in green). It also develops the axon initiation segment (marked with yellow cartridge). At stage 5, neurons are terminally differentiated and are ready to make synaptic connections. Neurons show the presence of dendritic spines (protrusions in grey) and axon initiation segment (Polleux and Snider 2010).

## 1.2 Axonal guidance

The precise wiring of the nervous system relies on the ability of axons and dendrites to recognize their synaptic partners. The axons are directed to their target cells in a highly directed and stereotyped manner, making very few errors. Axons move along the trail of adhesive molecules like the cell adhesion molecule (CAMs) and extracellular proteins

(laminin and fibronectin). Laminin is a 900 kDa extracellular protein first isolated from mouse Engelbreth-Holm-Swarm (EHS) tumor, consists of globular and rod like domains that are arranged in a cruciform shape (Beck, Hunter et al. 1990). It supports neurite outgrowth in cultured neurons and explants. Growth cones respond to an array of extracellular cues or molecules that are secreted or presented on the cell surface by cells along the axon path (Tessier-Lavigne and Goodman 1996; Dickson 2002) which include netrin (Kennedy, Wang et al. 2006; Round and Stein 2007), semaphorins (Kruger, Aurandt et al. 2005), slits (Dickson and Gilestro 2006), and ephrins (Mohamed and Chin-Sang 2006; Quinn and Wadsworth 2006). Cues may have duplex roles, attracting some axons while repelling others. Interaction between the substrate and the cue is necessary for axonal guidance, for example laminin and netrin-1 interaction guides retinal axons out of the eye (Mann, Harris et al. 2004). Guidance can be explained very well with an analogy discussed by Lowery et al., 2009 (Lowery and Van Vactor 2009).

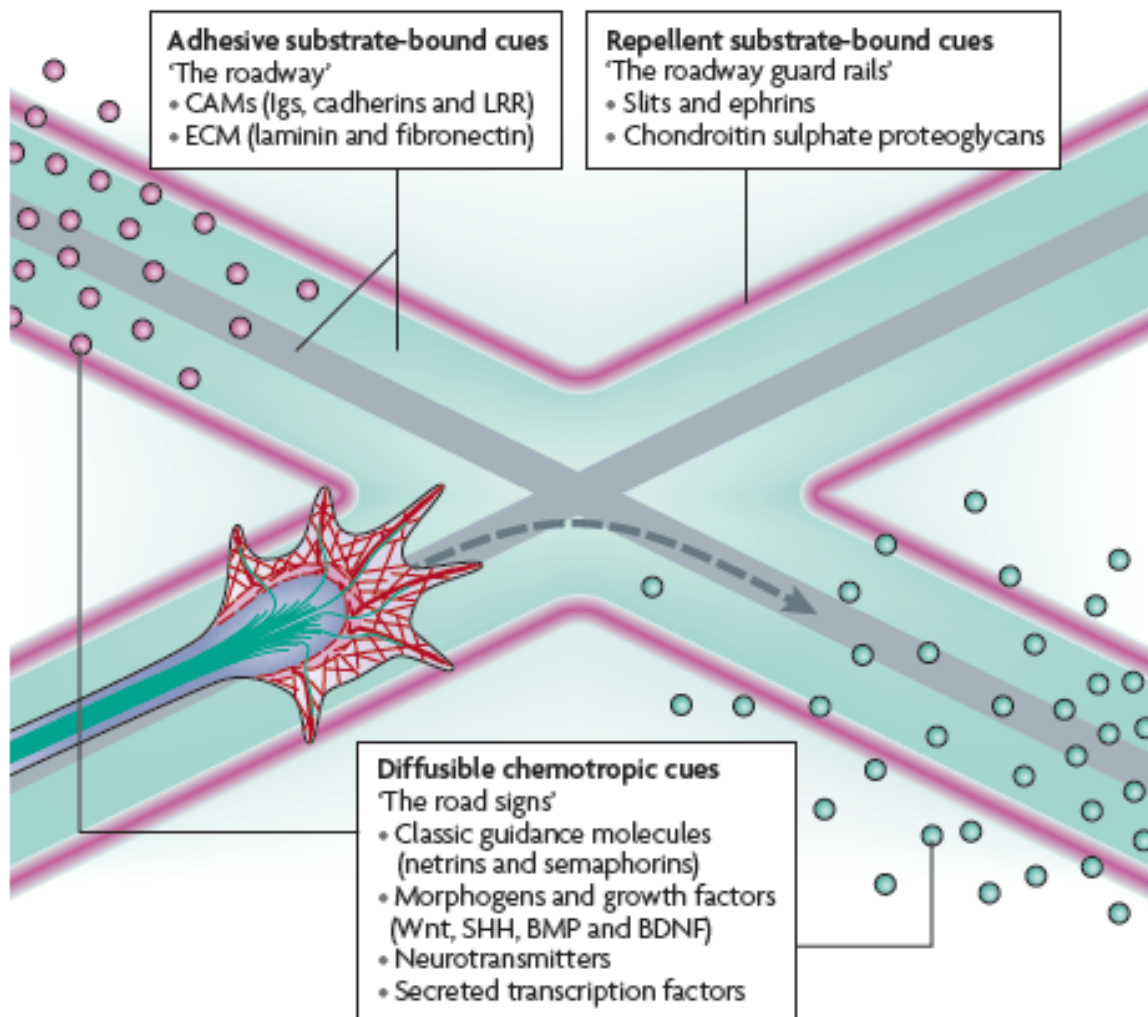


**Figure 4: Schematics of axonal guidance.** The growth cone (shown as hand like structure) travels using adhesive molecules (CAM and ECM) as the trails or the road (represented in green). The growth cone avoids repulsive guidance molecules (red circles) and grows towards the attractive guidance molecules (green circles) (Lowery and Van Vactor 2009).

### 1.2.1 Netrin

Netrins are dual function diffusible proteins and belong to a small family of guidance cues consisting of ~600 amino acids. The name is derived from the Sanskrit word 'Netr',



which means 'one who guides'. Structurally, netrins contain globular domain and EGF domain. Netrins are long-range chemoattractive and repulsive guidance cues. Their role has been well known in attracting axons ventrally towards the midline (Culotti and Merz 1998). The first insight came from the study in worm mutant *unc-6*, which affects the dorsal as well as the ventral migration of circumferential axons (Wadsworth 2002). The netrin signaling system is comprised of DCC (Deleted in Colorectal Cancer) and UNC5 receptors. DCC receptors induce attractive signaling whereas the association of DCC and UNC5 cytoplasmic domains convert the netrin induced attractive guidance to repulsive behavior in the neurons (Hong, Hinck et al. 1999). Netrin attracts certain neurons like commissural neurons but repels others, including trochlear motor neurons. It has been shown that netrin mediated chemoattraction is dependent on MAP1B. Netrin induces phosphorylation of MAP1B (Microtubule associated protein 1B) in a GSK-3 $\beta$  (Glycogen synthase kinase 3 $\beta$ ) and CDK5 (cyclin dependent kinase 5) dependent manner (Del Rio, Gonzalez-Billault et al. 2004). A netrin knockout mouse has axonal guidance problems, including defects in the formation of forebrain commissures, especially corpus callosum, and in spinal commissures. They also exhibit increased cell death (Serafini, Colamarino et al. 1996).

### **1.2.2 Semaphorins**

Semaphorins are a large family of cell surface and secreted guidance proteins. Semaphorins are expressed in most tissues but are best characterized in the nervous system development. Semaphorin expression can be seen in both neuronal as well as non-neuronal cells. Apart from that, semaphorins are expressed in many organ systems including the immune, musculoskeletal, renal, reproductive, respiratory and cardiovascular systems. The first semaphorin to be discovered was semaphorin-1a, a

transmembrane protein in the developing grasshopper (Kolodkin, Matthes et al. 1992). At the same time, a 100 kDa glycoprotein in the chick brain was identified as inducing growth cone collapse in sensory ganglion neurons *in vitro*. Initially termed as collapsin, it was later known as semaphorin 3A (sema 3A) (Luo, Raible et al. 1993). Based on their structures, the semaphorins can be divided into 8 classes. Class 1 and 2 are found in invertebrates; 3 to 7 are found in vertebrates and class 8 is found in viruses. All members of the family contain a highly conserved sema domain consisting of ~500 amino acids. The sema domain is critical in order for semaphorins to mediate their effects; in particular, a stretch of 70 amino acids within the domain is important for the effects of sema3A on repulsive axon guidance and the collapse of the growing tip or growth cones of axons, which stops their extension (Koppel, Feiner et al. 1997). Later on, another small stretch of amino acids homologous to tarantula hanatoxin, (K<sup>+</sup> and Ca<sup>2+</sup> ion-channel blocker) was indentified to be very important for the growth cone collapsing effects of sema3A (Behar, Mizuno et al. 1999). Semaphorins contain another highly conserved domain called plexin-semaphorin-integrin (PSI) domain, located at the c-terminal of the sema domain. Semaphorins also have N-linked glycosylation sites. In contrast, individual semaphorins have distinguishing characteristic features. For example, they may contain additional sequence motifs such as an immunoglobulin-like (Ig) domain or a stretch of basic amino acids and/or type 1 thrombospondin repeats (TSRs).

The majority of the semaphorins exert their effects by binding directly to single pass transmembrane receptors: plexins (Plex), as reviewed by (Kusy, Funkelstein et al. 2003). Further, plexins are divided in to 4 subfamilies: Plexin A1 to A4; Plexin B1 to B3; Plexin C1 and Plexin D1. In contrast to other semaphorins, class 3 semaphorins require another transmembrane protein, neuropilin (Npn) for their signaling.

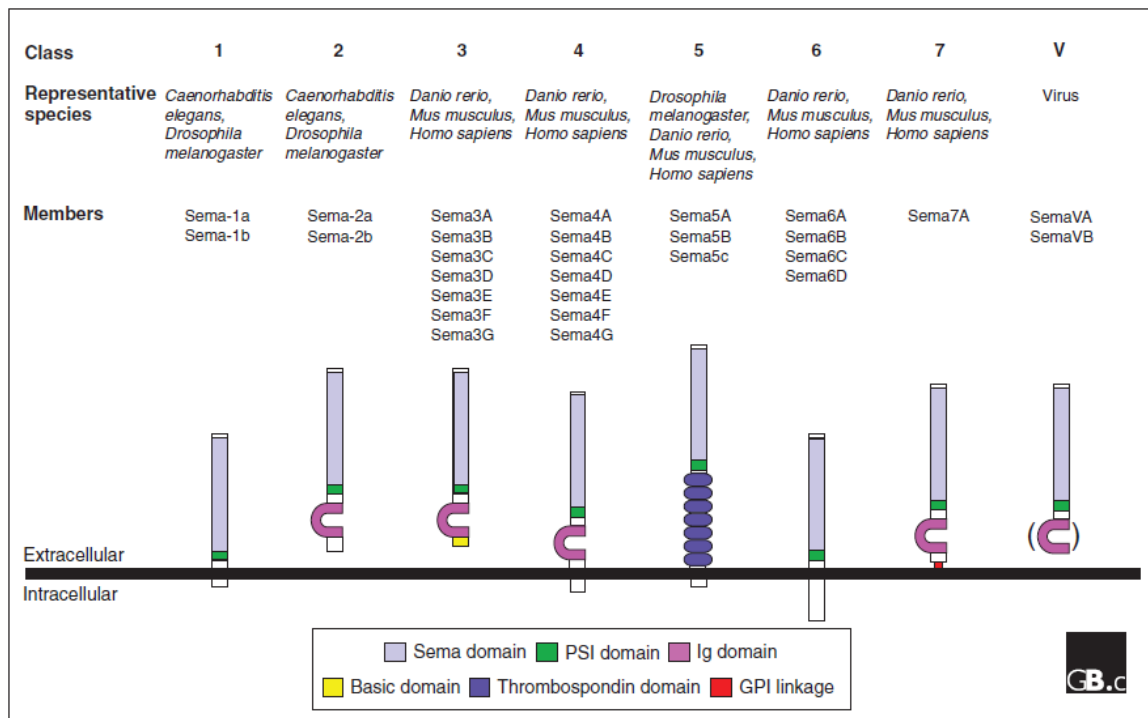


**Figure 7:** Structure of semaphorin receptor family. Semaphorins are divided into 8 classes. All the receptors of the family have both sema and PSI domains. Classes 2, 3, 4, 7 and 8 have immunoglobulin-like domains. Class 5 has thrombospondin domains, class 3 and 7 have basic domains and GPI linkage respectively (Yazdani and Terman 2006).

Sema4D/plexin B1 induces growth cone collapse in hippocampal neurons through the activation of PTEN and R-Ras Gase (Oinuma, Ito et al. 2010). sema4D/plexin B1 has also been shown to activate Rho through the interaction and to induce neurite retraction through the Rho/ROCK pathway (Aurandt, Vikis et al. 2002; Swiercz, Kuner et al. 2002). sema3A activates GSK-3 $\beta$  at the leading tip of the growth cones and induces growth cone collapse in neurons. sema3A regulates neuronal polarization and axonal branching (Shelly, Cancedda et al. 2011) (Bagnard, Lohrum et al. 1998). sema3A signaling is mediated through CDK5 and GSK-3 $\beta$  kinases. CDK5 and GSK-3 $\beta$  kinases phosphorylate CRMP2 (collapsing response mediating protein-2), reducing the tubulin binding affinity (Uchida, Ohshima et al. 2005).

### 1.2.3 Draxin

Draxin is a long range repulsive guidance cue involved in the development of spinal cord and forebrain commissures (Islam, Shinmyo et al. 2009). It consists of 349 amino acids with signal peptide sequences, suggesting that draxin is a secreted protein. Expression studies of draxin transcripts and protein using  $\beta$ -galactosidase staining show that draxin is expressed in many regions of the brain including the olfactory bulb, cortex, midbrain, cerebellum and pontine nuclei in new born mice.

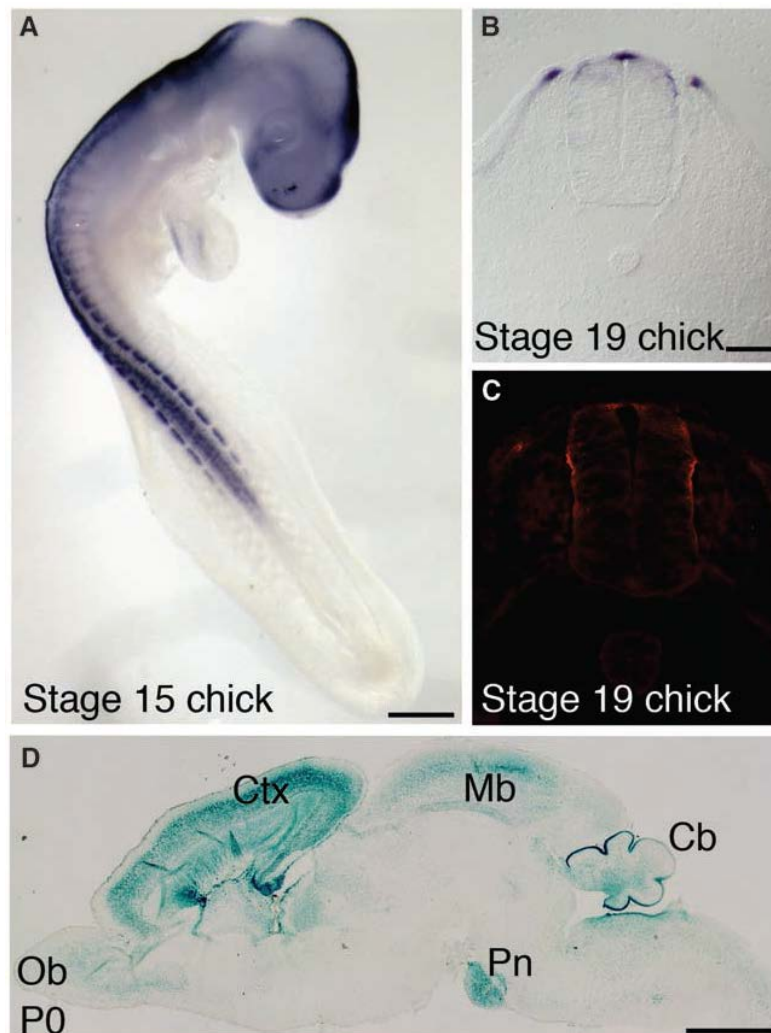


**Figure 8:** Expression of draxin in chick and mouse. (A) Whole mount *in situ* hybridization experiments showing the expression of draxin mRNA in the brain and

spinal cord of the chick. (B) Section *in situ* hybridization experiments showing the expression of draxin mRNA in the roof plate and dorsal lip of the chick embryos. (C) Detection of draxin protein in the dorsolateral basement membrane of the spinal cord using immunohistochemistry. (D) Sagittal section of newborn mouse brain showing the expression of draxin using  $\beta$ -galactosidase staining. Draxin is expressed in the olfactory bulb (Ob), cortex (Ctx), midbrain (Mb), pontine nuclei (Pn) and cerebellum (Cb). Scale bars in (A) and (D) indicate 1 mm; in (B) and (C), scale bar 100  $\mu$ m. (Islam, Shinmyo et al. 2009).

Draxin knockout mice are viable and fertile but display a severe abnormality in the formation of corpus callosum and hippocampal commissure (Islam, Shinmyo et al. 2009). Anterograde Dil (1, 1'-dioctadecyl-3, 3, 3', 3-tetramethylindocarbocyanine) tracing experiments show that callosal axons of draxin knockout mice fail to cross the midline. In strongly affected knockout mice IGG cells were absent (Islam, Shinmyo et al. 2009). Draxin plays an important role in the projection of thalamocortical axons. Recently it has been shown that draxin exerted growth cone collapse and neurite growth inhibition signal through multiple netrin receptors DCC, Neogenin, UNC5s H1, H2, H3), and DSCAM (Down's syndrome cell adhesion molecule) (Ahmed, Shinmyo et al. 2011).

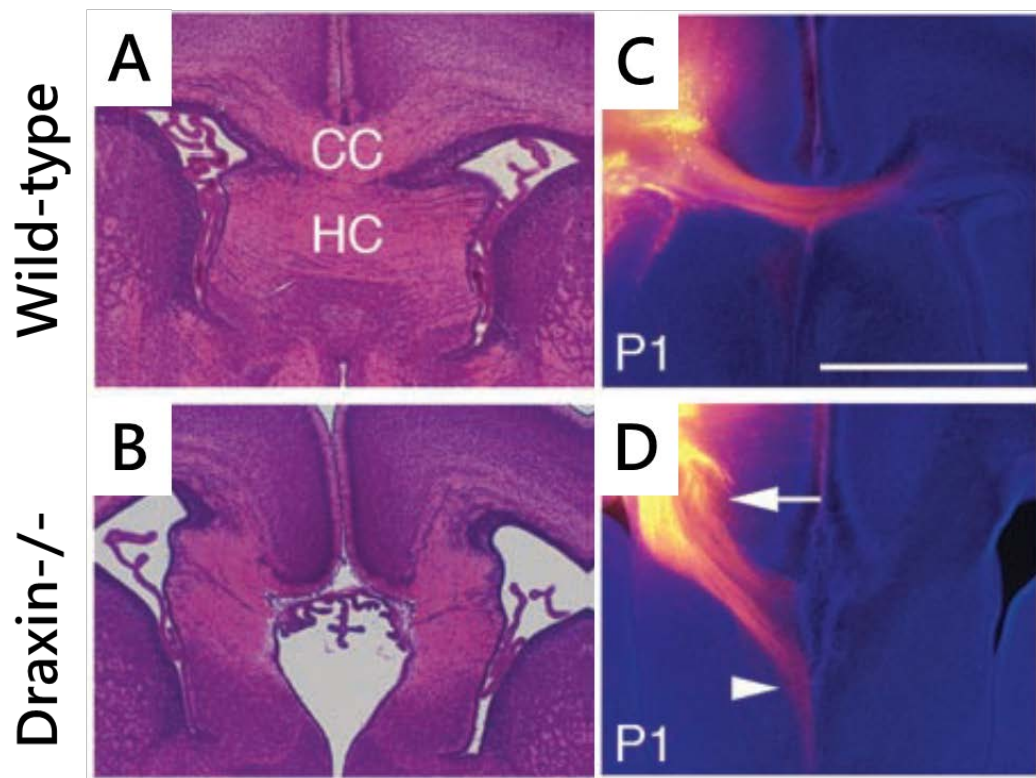


**Figure 9:** Abnormal development of corpus callosum in draxin knockout mice. (A and B) Coronal sections of P0 brains stained with hematoxylin and eosin. Wild-type mice show a nicely developed corpus callosum (marked as CC) and hippocampal commissure (HC), whereas as draxin<sup>-/-</sup> show a completely disrupted corpus callosum. (C and D) Coronal sections of brains were taken after injection of DiI into the neocortex. Callosal axons in the wild-type mice cross the midline and reach the other hemisphere whereas in draxin knockouts, callosal axons were unable to cross midline. Scale bar: (A and B) 500 $\mu$ m and (C and D) 1mm (Islam, Shinmyo et al. 2009).

#### 1.2.4 Slits

Slits are large proteins secreted by the midline glia (Rothberg, Hartley et al. 1988). They facilitate the commissural axons exit of the midline and also prevent them from re-

crossing the midline. Slits signal through the Roundabout (Robo) receptor. In Robo mutants, axons cross and recross the midline many times.

### **1.3 The growth cone**

The growth cones are sensitive and dynamic structures present at the tip of the axons. They are composed of finger-like projections, filopodia and a veil-like structure called lamellipodia. Two key components of the growth cone are actin and microtubules (MTs). The growth cone can be divided into three zones: peripheral domain (P), transition zone (T) and central domain (C). The peripheral (P) domain contains F-actin bundles, termed filopodia, as well as mesh-like F-actin networks. Furthermore, dynamic MTs explore preferentially in this region, usually along F-actin bundles. The central (C) domain encloses stable MTs that enter the growth cone from the axon shaft. Additionally, numerous organelles, vesicles and central actin bundles are present in this domain. Transition (T) zone is in between the P and C domains; it is composed of actin arcs and is adjacent to the F-actin bundles. During the neuronal navigation the growth cone detects the gradient of the cue and the level of receptor activation with a time window as the neurons move up and down along the gradient of the cue.

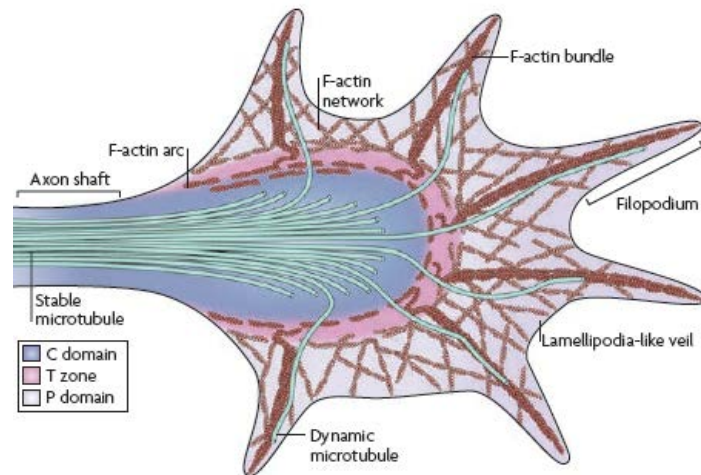


**Figure 4:** Schematic of the growth cone. The schematic shows three domains of the growth cone. Central domain (C), transition zone (T) and peripheral domain (P). C domain shows a bundle of MTs (represented in green), which are stable and entering from the axonal shaft. T zone is sandwiched between the C domain and P domain and contains acto-myosin contractile structures and actin arcs which help in the consolidation of MTs during growth. P domain is highly dynamic and is comprised of F-actin bundles and lamellipodia structures (Lowery and Van Vactor 2009).

#### 1.4 Growth cone cytoskeleton elements

The Cytoskeleton plays a very important role in neuronal development. Once the growth cones come in contact with the guidance cue various signal transduction pathways are activated and based on that neurons make the decision to either move toward or away from the source of the guidance cue. One of the noteworthy features of the growth cone cytoskeleton is the creation of a very dynamic yet steady framework. The growth cone cytoskeleton is composed of three major types of fibers: microtubules, microfilaments and intermediate filaments.



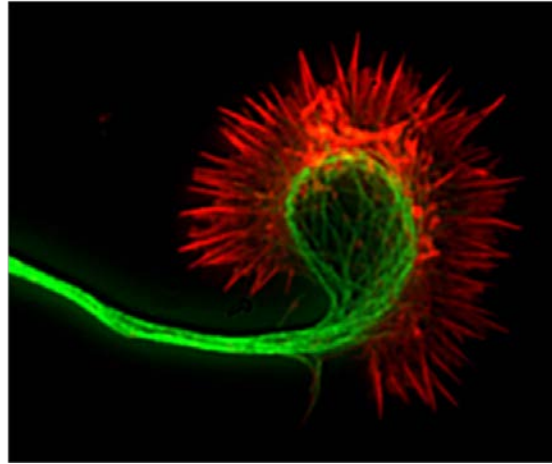


**Figure 6:** Image of cortical axon growth cone showing two major cytoskeletal elements. The growth cone shows actin (red) and microtubules (green). The actins are stained with phalloidin whereas the microtubules are stained with anti-tubulin antibodies. In the growth cone, dynamic microtubules occasionally enter and explore the peripheral regions and interact with actin filaments (Kalil, Li et al. 2011).

MTs are hollow tube-like structures with a diameter of 25nm. They are made up of  $\alpha$  and  $\beta$  tubulin heterodimers. In mammals, 13 tubulin protofilaments arrange laterally to form one circle. The arrangement of  $\alpha\beta$  in a head-to-tail configuration makes them polar. MT formation in the cell is instigated by the binding of  $\alpha\beta$ -tubulin heterodimers to the  $\gamma$ -tubulin ring complex at the centrosome, a MT organizing centre. MTs undergo many post-translational modifications including: phosphorylation, tyrosination, detyrosination, acetylation, polyglutamylation, and polyglycylation, as reviewed in (Ludueno 1998). MTs interact with microtubule associated proteins (MAPs), which regulate cytoskeletal arrangement and dynamics. MAPs also interact with other cytoskeletal polymers and link them to MTs reviewed in (Maccioni and Cambiazo 1995).

In growth cones, the first study on microtubule dynamics was reported using cultures of embryonic grasshopper limbs (Sabry, O'Connor et al. 1991). The study demonstrated that in growth cone steering events, microtubules have the ability of dynamic exploration of the entire growth cone. The study also showed that near guidepost cells, microtubules selectively invade filopodial branches that had contacted the guidepost cell. Both selective invasion and selective retention in the branches generate an asymmetrical microtubule arrangement within the growth cone.

Microfilaments are a helical structure of diameter 7 nm, composed of monomeric globular (G) protein termed as actin. Actin is 42 kDa versatile protein and accounts for 1-5% of the total protein in a non-muscle cell and about 20% in muscle cells. The monomeric subunits are assembled in a fashion whereby they have the same orientation. Due to this feature, microfilaments exhibit polarity. This polarity affects the growth of microfilaments; one end (plus end) typically assembling and disassembling faster than the other (minus end). *In vitro* G actins exist in three forms: ATP-actin, ADP-pi-actin (ADP with inorganic phosphate (pi) noncovalently bound in  $\gamma$  position) and ADP actin. Both ATP-actin and ADP-actin can associate or dissociate from barbed as well as growing ends, however kinetically ADP-actin dissociation is favored, resulting in the slow addition of monomers at the barbed ends and the slow dissociation of monomers at the barbed ends.

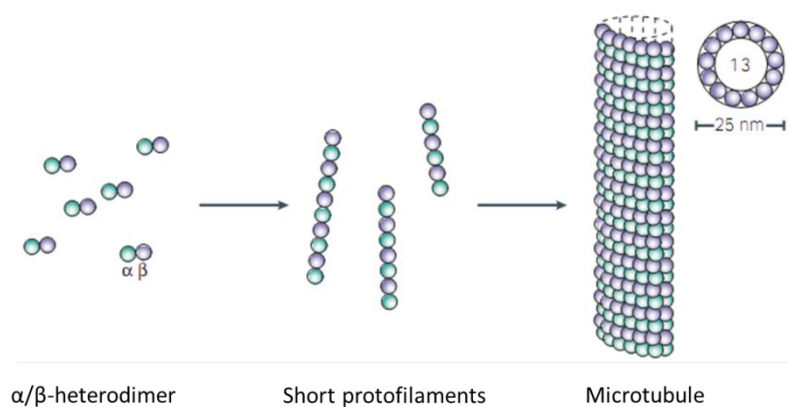


**Figure 7:** Polymerization of microtubules.  $\alpha/\beta$  heterodimers together form short protofilaments, which further form the cylindrical microtubule of 25nm in diameter. Scheme from (Westermann and Weber 2003).

## 1.5 Microtubule dynamics

Microtubules are extremely dynamic structures. MTs undergo switch between rapid polymerization and shrinkage, a process known as dynamic instability, powered by GTP hydrolysis (Mitchison and Kirschner 1984). MAPs regulate the microtubule dynamics either by stabilizing or destabilizing the microtubules. Plus-end tracking proteins (+TIPs) are the specialized MAPs which specifically accumulate at the microtubule growing ends. The first +TIPs to be described was cytoplasmic linker protein of 170 kDa (CLIP-170) reviewed in (Akhmanova and Steinmetz 2008). +TIPs come from different unrelated families. In- spite of this diversity they share common functions and co-localize with each other. They are classified into 5 different subgroups: EB family proteins, cytoskeleton associated proteins Gly-rich (CAP-Gly proteins), Proteins containing basic and Ser-rich sequences, HEAT and WD40-repeat proteins and

microtubule motor proteins. End-binding proteins (EB) are globular proteins typically contain calponin homology (CH) domains, which is the characteristics of actin binding protein. They have conserved N- and C- terminal domains that are connected through the linker sequence. EB1, EB2 and EB3 are the members of this family. The N-terminal domain is necessary for microtubule binding. The C-terminal region contains a coiled-coil domain which helps in dimerization of the EB monomers. CAP Gly proteins contain Gly-rich domains at their N-terminal which help them to bind to the microtubules. CLIP-170, CLIP-115 and p150<sup>Glued</sup> are few members of this family. Proteins containing basic and ser-rich sequences are the flexible multi-domain structure often mediating interaction with the microtubules and the EB proteins. CLASP1/2 (CLIP-associated proteins), adenomatous polyposis coli protein (APC), microtubule-actin crosslinking factor (MACF) and transmembrane protein stromal interaction molecule-1 (STIM1) are the few members belong to this group. HEAT- and WD40-repeat proteins contain several tumor over expressed gene (TOG) domains in their N-terminal which bind to microtubules. Microtubule motor proteins include both plus-end-directed and minus-end-directed motor proteins including kinesins, mitotic centromere-associated kinesin (MCAK) and cytoplasmic dyneins.

## **1.6 MAP1 proteins**

MAP1 family of proteins are members of the MAP family which binding along the MT lattice. The MAP1 family consists of two related but distinct proteins, MAP1A and MAP1B (Schoenfeld *et al.*, 1989; Garner *et al.*, 1990; Langkopf *et al.*, 1992). These MAPs are encoded by two distinct genes (Garner *et al.*, 1990) but they show amino acid similarities in amino acid regions. MAP1A has a molecular mass of 299 kDa whereas MAP1B has a molecular mass of 320 kDa. There are three proteins associated with the

microtubule-binding domains of both MAP1A and MAP1B, referred to as light chains: LCI (34 kDa); LC2 (30 kDa) and LC3 (19 kDa) (Vallee and Davis, 1983; Schoenfeld *et al.*, 1989).

Interestingly, MAP1A and LC2 and MAP1B and LC1 are transcribed by single mRNAs which give rise to pre-MAP1A/LC2 and pre-MAP1B/LC1 polyprotein precursors, which are further proteolytically processed (Hammarback *et al.*, 1991; Langkopf *et al.*, 1992).

## **1.7 MAP1B**

MAP1B is expressed at high levels during mammalian brain development (Schoenfeld 1994) and plays a role in neuronal migration and axon guidance *in vivo* (Takei, Kondo *et al.* 1997; Gonzalez-Billault, Demandt *et al.* 2000; Meixner, Haverkamp *et al.* 2000). The expression of MAP1B can be detected in neurons, Schwann cells, oligodendrocytes and astrocytes (Fischer, Konola *et al.* 1990; Ma, Chow *et al.* 1999). MAP1B is a cytoskeletal protein involved in modeling the central as well as the peripheral nervous system (Meixner, Haverkamp *et al.* 2000). It consists of heavy chain (300 kDa) and light chain (32 kDa) with microtubule and actin binding regions.

Within the subcellular compartments, MAP1B can be detected in dendrites, axons, postsynaptic terminals and soma of the neurons. MAP1B functions and biological properties have been studied extensively using biochemical as well as genetic approaches. Overexpression of the light chain of MAP1B (LC1) in PtK2 cells lead to the formation of thick, wavy and organized microtubule bundles (Togel, Wiche *et al.* 1998).

Until now, four MAP1B knockout mice have been generated displaying controversial phenotypes. First, MAP1B<sup>-/-</sup> was generated using the gene trap method, inserting a stop

codon at amino acid 571. In these mice the expression of MAP1B is absent. Homozygous mice die at embryonic day 8.5 (E 8.5). The heterozygotes survive but display a spectrum of phenotypes including slower growth, lack of visual acuity, smaller retina size and motor system abnormalities (Edelmann, Zervas et al. 1996). The second MAP1B<sup>-/-</sup> was generated by inserting a stop codon after amino acid 11. The knockout shows the expression of MAP1B splice variants. Heterozygous mice displayed no obvious abnormalities in their development and behavior, whereas the homozygotes showed a decrease in brain weight and delayed nervous system development as well as mild reduction in the axonal myelination (Takei, Kondo et al. 1997). The third MAP1B<sup>-/-</sup> was generated using a gene trapping strategy wherein a stop codon was introduced after amino acid 95. The knockout exhibit about 5% of normal protein and are hence considered as a hypomorphous model. Homozygotes die postnatally whereas the heterozygotes survive and show an absence of corpus callosum, deformity in commissures and malformation in the formation of cortex, hippocampus and cerebellum whereas heterozygotes are normal (Gonzalez-Billault, Demandt et al. 2000). The fourth MAP1B<sup>-/-</sup> was generated after introducing a large deletion (about 93%) of the coding region in the MAP1B gene. MAP1B expression was absent in these knockouts. Homozygotes survive but display 80% lethality. The most striking phenotype were reduced body size, agenesis of corpus callosum, misguided commissures forming Probst bundles, reduced diameter in peripheral axons and myelin sheath and reduced nerve conduction velocity in the sciatic nerve (Meixner, Haverkamp et al. 2000). Adult dorsal root ganglion (DRG) explants and dissociated neurons were also affected in MAP1B<sup>-/-</sup> mice.

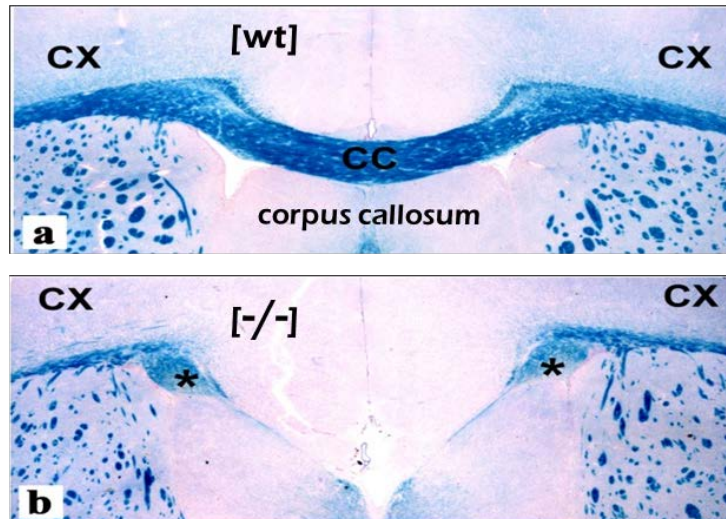


**Figure 8:** Coronal section of wild-type and MAP1B<sup>-/-</sup> mice brains. (a) Sections from the wild-type mice brain show well developed corpus callosum that connects the right and the left hemispheres whereas MAP1BKO show complete agenesis of corpus callosum (Meixner, Haverkamp et al. 2000).

### 1.7.1 MAP1B phosphorylation

MAP1B is phosphorylated by a number of kinases including GSK-3 $\beta$  (Lucas et al. 1998; Goold et al. 1999; Goold & Gordon-Weeks, 2001; Scales et al. 2009), cyclin-dependent kinase 5 (CDK5) (Pigino et al. 1997; Paglini et al. 1998) casein kinase 2 (CKII) (Díaz-Nido et al. 1988; Ulloa et al. 1993) and c-Jun N-terminal protein kinase 1 (JNK 1) (Chang et al. 2003; Kawauchi et al. 2003, 2005).

MAP1B is phosphorylated either by Mode I phosphorylation or by Mode II phosphorylation. Mode I phosphorylation is catalyzed by GSK-3 $\beta$  and CDK5 (Lucas, Goold et al. 1998) (Avila, Dominguez et al. 1994) whereas Mode II phosphorylation is catalyzed by CKII (Díaz-Nido, Serrano et al. 1988). MAP1B has both non-primed (Trivedi et al. 2005) and primed (Scales et al. 2009) GSK-3 $\beta$  phosphorylation sites. Antibodies against GSK-3 $\beta$  primed MAP1B phosphorylation sites label somato dendritic

compartments and axon in developing neurons (Scales et al. 2009) whereas antibodies against GSK-3 $\beta$  non-primed MAP1B phosphorylation sites label axons exclusively (Trivedi et al. 2005). In Mammalian neurons, spatial-distribution of GSK-3 $\beta$  primed and non-primed phosphorylation sites on MAP1B are conserved, particularly within the primed GSK-3 $\beta$  sites on MAP1B (Tymanskyj, Lin et al. 2010).

In vivo proteomic studies show that MAP1B has 33 phosphorylation sites (M.O Collins et al 2005). The GSK-3 $\beta$  phosphorylate seven sites (S829, S1247, S1347, S1395, S1793, S1911, S2094); CDK5, phosphorylate eight sites (S829, S1260, S1317, S1334, S1610, S1621, S1775, S1793); CKII phosphorylate have five sites (S828, S1307, S1382, S1768, S1877); cdc2 phosphorylate two sites (S1768, S1775); the p38MAPK phosphorylate six sites (S1307, S1373, S1384, S1391, S1781, T1784) ERK1 (S1255); the PKG phosphorylate one (T1806) and PKA two sites (S1371, S1778). INSR and src kinase phosphorylate tyrosine site at (Y1331), reviewed in (Riederer 2007). Despite the fact that many phosphorylation sites have been identified, very little is known about them due to the fact that out of all the sites only two have been mapped.

Guidance cues like netrin and reelin induce phosphorylation of MAP1B in neuronal migration and axonal guidance pathways (Del Rio, Gonzalez-Billault et al. 2004) (Gonzalez-Billault, Del Rio et al. 2005). Mode I phosphorylation by GSK-3 $\beta$  activity is detected using mAb-SMI 31 antibody (Johnstone, Goold et al. 1997). In vitro kinase assay, using cultured cerebellar granule cells, shows that MAP1B is phosphorylated by GSK-3 $\beta$ . Phosphorylated MAP1B in non-neuronal cells increases the population of



unstable microtubules at the cost of the stable microtubules (Goold and Gordon-Weeks 2004).

Another important post-translational modification of MAP1B is S-nitrosylation. Recent insights show that NO-induced axon retraction is dependent on the presence of MAP1B. Studies suggest that MAP1B as a target of S-nitrosylation; activation of neuronal nitric oxide synthase (nNOS) or extracellular application of an NO donor results in S-nitrosylation of the LC 1 of MAP1B on cystine 2457 residue. This modification leads to a conformational change and increases MAP1B binding to microtubules. Mutation analysis showed that S-nitrosylation of MAP1B is essential for NO-induced axon retraction (Stroissnigg, Trancikova et al. 2007).

## **1.8 Growth cone signaling**

### **1.8.1 DCC and UNC5 receptor**

DCC receptors are single pass type I transmembrane glycoprotein of molecular mass 175-190 kDa. It consists of large extracellular domain of about 1100 amino acids and a cytoplasmic domain with 325 amino acids. The extracellular domain has four immunoglobulin-like domains and six fibronectin type III domains. DCC cytoplasmic domain has three regions named P1, P2 and P3.

The expression studies show that DCC is linked to neuronal guidance and survival (Mehlen 2003). DCC gene inactivation studies show severe defects in brain development, complete absence of corpus callosum and hippocampal commissures that are similar to MAP1B<sup>-/-</sup> phenotypes. Axons fail to cross the midline instead they extend abnormally forming probst bundles.

The UNC-5 belongs to class of netrin receptors which mediate the repulsive guidance. They are single pass transmembrane proteins containing 2 immunoglobulin (Ig) like domains and 2 type I thrombospondin domain in the extracellular region. First identified as a tumor-suppressor gene on chromosome 18q later showed to be associated with brain development.

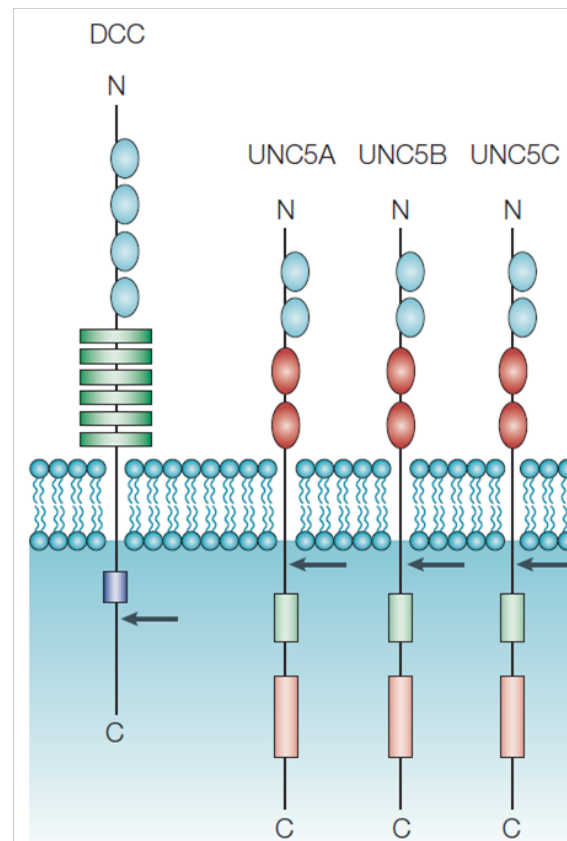


**Figure 10:** DCC and UNC5 receptors. DCC is type I transmembrane protein. It is composed of an extracellular domain consisting of four immunoglobulin-like repeats (light blue circles), six fibronectin type III-like repeats (green rectangles), a single transmembrane spanning region and a cytoplasmic domain including the dependence domain (dark blue square). UNC5A, UNC5B and UNC5C also are type I transmembrane proteins. All three proteins have an extracellular region, consisting of two immunoglobulin-like domains (light blue circles) and two thrombospondin-like repeats

(red circles) and a zonula occludens-1 domain (light green rectangles) and a death domain (pink rectangles) in the cytoplasmic region. Arrow indicate the capsase cleavage site (Arakawa 2004).

### **1.8.2 GSK-3kinase**

GSK-3 is a key downstream regulator molecule involved in many signaling pathways including insulin, Wnt and epidermal growth factors (Saito, Vandenhede et al. 1994; Eldar-Finkelman, Seger et al. 1995; Cook, Fry et al. 1996; Waltzer and Bienz 1999; Ding, Chen et al. 2000; Kennedy, Wang et al. 2006). GSK-3 belongs to the super family of mitogen-activated protein (MAP) kinases (Hanks and Hunter 1995). It has two isoforms: GSK-3 $\alpha$  and GSK-3 $\beta$  of molecular weights of 51 and 47 kDa, respectively (Woodgett 1990). They share about 95% homology. GSK-3 $\beta$  phosphorylates multiple substrates but not all targets are phosphorylated in the same mode and with the same efficiency.

GSK-3 $\beta$  is subjected to multi-level regulation mediated by its phosphorylation, subcellular localization, and protein–protein interactions. GSK-3 $\beta$  kinase undergoes multiple phosphorylation events, which affect its activity depending upon upstream signaling kinase. Phosphorylation of the GSK-3 $\beta$  kinase domain at Tyr216 leads to its activation (Dajani, Fraser et al. 2001), whereas phosphorylation of the n-terminal Ser9 results in inhibition of its activity (Stambolic and Woodgett 1994). GSK-3 $\beta$ , unlike other kinases, prefers prior phosphorylation of its substrate before it can phosphorylate the substrate. This is termed primed phosphorylation. It can also phosphorylate without priming. Primed phosphorylation is considered to be more efficient than without priming.

GSK-3 $\beta$  regulated the microtubule dynamics by modulating many substrates including adenomatous polyposis coli (APC), MAP1B, CRMP2, CLASP2 and Tau proteins, as reviewed by (Jope and Johnson 2004). In addition, many kinases and transcription factors are the targets of GSK-3 $\beta$  activity. Studies show that suppression of GSK-3 $\beta$  activity is necessary for axon formation and extension (Zhou, Zhou et al. 2004). In contrast, parallel studies also show that inhibition of GSK-3 $\beta$  prevents axon extension (Owen and Gordon-Weeks 2003). Phosphorylation of MAP1B by GSK-3 $\beta$  destabilizes the microtubules and maintains them in a dynamic state (Trivedi, Marsh et al. 2005). CRMP2 regulated microtubule polymerization is inhibited when it is phosphorylated by GSK-3 $\beta$  (Yoshimura, Kawano et al. 2005).

### **1.8.3 PI3 kinase**

PI3 kinases (PI3K) are heterodimeric lipid kinases activated by growth factor and hormone receptors. They are involved in various cellular processes, such as proliferation, apoptosis, cytoskeletal rearrangement growth and metabolism (Engelman, Luo et al. 2006). PI3Ks are composed of regulatory and catalytic subunits that are encoded by different genes.

PI3K divided into three classes based on their subunit composition and their substrate specificity for phosphoinositides (Vanhaesebroeck, Leever et al. 2001) : class I, II and III. Class I PI3k is divided in to two subsets, class IA and IB. The class IA PI3k is a heterodimer consisting of one 110 kDa catalytic subunit (p110 $\alpha$ ,  $\beta$  or  $\delta$ ) and one regulatory subunit (p85 $\alpha$ , p85 $\beta$ , p55 $\alpha$ , p50 $\alpha$ , or p55 $\gamma$ ). The Class IB PI3K is also a dimer, composed of one catalytic subunit (p110 $\gamma$ ) and one regulatory subunit (p101 or p87) (Wymann, Bjorklof et al. 2003). Class I enzymes utilize PIP2 as substrates and are thought to primarily produce PIP3 in cells reviewed in (Backer 2010).

PI3K plays an important role in neuronal migration, particularly radial and tangential migration of the neurons. For example reelin, an extracellular matrix protein controls the radial migration of neurons in a PI3K dependent manner. It induces PI3K regulatory subunit p85 $\alpha$  to associate with Disabled (Dab1) protein consequently leading to activation of Akt and inhibition of GSK-3 kinases (Beffert, Morfini et al. 2002). BDNF induced, tyrosine kinase receptor (TrkB) signaling for tangential migration of neurons takes place via PI3K.

PI3K also plays a vital role in regulating neuronal morphogenesis. For example segregation of axonal and dendritic compartments takes place via PI3K pathway (Cosker and Eickholt 2007).

#### **1.8.4 PKB/Akt kinase**

Akt is a serine/threonine kinase and is a critical signaling molecule involved in cellular growth, survival, proliferation, metabolism, migration and anticancer therapeutics, as reviewed in (Manning and Cantley 2007). Akt has three isoforms: Akt1/PKB $\alpha$ ; Akt2/PKB $\beta$  and Akt3/ $\gamma$ , which share homology. Akt isoforms are composed of the pleckstrin domain (PH) on their n-terminus, the regulatory domain on their c-terminus and the catalytic domain in the middle. Akt has many phosphorylation sites: threonine 308 (Thr308) 309, 305 in Akt1, Akt2 and Akt3 respectively and serine 473 (ser473), 474 and 472 in Akt1, Akt2 and Akt3 respectively. The primary outcome of PI3K activation is the production of PIP3 in the membrane, which functions as a second messenger to activate downstream signaling cascades that involve Akt and other proteins. Phosphorylation of PIP2 at the D3 position on the inositol head group leads to the formation of PIP3, which acts as a second messenger. Phosphorylation at the D3

position is necessary for the binding of the PH domain of Akt. The function of PIP3 is to recruit PH-domain-containing proteins to the inner surface of the cell membrane. At the membrane, PH-domain-containing serine/threonine kinases termed 3-phosphoinositide-dependent protein kinase-1 (PDK1) and 3-phosphoinositide-dependent protein kinase-2 (PDK2) phosphorylates Akt on Thr308 (Vanhaesebroeck and Alessi 2000) and Ser473 for its activity, as reviewed in (Vivanco and Sawyers 2002).

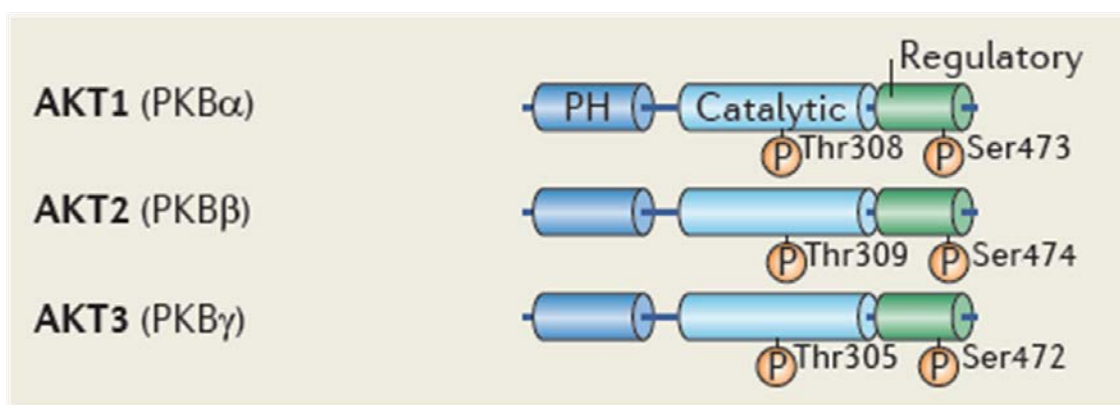


**Figure 11:** Structure of Akt isoforms. Akt1, Akt2 and Akt3 isoforms share more than 80% amino acid sequence homology and include an N-terminal pleckstrin homology (PH) domain, a central catalytic domain and a C-terminal regulatory domain. Phosphorylation of Thr308 in the catalytic domain of Akt1 (Thr309 in Akt2 and Thr305 in Akt3) by 3-phosphoinositide-dependent kinase 1 (PDK1) as well as Ser473 in the regulatory domain of Akt1 (Ser474 in Akt2 and Ser472 in Akt3) by mammalian target of rapamycin complex 2 (mTORC2) is required for activation of Akts.

### 1.8.5 PTEN

PTEN is a phosphatase involved in many cellular functions including cell proliferation survival and energy metabolism. PTEN gene is located on chromosome 10q23.3 and encodes a protein of 403 amino acids. PTEN can act on both polypeptide and

phosphoinositide substrates. PTEN is a critical regulator of PI3K signaling pathway and it has been shown that mutation or loss of PTEN leads to many diseases and tumorigenesis.

Role of PTEN in cell survival and proliferation became evident by the fact that mutation of PTEN lead to human cancers including prostate carcinoma, melanoma, glioblastoma and endometrial carcinoma (Maehama and Dixon 1999). Additionally, germline mutations in PTEN are linked with Cowden disease and Bannayan-Zonana syndrome, dominantly inherited diseases characterized by the development of multiple benign tumors and by the high risk of developing malignant tumors in breast and thyroid.

PTEN activity is regulated by many post-translational modifications including phosphorylation, acetylation, and oxidation which further regulate its localization. Phosphorylation of a group of serine and threonine residues located in the COOH-terminal region of PTEN renders it in closed inactive conformation whereas dephosphorylation leads to open active in conformation. CK2 and GSK-3 $\beta$  are implicated in phosphorylation some of these sites (Torres and Pulido 2001). CK2 mainly phosphorylates serine 370 (S370) and serine 385 (S385), whereas GSK-3 $\beta$  targets serine 362 and Threonine 366 (S362 and T366). Studies suggest that association of GSK-3 $\beta$  might be the part of a negative-feedback loop that regulates the activity of PTEN and PI3K (Al-Khoury, Ma et al. 2005). Additionally, evidences show that RhoA-associated kinase (ROCK) phosphorylates S229, T232, T319 and T321 in the C2 domain to activate PTEN and target it to the membrane in chemoattractant-stimulated leukocytes. The consequences underlying ROCK-mediated phosphorylation and activation of PTEN are not clear yet.

# Part I

---

## Results



## 2 RESULTS

### 2.1 Draxin-dependent neurite inhibition is suppressed in MAP1B<sup>-/-</sup> neurons.

#### 2.1.1 Draxin inhibits neurite outgrowth in cortical explants

To investigate whether draxin has repulsive guidance properties for cortical neurons, we cultured cortical explants from newborn pups in the presence of draxin-conditioned medium. The experimental procedure is summarized in Fig. 12. Draxin was expressed through transient transfection of COS7 cells with the mixture of myc tagged draxin construct and trans-activator plasmid. As a control we used mock-transfected conditioned medium. Draxin conditioned medium was harvested 48 hours post transfection and was diluted by adding 50% of fresh medium. The expression of myc tagged draxin protein was detected using immunocytochemistry and western blots (Fig 13A and 13B). Cortical explants from newborn pups were manually dissected and grown in matrigel for 48 hours in the presence and absence of conditioned medium.

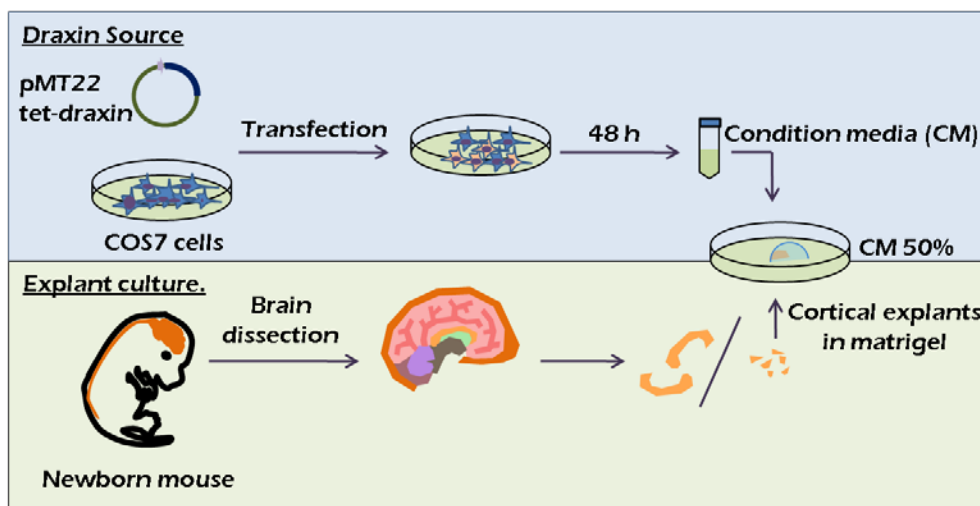


**Figure 12:** Experimental scheme to test the effect of draxin on cortical explants. Draxin conditioned medium was harvested 48 hours post transfection and was diluted by

adding 50% of fresh medium. Cortical explants from newborn pups were manually dissected and grown in draxin- or mock-conditioned medium.

Wild-type cortical explants cultured in the presence of draxin-conditioned medium displayed a reduced neurite outgrowth, consistent with previous study Islam et al in 2009 (Islam, Shinmyo et al. 2009). In contrast, explants growing in mock conditioned medium showed robust neurite outgrowth.

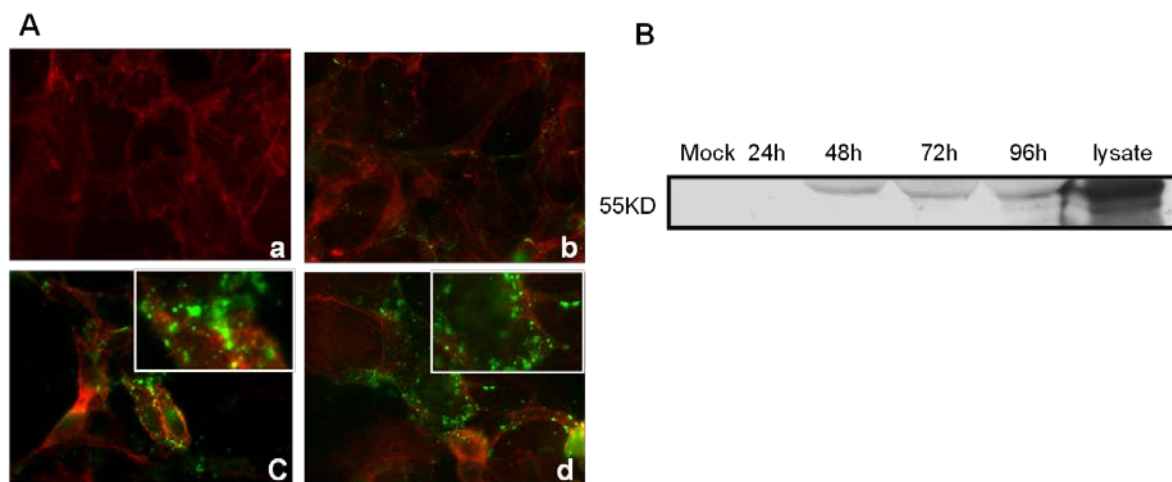


**Figure 13:** Ectopic expression of draxin protein in COS7 cells. A. (a) Mock (transfected with empty pMT22tet vector) (b) 24hours and (c & d) 48 hours post transfection of a myc-tagged draxin encoding construct into COS7 cells. Cells were fixed and stained for F-actin (phalloidin: red) and for myc (green). Draxin transfected cells displayed vesicular localization of draxin myc-fusion protein. B. Detection of expressed draxin protein in culture medium using immunoblotting. Draxin conditioned medium was harvested at 24 hours, 48 hours, 72 hours and 96 hours post transfection and detected using myc antibodies. The cell lysate was used as the control. The draxin expression was detected after 48h post transfection.

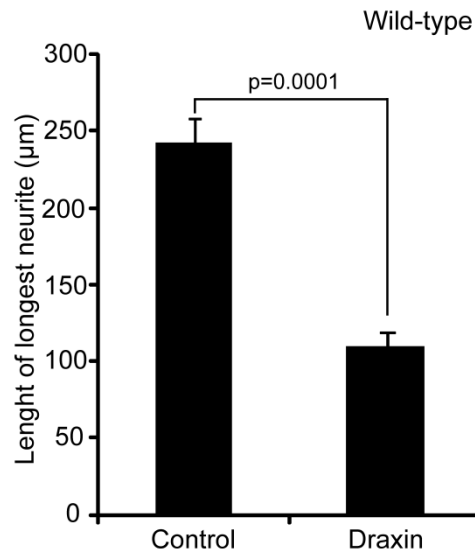


**Figure 14.** Quantitative analysis of neurite length of wild-type explants upon draxin treatment. The neurite length of wild-type explants, grown in presence and absence of draxin conditioned medium were quantified using student t-test. Draxin reduced the neurite outgrowth significantly compared to the control group. Quantification from three independent experiments in each experiment 30 explants measured. Values are shown in mean  $\pm$ SEM.

### 2.1.2 No inhibition of neurite outgrowth by draxin in MAP1B<sup>-/-</sup> cortical explants culture.

The resemblance of corpus callosum defects in draxin (Islam, Shinmyo et al. 2009) and MAP1B knockout mice (Meixner, Haverkamp et al. 2000) led us to examine the potential role of MAP1B in chemo-repulsive draxin signaling. Cortical explants from MAP1B<sup>-/-</sup> mice were grown in the presence and absence of draxin-conditioned medium as mentioned above. In contrast to wild-type explants, MAP1B<sup>-/-</sup> neurites showed insensitivity towards draxin. They showed a vigorous neurite out growth in the presence as well as absence of draxin. These experiments indicate that draxin signaling is mediated by MAP1B.

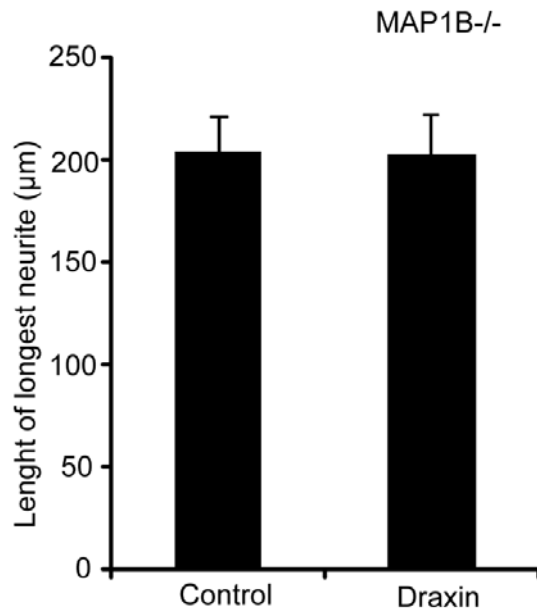


**Figure 15:** Quantitative analysis of neurite length of MAP1B knockout explants upon draxin treatment. Neurite length of MAP1B knockout explants, grown in presence and absence of draxin conditioned medium were quantified using student t-test. Neurite length was not inhibited by draxin in MAP1B deficient explants. Quantification from three independent experiment in each experiment 30 explants measured. Data represented in mean  $\pm$  SEM.

## 2.2 Draxin induced inhibition of neurite outgrowth are MAP1B dependent

We further tested the role of MAP1B in draxin signaling by using purified recombinant draxin protein. Cortical explants from newborn wild-type and MAP1B<sup>-/-</sup> mice were grown for 48 hours in matrigel in the presence or absence of draxin (10nM). For quantification, the length of the longest neurite from each explant was measured. The length of the longest neurite is a simple and sensitive parameter in determining the maximum neurite length that can be attained in the absence or presence of a given guidance cue (Islam, Shinmyo et al. 2009). Draxin inhibited neurite outgrowth significantly in wild-type cortical explants whereas MAP1B<sup>-/-</sup> neurons remained

insensitive to draxin (Fig. 16A and 16B). Additionally, I used another well-characterized repulsive guidance cue: Sema3A, to test whether this role of MAP1B is specific to draxin. I obtained similar results to the draxin. Hence our data suggests that MAP1B is a key component necessary for chemo-repulsion induced by guidance molecules.

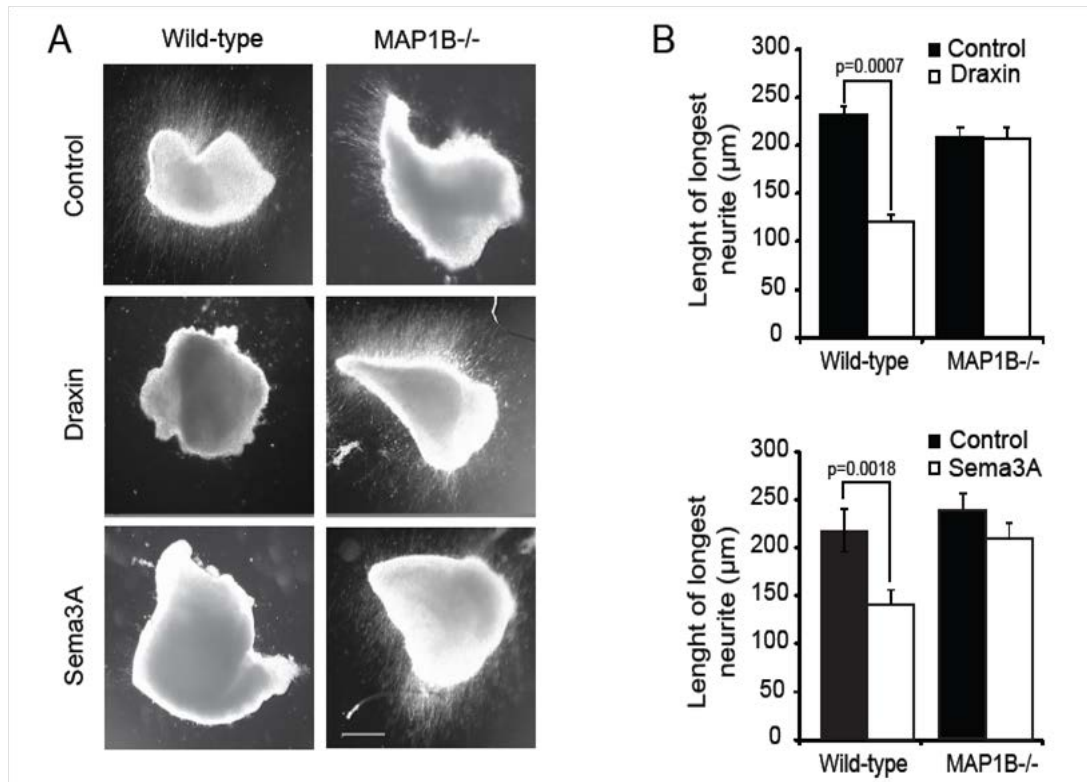


**Figure 16:** MAP1B is required for draxin- and sema 3A-induced neurite outgrowth inhibition. A. Cortical explants from newborn wild-type or MAP1B<sup>-/-</sup> mice, cultured for 48 hours in the presence or absence (control) of 10 nM draxin or 100 ng/ml of sema3A. Scale bar = 100 μm. B. Quantification of the longest neurites of 30 explants in each of 3 independent experiments. Data represented in mean ±SEM. p-values are indicated.

### 2.3 Draxin inhibits neurite outgrowth in dissociated cortical neurons.

To investigate the effect of draxin on individual neurons, I established a dissociated cortical neuron culture. Trypsin dissociated cortical neurons were grown on poly-l-

lysine (PLL) and laminin coated coverslips in the presence and absence of draxin conditioned medium. After 48 hours in the culture the neurons were fixed and quantified. For quantification, random pictures were taken from the coverslips. From each picture, the percentage of neurons in non-polarized stage, stage II and stage III (polarized) stage (refer Fig. 3 for neuron stages) were calculated.

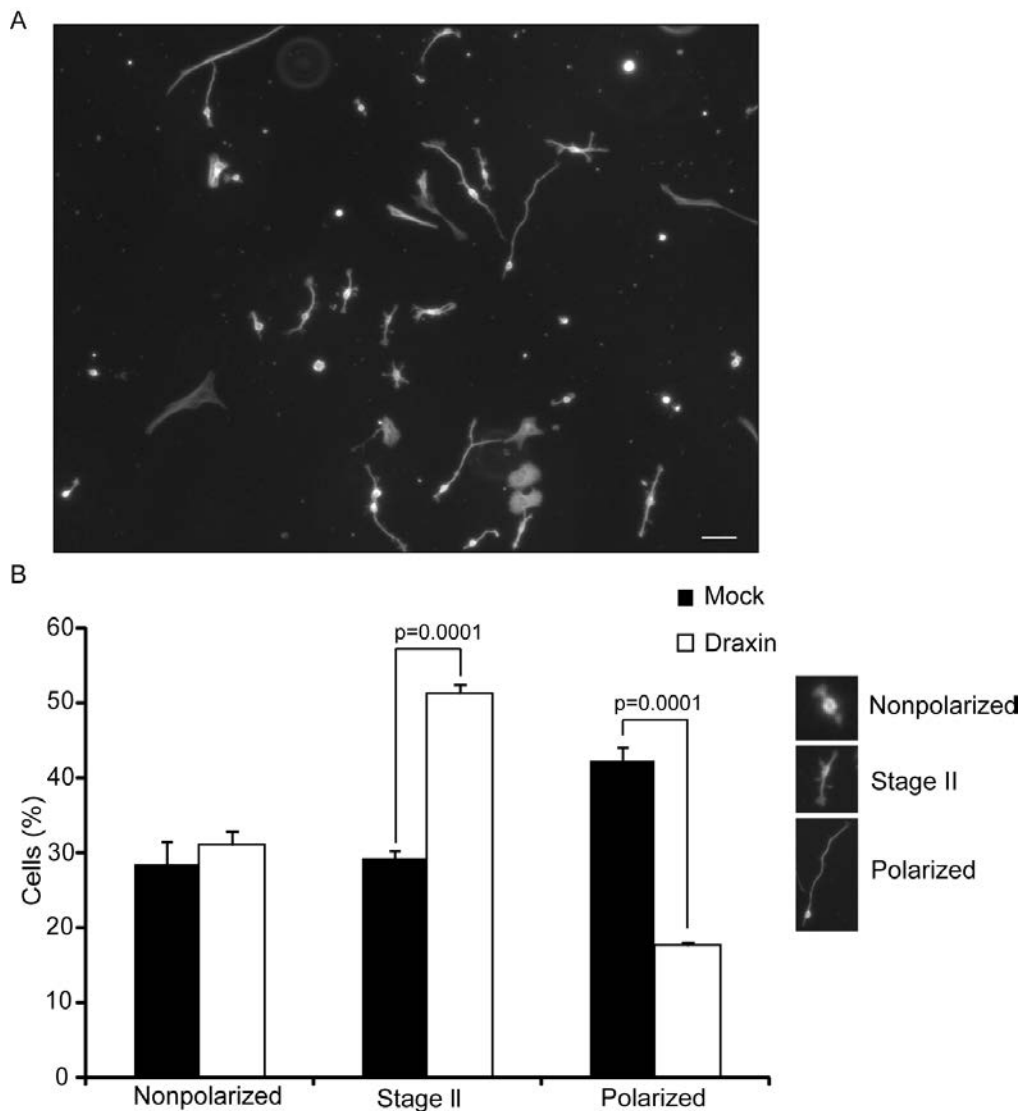


**Figure 17:** Draxin significantly reduced the percentage of polarized neurons in the cultures. A. A representative picture showing neurons growing in conditioned medium. Scale bar 100 $\mu$ m. B. Neurons growing in mock conditioned medium passed the stage II normally to reach the polarized stage after 48 hours in culture. In contrast, large

number of neurons remained in stage II in presence of draxin conditioned medium and a very small percentage of neurons entered the polarized stage. Quantification from two independent experiments in each 120 neurons measured. Values are shown in mean  $\pm$  SEM. p-values are indicated.

#### **2.4 Establishment of growth cone collapse assay.**

Growth cone collapse assay is a reliable method to identify and study the signaling mechanism of repulsive guidance cues. The assay uses the morphology of the growth cone as a readout to test the effects of various guidance cues. In neuronal cultures, locally applied repulsive guidance cues induce growth cone turning, hence avoiding the repellent stimulus. In contrast, bath application results in the loss of out spread morphology of the growth cone, leading to the transitory paralysis. To investigate the signaling mechanism of draxin, I established growth cone collapse. In growth cone collapse assay neurons were fixed after being treated with repulsive cues for various time points and were then quantified. Quantifications were carried out as mentioned in Kapfhammer et al in 2007 (Kapfhammer, Xu et al. 2007).

##### Results and quantitative evaluation

1. Basal level collapse of growth cones in culture conditions: we observed typically around 10-30% of collapse in cortical neurons in untreated or control conditions. This suggests that a proportion of growth cones naturally undergo collapse, which was considered the basal collapse.
2. Partial collapse and no collapse: Poor addition of collapsing inducing material lead to the partial collapse of growth cones. Sometimes poor fixation also

resulted in partial collapse. The concentration of collapsing inducing material was decided based on the percentage of collapse induced. Ideal concentration of the collapse inducing material should induce 60-85% of collapse.

3. Complete collapse of growth cones: Neurons showed complete absence of growth cones when the neurons were disturbed or kept outside the incubator for too long. Complete collapse of growth cones was also observed when the seeding density of neurons was too low.
4. Smaller growth cones: smaller growth cones were the result of uneven coating or poor substrate binding on plates. Laminin, being the most critical substrate, needs to be uniformly coated and should not be dry while seeding neurons.

#### Readouts

1. For quantification, only growth cones which are not in contact with other cells were considered.
2. Growth cones in a stage of filopodial thickening along with lamellar disintegration were scored as collapsed.

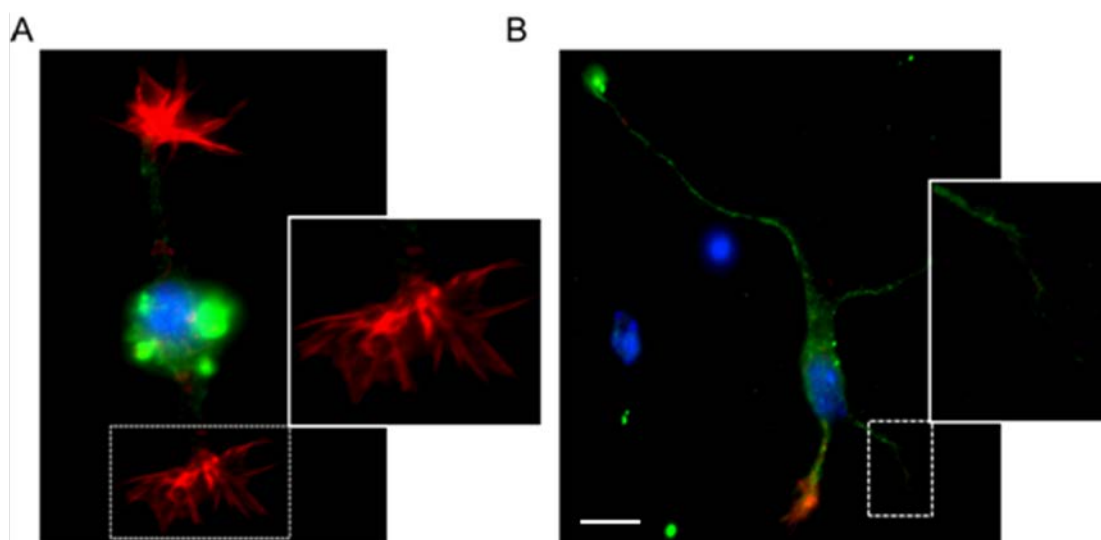




**Figure 18:** A representative picture showing extended and collapsed morphology of growth cones in cortical neuron culture. Cortical neurons fixed and stained for actin and  $\beta$ -III tubulin after 48 hour in culture. Neuron with extended (A) and collapsed growth cones (B). Insets show the magnified growth cone. Scale bar 10 $\mu$ m.

## **2.5 Draxin-induced growth cone collapses are suppressed in MAP1B deficient neurons.**

To investigate the acute effect of draxin on growth cone morphology, we performed growth cone collapse assays using dissociated cortical neuron cultures from newborn mice. Draxin induced growth cone collapse in over 70% of wild-type neurons, whereas in MAP1B<sup>-/-</sup> neurons the draxin effect was not significant (Fig. 19A and 19B). Growth cone collapse in wild-type neurons was apparent after 60 minutes of draxin incubation, consistent with previous results (Ahmed, Shinmyo et al. 2011). These outcomes suggest that draxin-induced attenuation of neurite outgrowth and growth cone collapses are mediated by MAP1B.

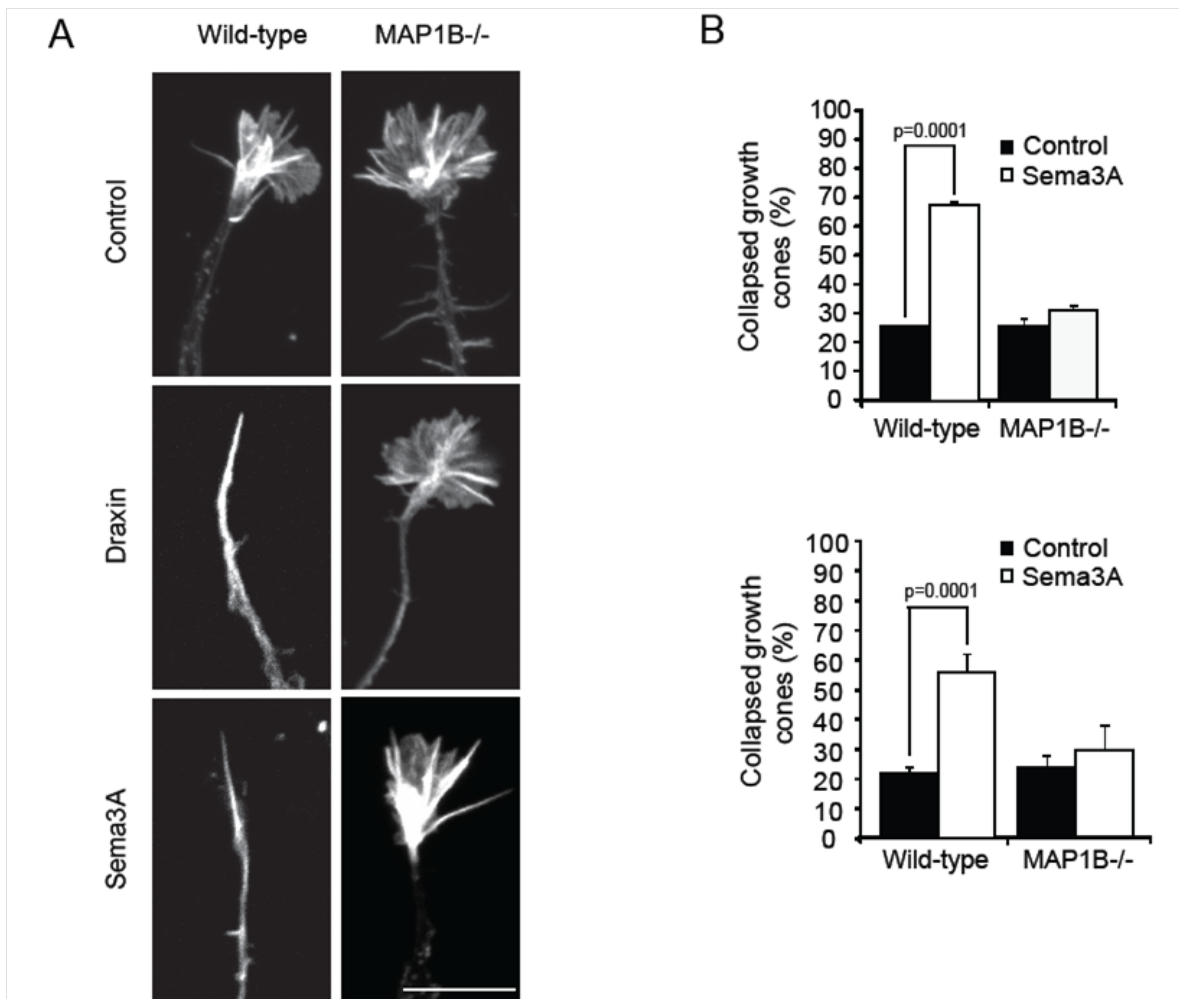


**Figure 19:** MAP1B is required for draxin and sema 3A-induced growth cone collapse. A. Growth cones of cortical neurons from newborn wild-type or MAP1B<sup>-/-</sup> mice cultured for 60 h, treated for 1 hour with 100 nM draxin or 30 minutes with 100 ng/ml sema 3A, fixed and stained for F-actin. Scale bar = 10  $\mu$ m. B. Percentage of collapsed growth cones. For each experimental condition the growth cones of 30 neurons in each of 3 independent experiments were evaluated. Data represented in mean $\pm$ SEM. *p*-value indicated.

## **2.6 Draxin increases MAP1B phosphorylation at a GSK-3 $\beta$ -dependent phosphorylation site**

MAP1B is subject to posttranslational modification by several serine/threonine kinases including GSK-3 $\beta$ , which phosphorylates MAP1B at Ser1260 and Thr1265 (Trivedi, Marsh et al. 2005). Phosphorylated MAP1B at these sites bind along tyrosinated microtubules and maintain a pool of dynamic microtubules (Goold et al., 1999). To test whether draxin induces phosphorylation of MAP1B at this site, cortical neurons from new-born mice were cultured for 2 days and were treated with draxin at different time points. The soluble-cell extracts were analyzed for the level of mode I phosphorylation using a monoclonal antibody which recognizes specifically the Ser1260/Thr1265 epitope in its phosphorylated form (Trivedi, Marsh et al. 2005). Draxin treatment elevated the level of MAP1B phosphorylation after 30 minutes of treatment whereas total MAP1B levels remained unchanged (Fig. 20A and 20B). To further identify that this increase in MAP1B phosphorylation was dependent on GSK-3 activity we used SB216763, a specific inhibitor of GSK-3. Treatment of GSK-3 inhibitor significantly decreased the phosphorylation level induced from draxin. Together, these results show that draxin treatment of cortical neurons causes a rapid GSK-3-dependent increase in MAP1B phosphorylation, which correlated with a time scale comparable to draxin induction of growth cone collapse.

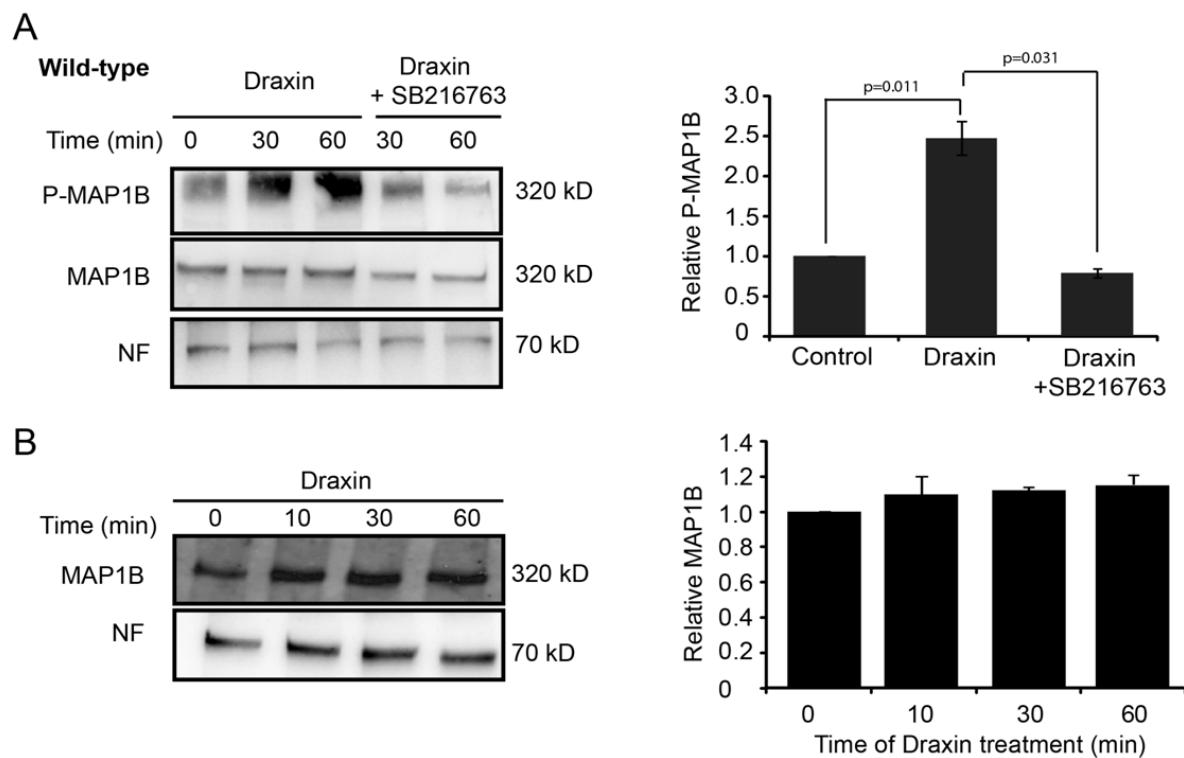


**Figure 20:** Draxin treatment increases the levels of GSK-3 $\beta$ -dependent phosphorylation of MAP1B on Ser1260. Immunoblot analyses of cortical neurons from newborn wild-type mice cultured for 60 h, treated with draxin in the absence or presence of the GSK-3 $\beta$  inhibitor SB216763 for the indicated times, lysed and probed using the indicated antibodies. A. The relative level of phosphorylated MAP1B (P-MAP1B) was determined by normalizing the P-MAP1B signal to the signal for total MAP1B. B. The relative level of MAP1B was determined by normalizing the MAP1B signal to the signal for neurofilament H in 3 independent experiments. Draxin treatment did not lead to a significant change in MAP1B levels. p-values indicated.

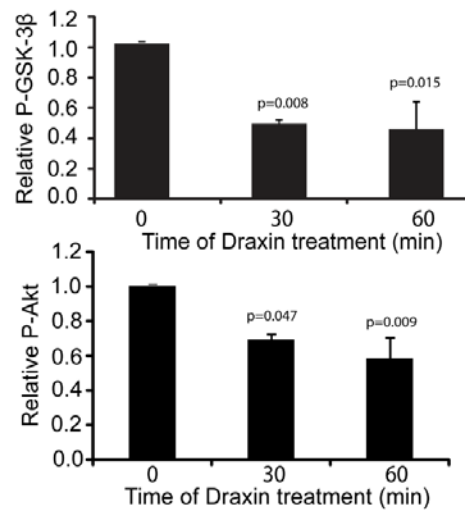
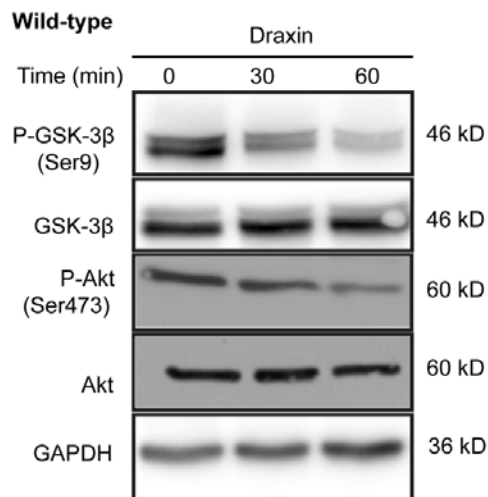
## 2.7 Draxin signaling involves activation of GSK-3 $\beta$ and inhibition of Akt

The increase in the phospho MAP1B immunoreactivity after draxin treatment indicated that draxin induced activation of GSK-3 is responsible for the increase in MAP1B phosphorylation. To test this possibility we treated cortical neurons with draxin and

analyzed phosphorylation of GSK-3 $\beta$  on Serine9 (Ser9) draxin. The treatments substantially reduced the Ser9 phosphorylation on GSK-3 $\beta$ , whereas total GSK-3 levels remained unchanged (Fig. 21A). As GSK-3 activity is negatively regulated by Ser9 phosphorylation, (Saito, Kidd et al. 1994; Cross, Alessi et al. 1995) the decrease in phosphorylation implies an increase in activity in response to draxin. This data suggests that draxin activates GSK-3. A similar activation of GSK-3 $\beta$  by draxin was observed in MAP1B $^{-/-}$  neurons, indicating that draxin signaling upstream of GSK-3 $\beta$  is not perturbed by lack of MAP1B (Fig. 21B). However, a more pronounced activation of GSK-3 $\beta$  in wild-type neurons was observed compared to MAP1B $^{-/-}$  neurons. This comparison suggests that MAP1B is required for the activation of GSK-3 upon draxin induction.

In axon growth, GSK-3 $\beta$  is a major downstream effector of PI3K and Akt where Akt negatively regulates GSK-3 $\beta$  by phosphorylating it on Ser9 (Saito, Vandenheede et al. 1994; Cross, Alessi et al. 1995). Thus, our finding that GSK-3 $\beta$  is activated and dephosphorylated at Ser9 in response to draxin could be the consequence of concomitant inactivation of Akt. To test this hypothesis I analyzed the level of Akt phosphorylated on Ser473, a marker for active Akt (Alessi, Andjelkovic et al. 1996). Draxin treatment of cortical neurons resulted in a decrease of Akt phosphorylation at the Ser473 site (Fig. 21A), indicating that draxin signaling inhibited Akt, while the total levels of Akt remained unaffected. Together our data suggest that draxin treatment leads to inhibition of the PI3K/Akt pathway, resulting in activation of GSK-3 $\beta$  and an increase in the level of MAP1B phosphorylation.

A



B

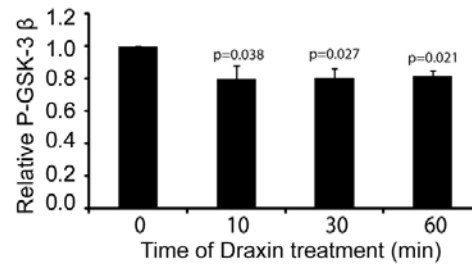
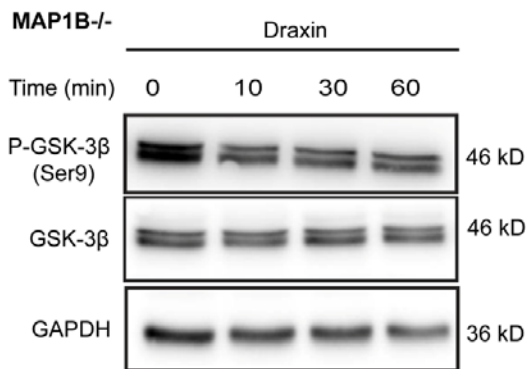


**Figure 21:** Draxin (100nM) treatment of cortical neurons inhibits Akt activity and activates GSK-3 $\beta$ . A. Immunoblot analyses of cortical neurons from newborn wild-type or B. MAP1B<sup>-/-</sup> mice. Neurons cultured for 60 hours, treated with draxin for the indicated times (min), lysed and probed using the indicated antibodies. The GSK-3 $\beta$  doublets in the blot represent the GSK-3 $\beta$ 1 and GSK-3 $\beta$ 2 isoform. The relative levels of GSK-3 $\beta$  phosphorylated at Ser9 (P-GSK-3 $\beta$ ) and Akt phosphorylated on Ser473 (P-Akt) were determined by normalizing the signals for the phosphorylated proteins to the corresponding signals for the total proteins in 3 independent experiments. Data represented in mean $\pm$ SEM. p- values are indicated.

Additionally, we checked the GSK-3 $\beta$  kinase activity using 10nM of draxin to rule out that different concentrations of draxin trigger different signaling pathways (Richard P.C Mannes et al., 2012). Our results showed a similar tendency in the activation of GSK-3 $\beta$  kinases (Fig. 22A and 22B).

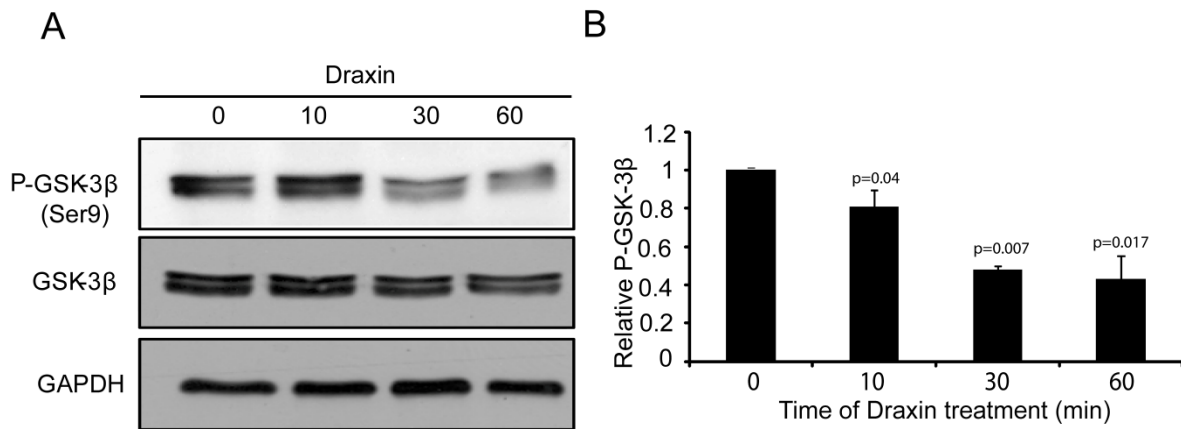


**Figure 22:** Draxin (10nM) treatment of cortical neurons activates GSK-3 $\beta$ . A. Immunoblot analyses of cortical neurons from newborn wild-type. Neurons were cultured for 60 hours, treated with draxin for the indicated times (min), lysed and probed using the indicated antibodies. The GSK-3 $\beta$  doublets in the blot represent the GSK-3 $\beta$ 1 and GSK-3 $\beta$ 2 isoform. The relative levels of GSK-3 $\beta$  phosphorylated at Ser 9 (P-GSK-3 $\beta$ ) were determined by normalizing the signals for the phosphorylated proteins to the corresponding signals for the total proteins in 3 independent experiments.

## 2.8 Involvement of GSK-3 $\beta$ and Akt pathway in draxin-induced growth cone collapse

To test whether activation of GSK-3 $\beta$  is necessary for draxin-induced growth cone collapse we analyzed the effect of draxin in the presence of the specific GSK-3 inhibitor

SB216763. Cortical neurons were pre-treated with SB216763 before draxin application. Treatment with SB216763 had no effect on its own, but completely blocked the draxin induced growth cone collapse (Fig. 23A and 23B). Additionally, the percentage of growth cone collapse in axons alone was also calculated (Fig 23D). These results demonstrate that activation of GSK-3 $\beta$  is necessary for the biological activity of draxin. Immunoblotting consistently revealed that treatment with draxin induces a substantial reduction in serine 9 phosphorylation (Fig. 21A). This activation was not evident when LiCl (20mM), a GSK-3 $\beta$  antagonist, was included in the cultures (Fig 23F and 23G).



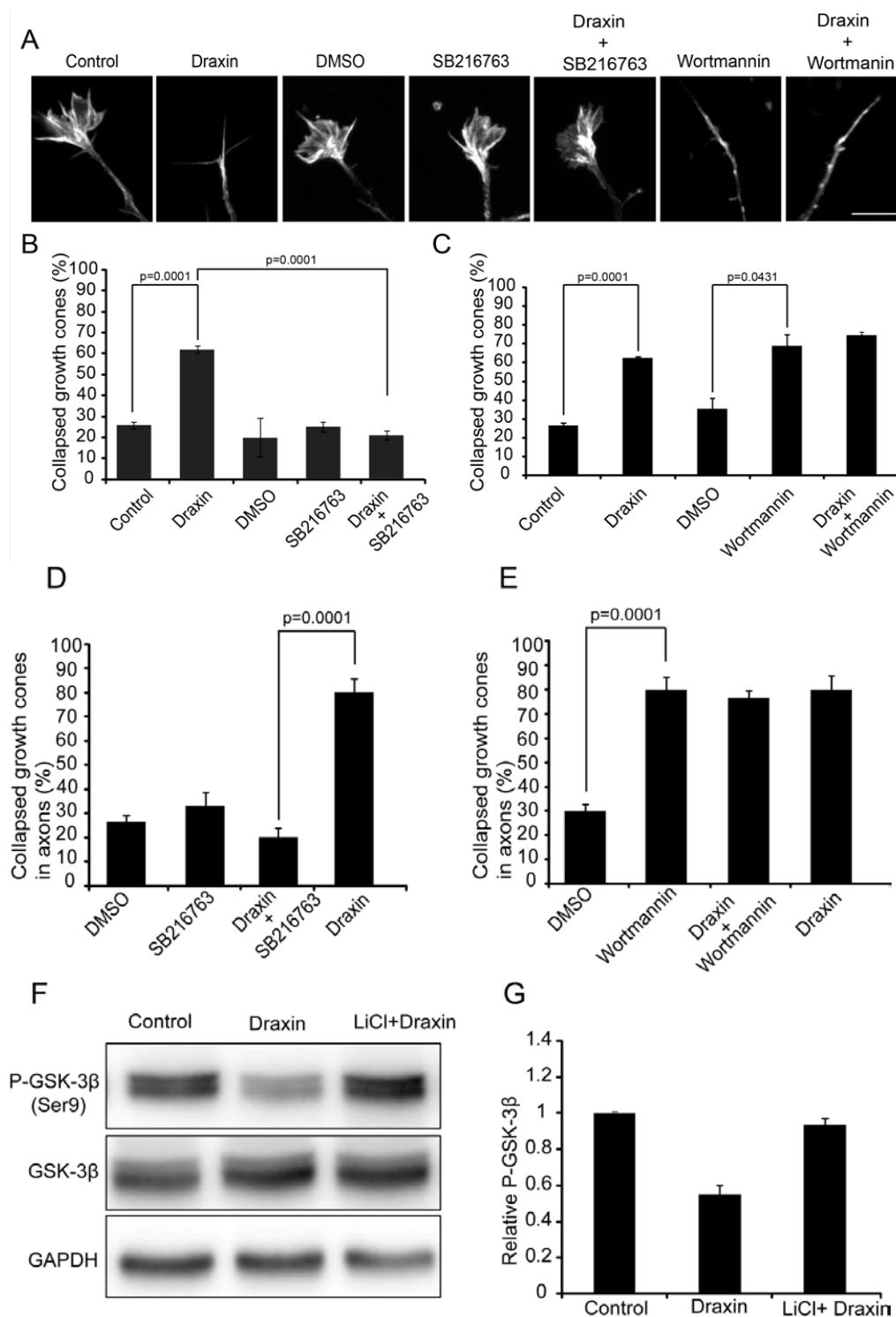


**Figure 23:** Draxin-induced growth cone collapse is dependent on GSK-3 $\beta$  activity and mimicked by inhibition of the PI3K. **A.** Growth cones of cortical neurons from newborn wild-type mice cultured for 60 h, pre-treated with solvent (DMSO) or the GSK-3 $\beta$  inhibitor SB216763 or the PI3K inhibitor wortmannin for 1 h followed by addition of draxin for 1 h as indicated. Cells were fixed and stained for F-actin. Scale bar = 10  $\mu$ m. **B**

and C. Quantification of growth cone collapse in neurites. D and E. Quantification of growth cone collapse in axons. F. Treatment with the GSK-3 inhibitor LiCl enhances GSK-3 $\beta$  phosphorylation and antagonizes the draxin-mediated decrease in Ser9 phosphorylation. For each experimental condition the growth cones of 40 neurons in each of 3 independent experiments were evaluated. Data represented in mean  $\pm$ SEM. p-values are indicated.

## **2.9 Draxin-induced growth cone collapse is dependent on activation of GSK-3 $\beta$ and inhibition of Akt.**

The phosphatidylinositol (PI) 3-kinase inactivates GSK-3 by stimulating Akt-dependent phosphorylation of Ser 21 and/or Ser 9 (Cross et al., 1995). Studies show that treatment with PI3K inhibitors (wortmannin and LY294002) induces a dramatic reduction in the phosphorylation of GSK-3 $\alpha$  on Ser21 and GSK-3 $\beta$  on Ser9 (Britta Eichholtz 2002) demonstrating that PI3K activity is required for inactivating GSK-3 in the growth cones of neurons. The western blot data in fig 10 show that draxin application reduces the Akt activity in cortical neurons which could be a consequence of inhibition of the Akt activator PI 3kinase.

To explore the relevance of Akt inhibition for growth cone collapse, wortmannin, an inhibitor of PI3K was used. Inhibition of PI3K on its own resulted in growth cone collapse, mimicking the effect of draxin. Wortmannin induced growth cone collapse in cortical neurons to about the same extent as draxin. Simultaneous treatment with draxin and wortmannin had no additional effect (Fig. 23C and 23E).

I further analyzed the necessity of the inhibition of Akt in draxin signaling. To test this hypothesis, cortical neurons were co-transfected with expression construct encoding GFP and ectopically expressing constitutively active Akt construct (Akt-CA) or dominant negative (Akt-DN) Akt. Cells co-transfected with the GFP construct and empty vector served as controls. Neurons were grown for 24-26 hours, stimulated with draxin and analyzed for growth cone collapse. Draxin failed to induce growth cone collapse in neurons expressing constitutively active Akt (Fig. 24A and 24B). Whereas cells expressing Akt-DN constructs displayed increased growth cone collapse even in the absence of draxin (24A and 24B). These results demonstrate that inhibition of the PI3K/Akt pathway is a critical step in draxin signaling. In parallel, the Akt-CA and Akt-DN constructs expression were analyzed from transfected cell lysates by immunoblotting using total and phosphor-specific (Ser473) Akt antibodies. The results confirmed the high level expression of total Akt proteins in the case of Akt-CA and Akt-DN compared to control lysates, whereas phosphor-specific (Ser473) Akt expression was significantly reduced in Akt-DN lysates (Fig. 24C).

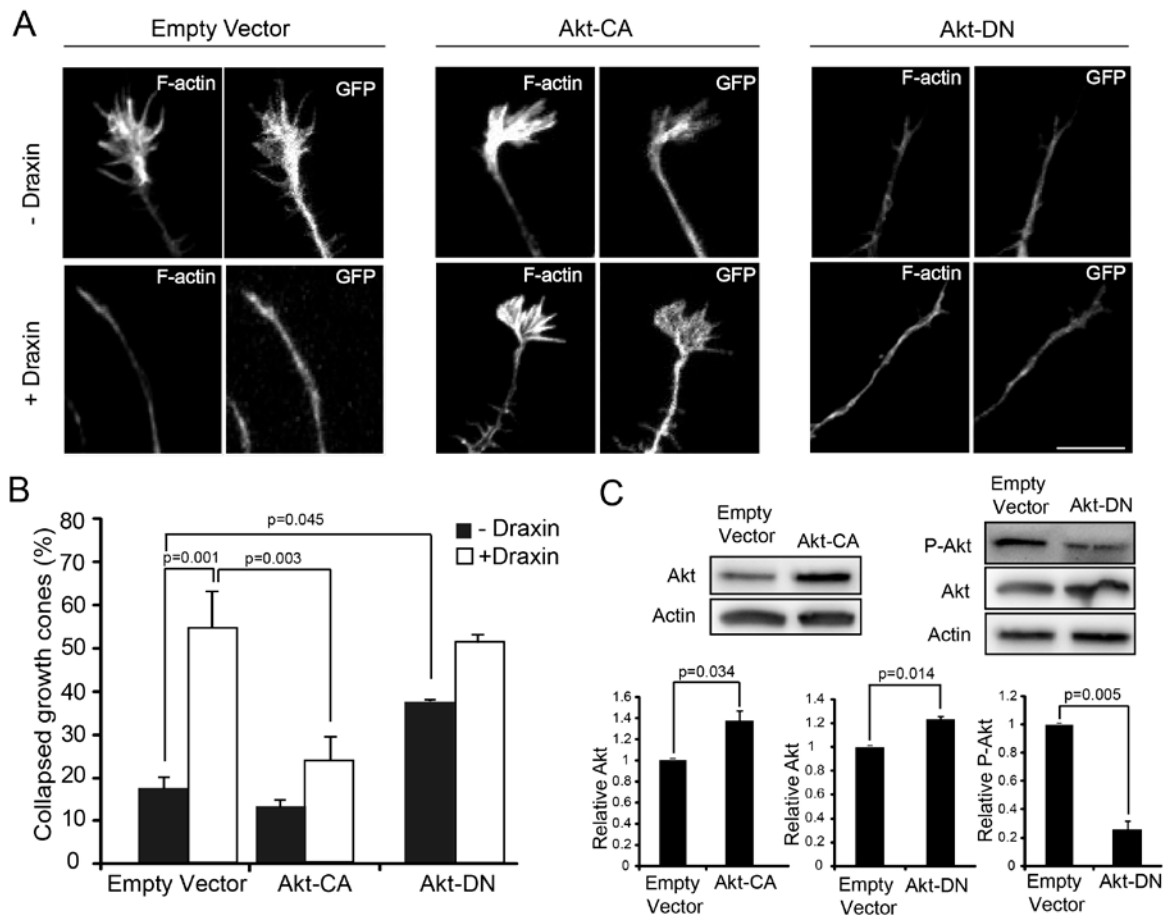


**Figure 24:** Draxin-induced growth cone collapse is prevented by constitutively active Akt. **A.** Growth cones of cortical neurons from newborn wild-type mice co-transfected with constructs encoding GFP and constitutively active (Akt-CA) or dominant negative (Akt-DN) Akt, cultured for 26 h and treated with or without draxin for 1 h as indicated. Cells were fixed and stained for F-actin. Scale bar = 10  $\mu$ m. **B.** Quantification of growth cone collapse. For each experimental condition the growth cones of 40 neurons in each of 3 independent experiments were evaluated. **C.** Expression level of Akt mutants were determined immunoblot using the indicated antibodies. For overexpression, the relative level of Akt was determined by normalizing the total Akt signal to the signal for actin. The effect of expressing Akt-DN was also seen as a suppression of active P-Akt relative to total Akt. The data represent results obtained in 2 independent experiments. Data represented in mean $\pm$ SEM. p-values are indicated.

## **2.10 Draxin-induced growth cone collapse is mediated by DCC receptor**

Draxin has been shown to exert its effects on axon growth through the netrin receptor DCC (Ahmed, Shinmyo et al. 2011). To test whether draxin-induced growth cone collapse of cortical neurons is mediated through DCC receptor I pretreated cortical neurons with a function blocking anti-DCC antibody (de la Torre, Hopker et al. 1997) or control antibodies prior to exposure to draxin. Pretreatment with low concentrations of anti-DCC antibody blocked the induction of growth cone collapse by draxin, while the control antibody had no effect (Fig. 25A and 25B).

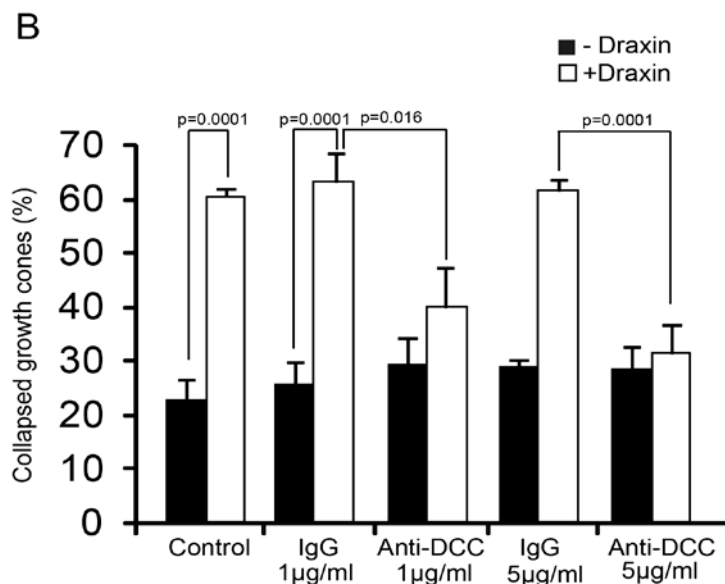
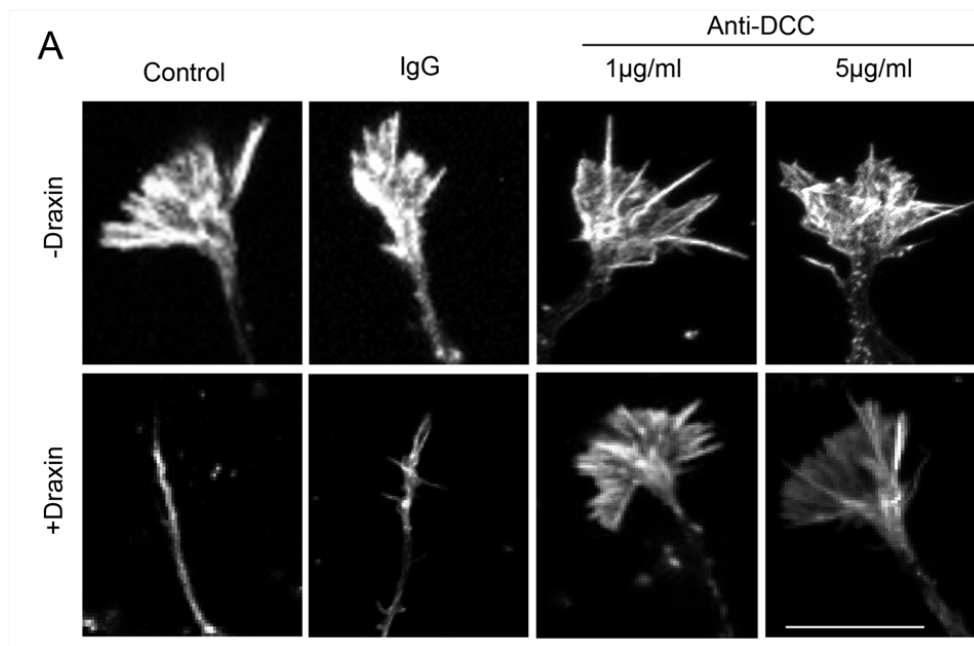


**Figure 25:** Draxin-induced growth cone collapse is mediated through DCC. A. Growth cones of cortical neurons from newborn mice cultured for 60 hours, pretreated for 1 hour with function blocking anti-DCC antibodies (anti-DCC) or unrelated IgGs at the indicated concentrations followed by addition of draxin for 1 h as indicated, fixation and staining for F-actin. Scale bar = 10  $\mu$ m. B. Quantification of growth cone collapse. For each experimental condition the growth cones of 40 neurons in each of 3 independent experiments were evaluate. Data represented in mean $\pm$ SEM. p-values are indicated.

# Part I

---

## Discussion

### 3 DISCUSSION

Draxin, a recently known novel chemo-repulsive guidance cue has garnered significant interest in the development of the central nervous system, in particular the formation of the corpus callosum (Islam, Shinmyo et al. 2009; Naser, Su et al. 2009; Ahmed, Shinmyo et al. 2011). However, the signaling cascade involved in draxin induced growth cone collapse and neurite outgrowth inhibition has not been reported; so far, our results demonstrate that draxin induces growth cone collapse through interaction with DCC, inhibition of the PI3K/Akt signaling pathway and activation GSK-3 $\beta$ . GSK-3 $\beta$  increases the level of MAP1B phosphorylation on Ser1260, a GSK-3 $\beta$  target site (Trivedi, Marsh et al. 2005). In our study we show that GSK-3 activity and MAP1B are necessary to convey the draxin signal. Thus, our study links draxin, DCC and MAP1B. This might explain why deletion of any of the three genes leads to developmental defects in the formation of the corpus callosum (Fazeli, Dickinson et al. 1997; Meixner, Haverkamp et al. 2000; Islam, Shinmyo et al. 2009).

The role of the PI3K/Akt pathway is well established in neuronal morphogenesis and neuronal migration (Waite and Eickholt 2010). For example, NGF induced activation of PI3K/Akt signaling has been implicated in axon elongation (Segal 2003). Conversely, growth cone collapse by repulsive guidance cues such as sema 3A, 3F and 4D and the growth inhibitory myelin component myelin-associated glycoprotein 1 have been correlated with downregulation of the PI3K/Akt signaling pathway (Atwal, Singh et al. 2003; Chadborn, Ahmed et al. 2006; Oinuma, Ito et al. 2010; Henle, Carlstrom et al. 2013). The inhibition of PI3K is also linked with neurite retraction (Sanchez, Sayas et al. 2001). Akt activity is the crucial output, which is directly linked to the level of PIP<sub>3</sub> in the plasma membrane, which is regulated by PI3K. The PI3K pathway is negatively regulated by PTEN phosphatase. (von Philipsborn and Bastmeyer 2007; Kölsch, Charest



et al. 2008). The downregulation or the inhibition of the PI3K/Akt pathway mimics draxin-induced growth cone collapse, extending previous studies with dorsal root ganglia explants (Edstrom and Ekstrom 2003) and neuroblastoma (N2a) cells (Sanchez, Sayas et al. 2001). These findings emphasize the importance of downregulation of the PI3K/Akt pathway for growth cone collapse and neurite retraction, but they do not show that draxin inhibits PI3K. An alternative pathway would be that draxin activates PTEN. Indeed, this pathway has been implicated in the induction of growth cone collapse by semaphorins 3A and 4D and the growth inhibitory myelin component myelin-associated glycoprotein 1 (Chadborn, Ahmed et al. 2006; Oinuma, Ito et al. 2010; Henle, Carlstrom et al. 2013).

DCC has been linked to PI3K/Akt signaling in *Xenopus laevis* spinal neurons (Ming, Song et al. 1999) and in *Caenorhabditis elegans* motor neurons (Adler, Fetter et al. 2006). However, in both of these paradigms netrin-1 binding to DCC leads to activation of the PI3K/Akt pathway, while draxin reduces Akt activity (Fig. 21A). One possible explanation would be that draxin binding to DCC may also recruit the UNC5 receptor, which is involved in the repulsive activity. Further, it would be of great interest to understand the molecular details of the link between DCC and the PI3K/Akt pathway.

MAP1B is essential for axon guidance by cues as diverse as reelin, netrin 1, lysophosphatidic acid and nitric oxide (Del Rio, Gonzalez-Billault et al. 2004; Gonzalez-Billault, Del Rio et al. 2005; Bouquet, Ravaille-Veron et al. 2007; Stroissnigg, Trančíková et al. 2007). The current study show that two additional chemo-repulsive cues, draxin and sema 3A, depend on MAP1B to exert their effects. In the model (Fig. 26) MAP1B is depicted in its canonical function as a microtubule regulator downstream of GSK-3 $\beta$ .

However, one cannot exclude the fact that MAP1B also impacts on GSK-3 $\beta$ , since I observed a decrease activity of GSK-3 $\beta$  in response to draxin in MAP1B<sup>-/-</sup> neurons in comparison with the wild-type neurons (Fig. 21B). Further studies will be needed to explore this interesting possibility (Villarroel-Campos and Gonzalez-Billault 2014).

Remarkably, both attractive (netrin-1) and repulsive (draxin) guidance cues trigger phosphorylation of MAP1B and activation of GSK-3 $\beta$ . The possible reason could be the recruitment of different receptors complexes. This modification by itself does not change MAP1B interaction with microtubules (Goold, Owen et al. 1999), but correlates with changes in microtubule stability (Lucas, Goold et al. 1998; Goold, Owen et al. 1999; Kawauchi, Chihama et al. 2003). Together, these results suggest that MAP1B phosphorylation on Ser1260, although a critical event in growth cone response is not involved in determining the outcome (growth cone collapse versus axon extension). Instead, it appears that MAP1B is a key component of a general pathway involved in linking attractive as well as repulsive guidance cue signals to the cytoskeleton. This notion could be very well addressed in the light of recent study, which emphasizes the new roles of MAP1B as a signaling molecule involved in normal physiology.

The crucial role of GSK-3 $\beta$  in repulsive axon guidance has previously been characterized for sema 3A (Eickholt, Walsh et al. 2002). Active GSK-3 $\beta$  targets in this respect are CRMP-2 (Fukata, Itoh et al. 2002; Brown, Jacobs et al. 2004; Uchida, Ohshima et al. 2005; Yoshimura, Kawano et al. 2005) and CLASP (Hur, Saijilafu et al. 2011), two proteins that regulate microtubules dynamics. I show here that growth cone response to sema 3A and to draxin is also critically dependent on MAP1B. Thus, my results identify a third essential GSK-3 $\beta$ -dependent pathway that impacts on microtubules. Together,

these findings demonstrate that GSK-3 $\beta$  regulates microtubules by a multipronged mechanism involving the phosphorylation of at least three microtubule regulators, further emphasizing that the precise regulation of microtubule dynamics is a key determinant in growth cone guidance.

### 3.1 Model of draxin signaling

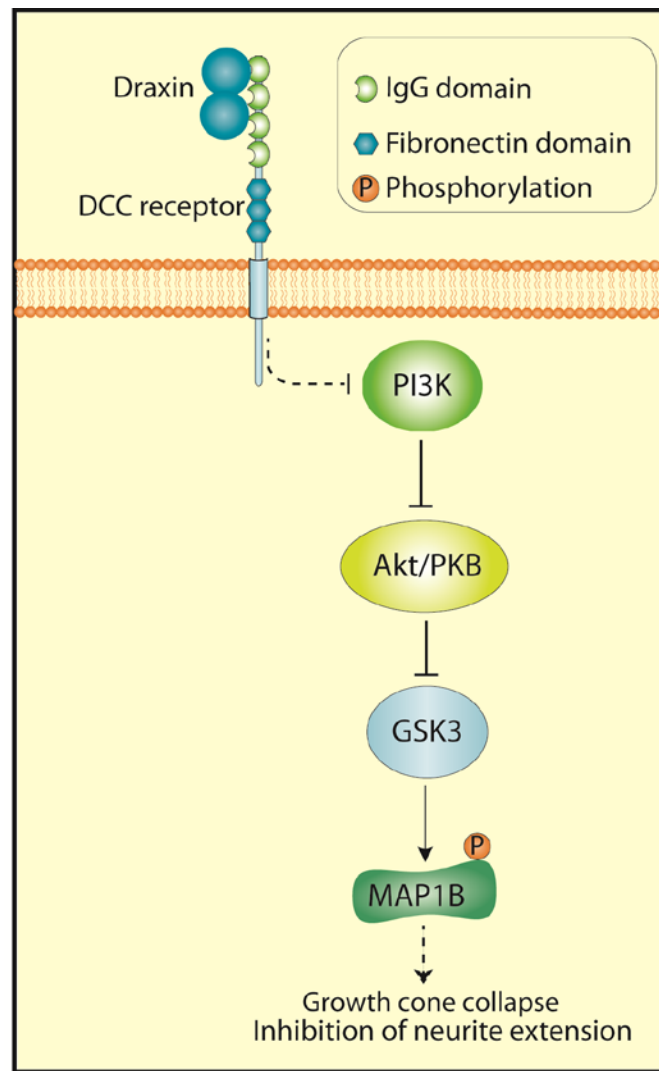


**Figure 26:** A model for repulsive draxin signaling. Draxin interaction with DCC triggers inactivation of the Akt pathway. This relieves GSK-3 $\beta$  from Akt-mediated inhibition leading to an increase in phosphorylation of MAP1B and reconfiguration of the cytoskeleton to promote growth cone collapse and inhibition of neurite extension.

# Part II

---

## Introduction

## **4. INTRODUCTION**

### **4.1 Nitric oxide and its signaling**

Nitric oxide (NO) is a multifunctional, gaseous signaling molecule involved in maintaining physiological processes including host defense, neuronal communication and the regulation of vascular tone reviewed in (Bryan, Bian et al. 2009). NO is produced by a family of enzymes named as nitric oxide synthases (NOS). There are four members in the NOS family: neuronal NOS (nNOS), endothelial NOS (eNOS), inducible NOS (iNOS) and mitochondrial NOS (mtNOS). All the members of the NOS share about 50 to 60% sequence homology (Lamas, Marsden et al. 1992). In mammals, nNOS and eNOS are constitutively expressed in cells and are Ca<sup>2+</sup>-calmodulin-dependent enzymes. In contrast, iNOS is Ca<sup>2+</sup>-calmodulin independent and is dependent on de novo synthesis. Inflammatory stimulation in macrophages, astrocytes, microglia and other cells leads to the activation of iNOS and production of high amounts of NO. All the NOS isoforms comprise four prosthetic groups: flavin adenine mononucleotide (FMN), flavin adenine dinucleotide (FAD), iron protoporphyrin IX (heme) and tetrahydrobiopterin (BH<sub>4</sub>) (Fig. 27).

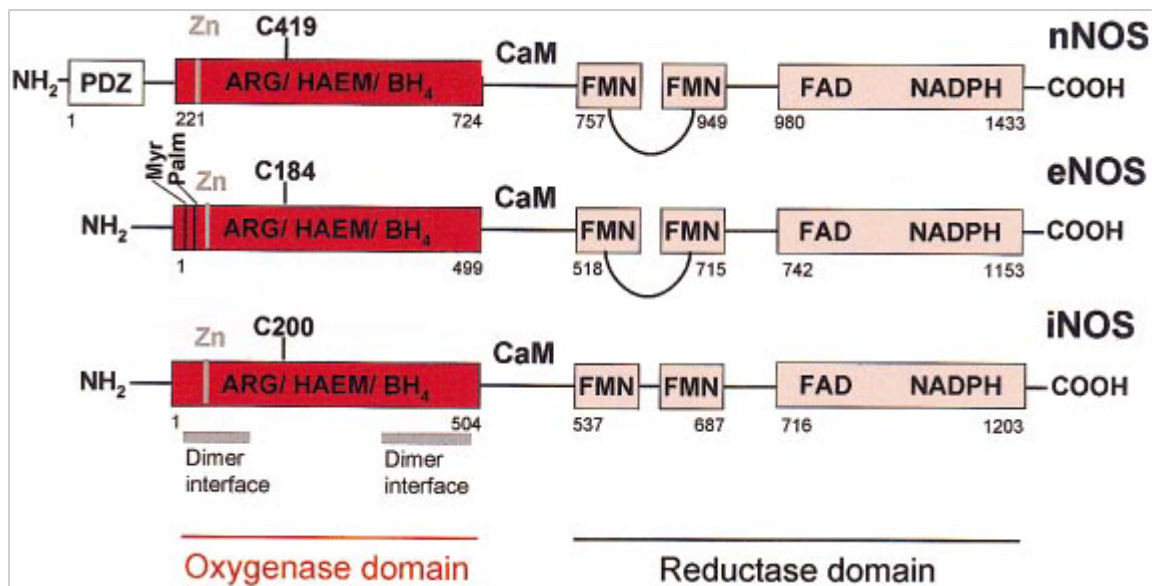


**Figure 27:** Structure of three nitric oxide synthase. All the synthases have an oxygenase domain and reductase domain. All NOSs have calmodulin (CaM) regions. The reductase domain consists of FAD and NADPH regions. Only nNOS has PDZ domain on the N-terminal (Alderton, Cooper et al. 2001).

Many of the physiological functions of NO are mediated through its primary receptor, soluble guanylyl cyclase (sGC). sGC is a heme-containing, heterodimeric NO receptor which can exert many physiological effects including maintaining fluid and electrolyte homeostasis, mediating smooth muscle tone and motility and phototransduction. To do this, Guanylyl cyclase enzyme catalyses the production of cyclic GMP (cGMP) which further acts directly with downstream effectors such as the family of cGMP-dependent protein kinases, cGMP-regulated phosphodiesterases and cyclic nucleotide-gated channels.

#### 4.1.1 Rho kinase

Rho-associated kinase (Rho-kinase) is as an effector of the small GTPase Rho (Leung, Manser et al. 1995) (Ishizaki, Maekawa et al. 1996) (Matsui, Amano et al. 1996),

involved in rearrangements of the actomyosin cytoskeleton. It belongs to AGC (Protein kinase A, G, C) family of proteins. The Rho-like small GTPases such as RhoA, Rac, and Cdc42 regulate cytoskeletal remodeling by binding to downstream effectors (Maekawa, Ishizaki et al. 1999) (Etienne-Manneville and Hall 2002). Rho regulates stress fiber formation, cell contraction and suppression of neurite outgrowth, whereas Rac and Cdc42 regulate the formation of lamellipodia and filopodia, respectively, and promote protrusive activities (Nakagawa, Fujisawa et al. 1996; Riento and Ridley 2003; Hall 2005). Rho family GTPases also modulate microtubule dynamics and cell polarity.

Two closely related kinases, Rho-associated coiled-coil serine/threonine kinase-1 (ROCK1) and -2 (ROCK2) have been identified as key downstream effectors of RhoA (Nakagawa, Fujisawa et al. 1996). ROCK1 and ROCK2 have distinct biological roles even though they share 92% amino acid sequence identity in their kinase domains (Lock and Hotchin 2009). Additionally, genetic deletion of ROCK2 is embryonically lethal and the loss cannot be compensated by ROCK1. They are ubiquitously expressed in most tissues; however, higher levels of ROCK1 are found in non-neuronal tissues including liver, lung and testis and ROCK2 are found in brain and muscles (Nakagawa, Fujisawa et al. 1996) (Leung, Chen et al. 1996).

ROCK1 and ROCK2 are composed of kinase domain on N-terminal, coiled-coil domain, Rho-binding domain, and PH domain. Myosin light chain 2 (MLC2) is a major substrate of ROCK, involved in the regulation of actomyosin contraction (Kureishi, Kobayashi et al. 1997) and the myosin-binding subunit of myosin phosphatase (MYPT) (Kawano, Fukata et al. 1999). ROCKs are inhibited by Y-27632 (Narumiya, Ishizaki et al. 2000), a compound that blocks microfilament bundles formation and contraction in cells reviewed in (Yoneda, Mulhaupt et al. 2005) (Davies, Reddy et al. 2000).



# Part II

---

## Results

## 5. RESULTS

### 5.1 NO induced myosin activation is ROCK dependent.

Myosin II is a major force necessary for growth cone motility. It regulates F-actin networks through depolymerization of actin (Medeiros, Burnette et al. 2006). The myosin II activity is regulated through spatial signaling by guidance cues, hence providing directional motility to the growth cones. A study suggests that Sema 3A treatment leads to redistribution of myosin IIB in growth cones (Brown, Wysolmerski et al. 2009). Genetic deletion or inhibition of myosin II activity blocks the retraction, suggesting that repulsive guidance cues require myosin II activity for their effects (Brown, Wysolmerski et al. 2009).

The aim of my second part of the study was to understand the role of acto-myosin in draxin mediated growth cone collapse. To do this, I started with an assay/system which was already established in the lab, where an interesting question was addressed: role of acto-myosin in NO mediated retraction in N2a cells.

Axon retraction requires the orchestrated regulation of F-actin and MTs can be induced by a variety of signaling molecules including NO. NO can induce axon retraction in vertebrate primary neurons (Hess, Patterson et al. 1993; Renteria and Constantine-Paton 1996; He, Yu et al. 2002). Interestingly, it has been shown that NO-induced axon retraction coincides with a change in the configuration of axonal microtubules to sinusoidal bundles (He, Yu et al. 2002). In addition, a role for F-actin in NO-induced axon retraction has been proposed but has never been demonstrated.

Recent insights suggest that NO-induced growth cone retractions are dependent on the presence of MAP1B (Stroissnigg, Trancikova et al. 2007). MAP1B is a target of S-

nitrosylation. Activation of neuronal nitric oxide synthase (nNOS) or extracellular application of an NO donor results in S-nitrosylation of the light chain 1 of MAP1B on cysteine 2457. This modification leads to a conformational change and increases MAP1B binding to microtubules. Mutational analysis showed that S-nitrosylation of MAP1B is essential for NO-induced axon retraction (Stroissnigg, Trancikova et al. 2007).

Since axon retraction induced by a number of repulsive axon guidance cues is crucially dependent on activation of acto-myosin contractility I asked the question whether NO, in addition to potentially modulating microtubule function through S-nitrosylation of MAP1B, also stimulates acto-myosin contractility. To this end I analyzed monophosphorylation of the myosin regulatory light chain (MLC) at Ser19 (phospho-MLC) as an indicator of myosin activity (Somlyo and Somlyo 2003). For this biochemical analysis N2a cells were used instead of primary DRG neurons, because the scarcity of the latter does not permit biochemical analysis. Similar to DRG neurons, N2a cells express MAP1B and display neurite retraction in response to nNOS activation or addition of the NO donor SNAP (Stroissnigg, Trancikova et al. 2007). Studies using ROCK and myosin inhibitors show that N2a cells can faithfully replicate neurite retraction observed in DRG neurons. The neurite retraction in N2a cells is dependent on ROCK and myosin, suggesting that the underlying mechanisms might be similar to those operating in DRG neurons. SNAP treatment of N2a cells enhanced monophosphorylation of MLC2, indicating that it increased acto-myosin contractility (Fig. 28). This SNAP-dependent increase in MLC phosphorylation was partially inhibited by the ROCK inhibitor Y27632, suggesting that ROCK is key to myosin activation in response to SNAP. In contrast, ML7, an inhibitor of myosin light chain kinase, did not have consistent effects on MLC

phosphorylation in SNAP treated N2a cells (not shown). Together, these results demonstrated that ROCK and myosin are necessary for axon retraction induced by NO.

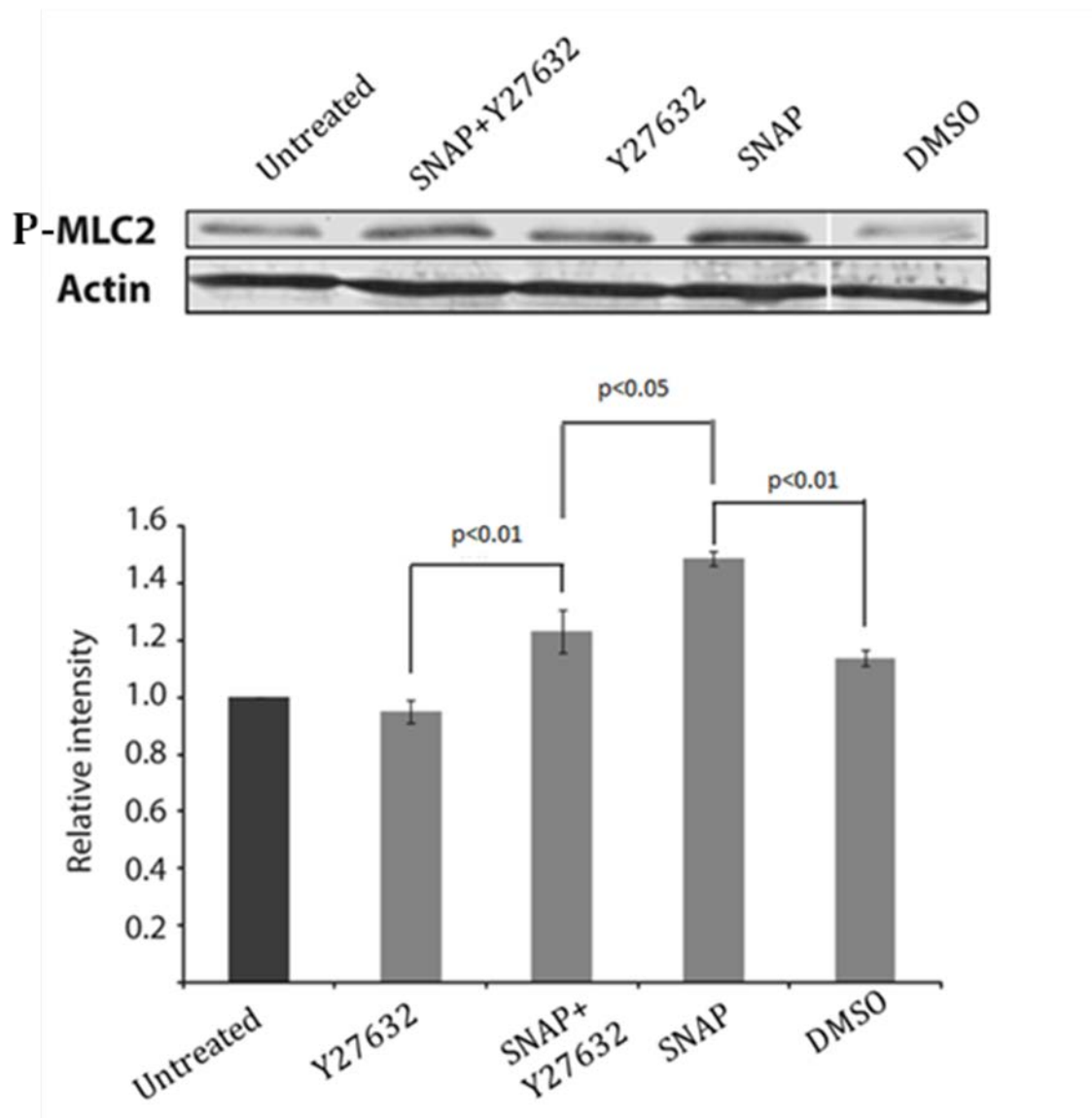


**Figure 28:** NO-induced myosin activation is ROCK dependent. Following treatment with SNAP and/or Y27632, N2a cells were lysed and analyzed by immunoblotting. Blots were incubated with anti-ser10 (phospho-MLC) or anti-actin antibodies. Blots were quantified using image J 1.44p software. The values show levels of phospho-MLC normalized to actin, which was used as a loading control. The level of phospho-MLC was expressed relative to the level of phospho-MLC detected in untreated cells. Bars are

# Part II

---

## Discussion

represented mean values  $\pm$  SD from 2 independent experiments. The p-values are indicated.

## **6. Discussion**

Axon guidance and retraction, F-actin and microtubules are believed to be key targets of guidance cue signaling. Both filament systems are highly dynamic and their dynamicity is critical for their function in growth cone migration, collapse and retraction. For example, actin filaments at the periphery of the growth cone undergo constant turnover. Together with the action of myosin this creates a retrograde flow of filamentous actin structures (Burnette, Schaefer et al. 2007; Lee and Suter 2008; Lowery and Van Vactor 2009). On the other hand, microtubules too need to be in a dynamic state to support growth cone turning (Challacombe, Snow et al. 1997; Buck and Zheng 2002; Schaefer, Schoonderwoert et al. 2008). It is generally accepted that local modulation of the constitutive dynamicity of the acto-myosin system and of microtubules is the basis for growth cone migration as well as retraction.

NO can act as a repulsive guidance signal and its potential role in brain development is well documented (Hess, Patterson et al. 1993; Wu, Williams et al. 1994; Cramer, Angelucci et al. 1996; Renteria and Constantine-Paton 1996; Mize, Wu et al. 1998; Song, Ming et al. 1998; Ernst, Wu et al. 1999; Castellani, De Angelis et al. 2002; He, Yu et al. 2002; Nishiyama, Hoshino et al. 2003; Tedeschi, Nguyen et al. 2009; Tojima, Itofusa et al. 2009). However, few details of NO-induced changes in acto-myosin and microtubule networks have emerged. We show here that NO treatment increases myosin activity. This was monitored by phosphorylation of MLC on Ser19. This is reminiscent of a previously demonstrated increase of MLC phosphorylation preceding NO-induced

synapse withdrawal from hypoglossal motoneurons (Sunico, Gonzalez-Forero et al. 2010). Previous work in our lab show that NO-induced growth cone collapse and axon retraction are strictly dependent on myosin activity (unpublished data). In this respect, NO resembles other repulsive guidance molecules, such as lysophosphatidic acid (LPA) and sema 3A (Arimura, Inagaki et al. 2000; Zhang, Schaefer et al. 2003; Gallo 2006).

---

# Materials and methods



## **7. MATERIALS AND METHODS**

### **7.1 Animals:**

Newborn MAP1B<sup>-/-</sup> mice of either sex homozygous for a MAP1B-null allele (Meixner, Haverkamp et al. 2000) and wild-type controls were decapitated in compliance with the Austrian law regulating the use of animals in biomedical research, Tierversuchsgesetz, BGBl. Nr. 501/1989 and BGBl. I Nr. 162/2005.

### **7.2 Cortical explants preparation and primary cell culture**

#### **7.2.1 Dissection of mouse cerebral cortex:**

##### **7.2.1.1 Materials required**

- Dissecting medium (ice cold Hank's balanced salt solution supplemented with 7 mM HEPES, 2 mM L-glutamine and antibiotics).
- Newborn pups
- Dissection microscope
- Dissection tools- general scissor, micro scissor and forceps,
- Ethanol 95%
- Dissection tray
- Matrigel
- Growing medium (Neurobasal medium supplemented with B27, L-glutamine and antibiotics).

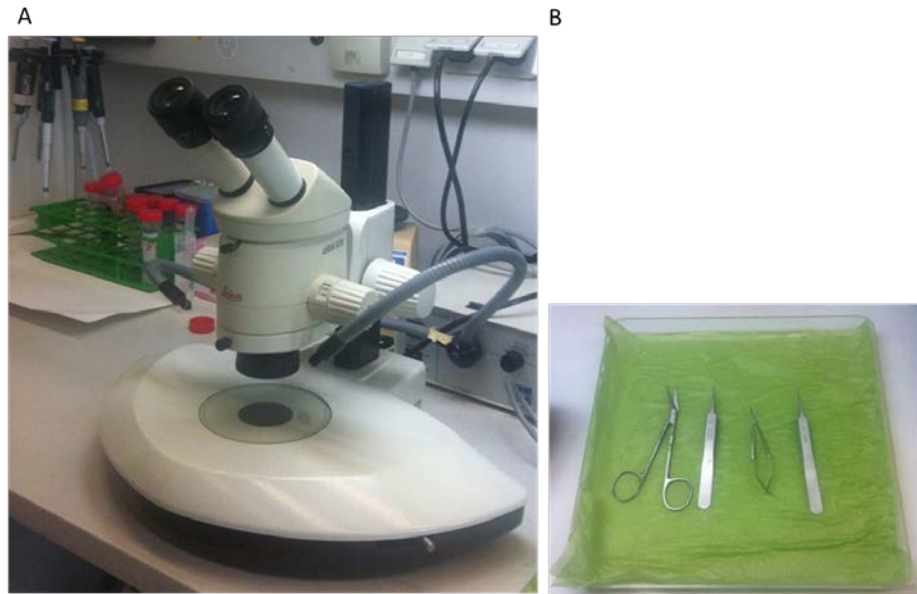


**Figure 29:** Tools used for dissection of the mouse cerebral cortex. A. Dissection microscope from Leica .B. Dissection tray showing instruments required for the dissection including general scissor, micro scissor and angled forceps.

#### 7.2.1.2 Dissection of the brain

- a. Newborn pups were decapitated.
- b. Small incisions were made to remove the skin. Then, carefully skull was removed. In newborn pups the skull is still a soft layer hence should be removed cautiously using angled forceps.
- c. Dissect the brain out from the skull and place it into a 35mm dish containing ice-cold ice cold Hank's balanced salt solution supplemented with 7 mM HEPES and 2 mM L-glutamine.
- d. Place the brain containing dish under the microscope.
- e. Remove the meningeal tissue with forceps.
- f. Make a sagittal incision to separate the two hemispheres and remove the hindbrain region.

- g. Place each hemisphere's cortex upside down and remove any noncortical tissue including hippocampus which is visible as a white banana shaped structure.
- h. Rinse the cortex with fresh dissection solution and collect.

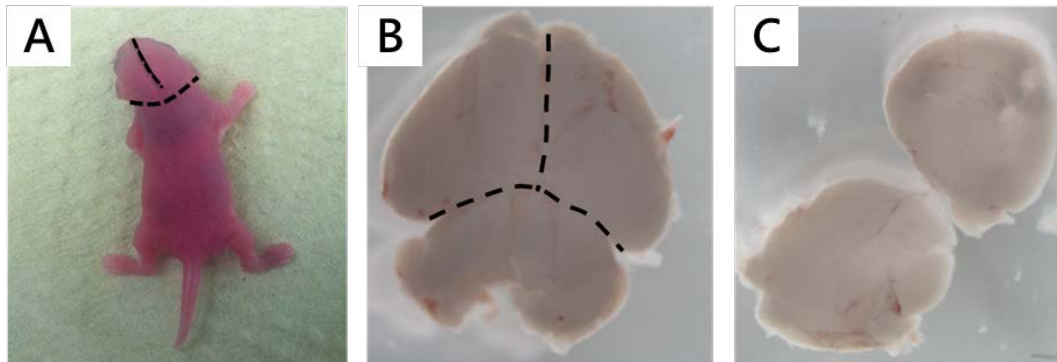


**Figure 30:** Picture shows dissection procedure for the cortex. A. Newborn pup is decapitated (along the horizontal dotted line shoed in the picture) and the incision was made to cut open the skin above the skull (vertical black dotted line). B. Whole brain is take out and placed in the dissection medium. The brain is cut in to two halves (shown as vertical dotted line) and the cortex is separated from the midbrain (as shown with the black dotted line). C. Separated cortices from the rest of the brain.

#### 7.2.1.3. Cortical explants culture

- a. Cerebral cortices of newborn pups were dissected in to small pieces manually.
- b. Take 24 well plates and place 8-10  $\mu$ l of matrigel in the center of each well.

- c. The cortical pieces should be placed on top of the matrigel and cover the tissue with another 8  $\mu$ l of matrigel. While working the matrigel should be kept on ice.
- d. The matrigel embedded tissues are placed in 37°C for 1-2 hours till the matrigel is polymerized.
- e. Gently add 600 $\mu$ l of medium in each well and allow them to grow for 24 hours at 37°C.

#### **7.2.1.4 Neurite outgrowth assay**

##### **7.2.1.4.1 Outgrowth assay using draxin condition medium.**

- a. Draxin condition medium was collected from COS7 cells after 48 hours of transient transfection of draxin expressing plasmid and as a negative control mock transfection with empty vector was used. Briefly, the medium was collected and centrifuged at 1000 rpm for 3 min in order to remove cellular debris and filtered with 0.2 $\mu$ M microfilters. The medium was frozen at -80°C until used and aliquot was tested for expression of Draxin with western blot for expression conformation.
- b. For explants cultures, 50% of the conditioned medium was diluted with fresh culture medium just before use.

##### **7.2.1.4.2 Outgrowth assay using recombinant draxin.**

- c. After the explants matrigel embed is polymerized add Add carefully culture medium containing neurobasal supplemented with B27, L-glutamine (2mM) and penicillin/streptomycin (50 units/ml) in the presence of PBS (control) or draxin (10 nM) or sema 3A (100ng/ml). After 48 hours, photographs of live explants were taken using an Axio-observer microscope (Zeiss) and the length of the longest neurite of each

explant was measured using image J software as described Islam et al 2009

## **7.2.2 Preparation of cortical primary neuronal cell culture**

### **3.2.2.1 Materials required**

- Cerebral cortical tissue
- Poly-L-Lysine
- Laminin
- 0.25% Trypsin-EDTA
- Plating medium (DMEM, 5% horse serum, 5% fetal calf serum and L-glutamine)
- Growing medium (Neurobasal medium, B27 supplement and L-glutamine)
- PBS
- Cell strainer 100 µm and 40µm mesh size.

### **7.2.2.2 Protocol**

- a. Cortical neurons from newborn mice were isolated and cultured as described previously with minor modifications (Anilkumar, Weisova et al. 2013).
- b. Cortical tissues were collected in 14ml tubes containing ice cold dissection medium.
- c. Pellet the tissues at 800 rpm/ 3 minutes and discard the supernatant carefully as this pellet is loosely attached to the bottom. It is always recommended to remove the supernatant using pipette rather than suction pump.
- d. Incubate the tissues with 0.25% trypsin-EDTA solution at 37°C for 20 min with in-between stirring every 5 min.
- e. After 20 minutes DMEM/FCS medium is added to inhibit the trypsin activity.

- f. Triturate the neurons and seed them on poly-L-lysine (100  $\mu\text{g/ml}$ , 1 h or overnight, 37°C) and laminin (20  $\mu\text{g/ml}$ , 3 h, 37°C) coated plates for various experiments in presence of DMEM +Glutamax medium supplemented with 5% Fetal calf serum and 5% horse serum.
- g. After 2 hours in culture, replace the plating medium with Neurobasal media supplemented with B27 and L-glutamine. Neuronal cultures were maintained at 37°C with 5% CO<sub>2</sub> in a humidified chamber.
- h. After 24h the neurons are washed to remove the dead cells. After 24h the cells look as shown in the following figure.

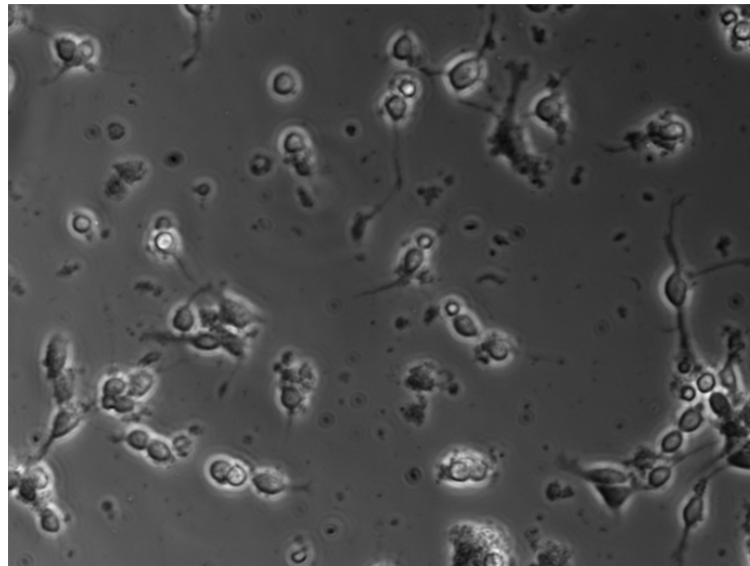


**Figure 3.** Picture showing dissociated cortical neurons after 24 hours in culture.

#### **7.2.2.2.1 Growth cone collapse assay**

- a. Neurons were seeded at low density about 50,000 cells per 13 mm coverslips coated with PLL and laminin.
- b. Neurons were treated and were fixed with 4% paraformaldehyde/11% sucrose solution for 20 min and stained with Texas red-conjugated phalloidin.

- c. Images were acquired on an LSM 710 microscope using 63X magnification objective.
- d. Quantification was carried out as described previously with modifications (Kapfhammer, Xu et al. 2007). Growth cone collapse was defined as the complete absence of lamelliopodia and not more than two filopodia at tip of the neurites. Only growth cones were considered which are not in contact with other growth cones. Processes longer than 20  $\mu\text{m}$  were considered as branches ( Li Li et al 2009).

### **7.3 Neuronal treatments**

Cortical neurons were treated with either draxin (100nM) or sema 3A (100ng/ml) for 60 and 30 min respectively. For inhibitor experiment, GSK-3 inhibitor (SB216763), PI3 kinase inhibitor (Wortmanin) and anti-DCC function blocking antibody (AF5) were applied at given (refer inhibitors and blockers section 3.2.2.3.1.3) for 1 h before draxin application.

### **7.4 Plasmids and Nucleofection**

Cortical neurons from newborn pups ( $1.5 \times 10^6$  cells) were suspended in 100  $\mu\text{l}$  of nucleofactor solution (Amaxa® Mouse Neuron Nucleofector® Kit-LONZA) and were mixed with constitutively active myristoylated Akt kinase construct (AktCA) or Akt kinase dead domain constructs (AktDN) were co-transfected with pmax -GFP plasmid (LONZA). pcDNA3 was used as the empty vector control for above vectors. Total 3 $\mu\text{g}$  of plasmid DNA (GFP: plasmid) in ratio 1:3 and were nucleofected using program G-013 before plating. 24-26h after, the cells were stimulated with draxin (100nM) for 1 h. The cells were fixed with 4% paraformaldehyde/11% sucrose solution for 20 min and stained with Texas red-

conjugated phalloidin (Sigma). The percentage of collapsed cells was counted from GFP positive cells.

## **7.5 Inhibitors and blockers**

The GSK-3 inhibitor SB216763 (Sigma-Aldrich) was used at 1  $\mu$ M, the PI3K inhibitor wortmannin (Sigma-Aldrich) at 0.1  $\mu$ M or the corresponding amount of DMSO as solvent control were treated 1h before draxin (1h) treatment. For DCC receptor function blocking experiments, Anti-DCC function blocking antibody (AF5, Calbiochem) was used at 1 $\mu$ g/ml or 5 $\mu$ g/ml or total IgG (1 $\mu$ g/ml or 5 $\mu$ g/ml) were used as a control.

## **7.6 Cell culture methods**

### **7.6.1 Materials required**

- Disposable latex gloves
- 75% Ethanol spary bottles
- Aspirating pipets
- 5 mL, 10 mL sterile pipets (glass or plastic)
- Confluent cells in 100mm culture dishes.
- Fresh culture dishes (100mm, 60mm and 35mm)
- Culture medium containing DMEM Medium with 10% serum, L-glutamine and antibiotics
- Trypsin
- PBS
- 15 mL centrifuge tube
- Vaccum system



### 7.6.2 Procedure for Passaging/ splitting Cells

- a. Warm DMEM medium and trypsin in 37°C waterbath 20 min before starting the procedure.
- b. Check cells in the flask under microscope to confirm the confluence and also check the cells carefully for any infection and cell morphological changes.
- c. Spray hands with ethanol and quickly place the dishes in hood. As a general rule do not spray flasks with ethanol.
- d. Using the Pasteur pipette aspirate the medium without touching the bottom of the plates.
- e. Add 10 mL of PBS to dishes making sure that it covers the entire surface of the flask or dish.
- f. Aspirate PBS and add 5ml trypsin to 100mm dishes, 2.5 ml to 60mm dishes and 4 mL trypsin to T-75 flask.
- g. Place back the dishes or flask in incubator for 4-5 min, or until the cells detached. This is critical step as over trypsinization affects the cell viability.
- h. Remove cells from incubator. Tap sides of the dishes gently to dislodge the remaining adherent cells and check that lumps are dispersed.
- i. Add equal volume media to stop the trypsin activity.
- j. Collect the cell suspension mixture in 15 mL centrifuge tube. Label tube.
- k. Centrifuge cells for 3 min at 1000 rpm.
- l. While centrifuge is still spinning prepare the dishes for plating with appropriate volume of fresh media (see Table 1, column 2) and label with name, date, cell type, passage number and passage dilution.

- m. After centrifugation, gently aspirate the supernatant without disturbing the Cell pellet.
- n. Resuspend cells in appropriate amount of fresh medium.
- o. Aliquot appropriate volume of cell suspension into freshly prepared dishes/flasks with media.
- p. Swirl the dishes gently so the cells to mix and spread uniformly and place back the dishes and flasks in incubator.
- q. Cells were maintained at 37 °C with 5%CO<sub>2</sub>.

### **7.6.3 Thawing cells**

- a. Frozen cells from liquid nitrogen were thawed at 37°C in water bath and immediately transferred to 15 ml falcon tube (as the cells were stored in DMSO it is highly recommended not to leave too long).
- b. Add 10-12 ml of DMEM medium with 10% serum, 2mM of L-glutamine and 50u/ml of penicillin/streptomycin was added, centrifuged at 1000rpm/3 min.
- c. Discard the supernatant, leaving behind the pelleted cells.
- d. Resuspend the cells in the fresh medium and plate on plastic dishes.

### **7.6.4. Treatment of N2a cells for NO-induced axon retraction experiment**

- a. Seed N2a cells at a density of  $5 \times 10^5 - 1 \times 10^6$  in 60mm petridishes containing DMEM medium supplemented with 10% FCS, L-glutamate and antibiotics (approximately 2 days before treatments).
- b. Once the cells are 80% confluent replace the medium with DMEM serum free medium in order to induce neuritogenesis for 6h. During this time the round cells start to develop processes.

c. Treat cells as following:

Dish	Treatments
1	10 $\mu$ M Y27632/1h followed by 100 $\mu$ M of SNAP
2	10 $\mu$ M of Y27632/1h
3	100 $\mu$ M of SNAP/1h
4	10 $\mu$ M ML-7/1h followed by 100 $\mu$ M of SNAP
5	10 $\mu$ M ML-7/1h
6	Untreated
7	6 $\mu$ l of DMSO/1h followed by 6 $\mu$ l of DMSO/1h
8	6 $\mu$ l of DMSO/1h

- d. All the treatments were carried out in dark and after every treatment the cells were placed back in to the incubator.
- e. After the treatments the medium was removed without disturbing the cells and wash the cells with 1X PBS.
- f. Lyse the cells by adding 200 $\mu$ l of 2x sample buffer (100mM Tris-HCl pH 6.8, 4% SDS, 20% (v/v) glycerol, 12mM EDTA, 0.2% bromphenol blue, 0.3% DTT and Complete Mini protease inhibitors tablets) uniformly all over the dish.
- g. Scrape the cells with plastic cell scrapers and transfer to eppendorf tubes.
- h. Further the cells are lysed completely by passing through the syringes 3-4 times.
- i. Heat at sample at 95°C for 5 min.
- j. Samples were separate on 12% SDS polyacrylamide gels and transferred to nitrocellulose membrane.
- k. After the transfer proteins were stained with Ponceau solution or amidoblack solution.
- l. The membranes were cut into two parts in regard to the size of Phophorylated-myosin and actin/tubulin.
- m. Membranes were washed with PBS/0.25% Tween20 for 3 times.

- n. Block membrane in 2% BSA in PBS/0.25% Tween20 for 1h at RT or over night at 4°C.
- o. After blocking wash membrane 3 times for 5 min with PBS/0.25% Tween20.
- p. Incubated with primary antibodies diluted in 1% BSA in PBS/0.25% Tween20 for 1h at RT or over night at 4°C:
- q. Blots were incubated with either Phospho myosin light chain 2 (Ser19) antibody (1:1000) or anti- actin antibody (1:1000) for overnight in 4 °C.
- r. Membranes were washed 3 times for 5 min with PBS/0.25% Tween20.
- s. Incubate membranes with secondary antibodies conjugated with alkaline phosphatase (AP) for 1h at room temperature.
- t. Membranes were washed 3 times and were incubated AP solution for 5 min and the membranes were developed with NBT and BCIP solutions.

#### **7.6.5. Transfection of cell lines**

About 1-1.5 X 10<sup>6</sup> cells were plated on 60mm plastic dishes. Cells were grown till they attain confluency. For one 60mm dish, 20µl of fugene reagent was added into 200µl Of Serum free media and incubated for 5min. Meanwhile in another tube DNA mix was prepared (In case of trans-activator/co-transfector). About 4.5µg of DNA was used for each transfection in 60mm dishes .Drop wise add the fugene mix in to the DNA containing tube. Gently tap and incubate the tube for 15-20min at room temperature. Add drop wise the incubated mixture on to the cells swirl and plate the dishes back in the incubator. Change the media next day. In case of sensitive cells media was changed after 5-6 h.

## **7.7 Immunocytochemistry**

For immunocytochemistry neurons were grown on glass coverslips in 24 well plates. Treated cells were fixed with 4% paraformaldehyde supplemented with 11% sucrose followed by washing with phosphate-buffered saline (PBS) (twice) and permeabilization with 0.1% of Triton X-100 in PBS for 10min. Further the cells were blocked with 2% BSA (PAA) in PBS-Tween 20 (0.01%) for 1 h. Cells were further incubated with primary antibodies, diluted in blocking buffer for 3h at room temperature or 4°C /overnight. Incubations were done in the humidified chamber. Excess antibody on the cells was washed with PBST for 3 times with 5min of incubation. Cells were incubated with secondary antibodies for 1h at room temperature followed by washing the cells with PBST and one time with water. 8µl of Mowiol was placed on the glass slides and the glass coverslip is placed on top of the mowiol drop keeping the cells upside down position. Overnight the coverslips are kept to dry in darkness and the next day the slides are stored at 4°C.

## **7.8 Preparation of protein extracts and their separation.**

1. Neurons were lysed in RIPA buffer (Sigma) in the presence of protease inhibitors (cOmplete ULTRA Tablets, EDTA-free, (Roche) and Phosphatase Inhibitor Cocktail (1:100; Sigma-Aldrich) and sodium orthovanadate. After centrifugation, the supernatant is collected and analysed using western blot.
2. Protein lysates (25µg/ lane) were separated on 6% or 10% SDS-PAGE (sodium dodecyl sulfate polyacrylamide gel electrophoresis). The Resolving gels contained Acrylamide (30%), Tris 1.5M (ph 8.8), H<sub>2</sub>O, Ammonium per sulphate [freshly prepared (10%)], SDS (10%), TEMED and the stacking gels contained Acrylamide (30%), Tris 0.5M (ph 8.8), H<sub>2</sub>O, Ammonium per sulphate [freshly prepared (10%)],

SDS (10%), TEMED). SDS-gel electrophoresis: Gels were run at 80mA with 500V for 1.5-2h using Bio-Rad mini gel running unit and were transferred to nitrocellulose membrane.

#### Western Blotting

1. Proteins of low molecular weight (10 – 100 kDa) were transferred using Trans-blot SD semi-Dry electrophoretic transfer cell from Bio-Rad. gels were transferred at 150mA at 500V for 1.5h
2. Wet blot transfer was carried out for high molecular weight proteins. Transfer was carried out at 4°C at 65 Volts for 4 hours. The transfer system was kept in a box packed with ice in order to reduce the heat produced during the process. Transfer buffer for supplemented with 0.01% SDS.
3. Post transfer the proteins were visualized using Ponceau staining. The membranes were blocked with 2% low fat milk or (MAP1B total, phospho-MAP1B and neurofilament H blots) or 5% low fat milk (GSK-3 $\beta$  blots) or 3% BSA (Akt blots) in Tris buffered saline (TBS) containing 0.1% Tween-20 and Further they were incubated with Primary antibodies (Reference section List of primary antibodies).
4. Secondary Antibodies: Anti-mouse and anti-rabbit horse radish peroxidase-conjugated (1:10,000; Jackson) secondary antibodies were used for detection of proteins on blots. Blots were developed using SuperSignal® West Pico Chemiluminescent substrate. Immunoblot images were acquired using X-ray films or the Fusion-FX7 Advance system (Peqlab). Quantification was performed by Image J version 1.44p software (National Institutes of Health, USA).

## **7.9. Statistical analysis methods**

Independent Student's *t*-test (cortical explants experiment), or one-way ANOVA and Tukey's post hoc analyses (time dependent draxin application experiment) were performed using SPSS software (SPSS GmbH Software, Munich, Germany). The results are shown as mean values  $\pm$  SEM. Where the *p* value was less than 0.05, results were determined as significantly different.

## **8. Reagents and chemicals**

### **8.1 Buffers and solutions**

#### **1. 5X electrophoresis buffer for SDS-PAGE (1L)**

Tris base (15.1g), Glycine (94g), 10% SDS (50ml) and volume adjusted with water.

#### **2. 1X Transferbuffer (semidry transfer)(1L)**

Tris base (3.03g), Glycine (14.4g), Methanol (200ml) and adjusted with water.

#### **3. 10X Tris Buffered Saline (TBS)**

Tris Base (15.76g), NaCl (87.76g) add water.

#### **4. 6X loading buffer**

0.5M Tris/HCl (7ml), Glycerol, SDS, DTT and Bromophenol blue (1.2g).

#### **5. 0.5M Tris/HCl (6.8)**

Tris (30.25g) adjusted to pH 6.8 with HCl and add water.

#### **6. 1.5M Tris/HCl (8.8)**

Tris (181.7g) adjust pH to 8.8 and add water.

#### **7. 10% Ammonium persulfate solution**

Ammonium persulfate solution (2g) and add water.

#### **8. 10X Ponceau**



Ponceau S (2g), Trichloroacetic acid (30%), Sulfosalicylic acid (30%) adjust with water.

## 8.2 Common reagents.

Chemical	Company	Catalog number
Acetic acid	Sigma	A6283
Acetone	VWR	20066296
Acrylamide-bis	Gerbu	1108
Ammonium per sulphate	Gerbu	1708
BCIP	Gerbu	03937
Boric acid	Sigma	B0394
Bovine serum albumin	PAA	A9418
Bromophenol blue	Sigma	114391
Complete tablet EDTA free	Roche	11873580001
D-Glucose	Sigma	G8270
Dithiothreitol	Sigma	D0632
DMSO	Sigma	D2650
EDTA	Gerbu	1034
Ethanol	Merk	1009835000
Glycerol	Sigma	G5516
Glycine	Gerbu	1023
Hydrochloric acid	Sigma	258148
Isoflurane	Abbott Lab	05260-05
Isopropanol	Merk	1070222511

Methanol	VWR	1.06012
Mowiol-4-88	Calbiochem	475904
N,N,N',N'-Tetramethylethylenediamine(TEMED)	Sigma	T9281
Nitro blue tetrazolium (NBT)	Sigma	N5514
	Agar	
Para formaldehyde	scientific	AGR1018
Phosphate buffered saline (PBS)	Invitrogen	10010023
Skimmed Milk Powder	Gerbu	1602
S-Nitroso-N-acetyl-DL-penicillamine (SNAP)	Sigma	N3398
Sodium chloride	Sigma	S9888
Sodium dodecyl sulfate (SDS)	Sigma	L4390
Sodium hydroxide	Sigma	221465
Sucrose	Gerbu	1331
Tris X	Gerbu	1018
Triton X-100	Sigma	T8787
Tween-20	Gerbu	2001
$\beta$ -Mercapto ehanol	Sigma	M6250

### 8.3 Inhibitor and guidance molecules

Chemical	Company	Catalog number
Anti-DCC Mouse mAb (AF5)	Calbiochem Millipore	OP45, US10P45
Draxin	ECM Biosciences	DP3671
Draxin, Mouse, recombinant	R&D Systems	6149 - DR/CF
Semaphorin 3A Mouse, recombinant	R&D Systems	5926 - S3
Wortmannin	Sigma	W-1628
Y27632	Sigma	Y-0503
ML 7 = MLC Kinase Inhibitor	Alexis	270-088-M005
ML-7 hydrochloride	Calbiochem Millipore	475880

## 8.4 Cell Culture Reagents

Chemical	Company	Catalog number
100X Penicillin/Streptomycin mix	Gibco	15070
Fungizone	Gibco	15290-026
L-Glutamine	Invitrogen	25030
FBS (FCS)	Sigma	F7524
DMM+Glutamax	Gibco	10569-010
Trysin	Sigma	T3924
Glutamax (100×)	Invitrogen	61965-026
Horse serum heat inactivated	Gibco	26050-088
Neurobasal medium A	Invitrogen	10888-022
Neurobasal medium A w/o phenol red	Invitrogen	12349-015
B27 supplement	Invitrogen	17504-044

## 8.5 List of primary antibodies

Name	Dilutions	Host	Suppliers	Catalog number
Akt	1:1000	Rabbit	Cell signalling	9272
P-Akt	1:1000	Rabbit	Cell signalling	9271
GSK-3 $\beta$	1:1000	Rabbit	Cell signalling	9315
P-GSK-3 $\beta$	1:1000	Rabbit	Cell signalling	9336
GAPDH	1:2500	Mouse	Cell signalling	G9545
P- MLC	1:1000	Mouse	Cell signalling	3675
SMI31(P-MAP1B)	1:2500	Mouse	COVANCE	SMI-31R
891(total MAP1B)	1:800	Rabbit	In house	In house
4453(total MAP1B)	1:	Rabbit	In house	In house
9E11(Myc)	1:1	Mouse	In house	In house
N19 (total MAP1B)	1:500	Rabbit	Santa cruz	SC-8970
Phalloidin	1:200		Sigma	P2141
Tubulin	1:2500	Mouse	Sigma	T9026

---

# References

## 9. References

- Adler, C. E., R. D. Fetter, et al. (2006). "UNC-6/Netrin induces neuronal asymmetry and defines the site of axon formation." Nature Neuroscience **9**(4): 511-518.
- Ahmed, G., Y. Shinmyo, et al. (2011). "Draxin inhibits axonal outgrowth through the netrin receptor DCC." J Neurosci **31**(39): 14018-14023.
- Akhmanova, A. and M. O. Steinmetz (2008). "Tracking the ends: a dynamic protein network controls the fate of microtubule tips." Nat Rev Mol Cell Biol **9**(4): 309-322.
- Al-Khouri, A. M., Y. Ma, et al. (2005). "Cooperative phosphorylation of the tumor suppressor phosphatase and tensin homologue (PTEN) by casein kinases and glycogen synthase kinase 3beta." J Biol Chem **280**(42): 35195-35202.
- Alderton, W. K., C. E. Cooper, et al. (2001). "Nitric oxide synthases: structure, function and inhibition." Biochem J **357**(Pt 3): 593-615.
- Alessi, D. R., M. Andjelkovic, et al. (1996). "Mechanism of activation of protein kinase B by insulin and IGF-1." EMBO J **15**(23): 6541-6551.
- Anilkumar, U., P. Weisova, et al. (2013). "AMP-activated protein kinase (AMPK)-induced preconditioning in primary cortical neurons involves activation of MCL-1." Journal of Neurochemistry **124**(5): 721-734.
- Arakawa, H. (2004). "Netrin-1 and its receptors in tumorigenesis." Nat Rev Cancer **4**(12): 978-987.
- Arimura, N., N. Inagaki, et al. (2000). "Phosphorylation of collapsin response mediator protein-2 by Rho-kinase. Evidence for two separate signaling pathways for growth cone collapse." J Biol Chem **275**(31): 23973-23980.

- Atwal, J. K., K. K. Singh, et al. (2003). "Semaphorin 3F antagonizes neurotrophin-induced phosphatidylinositol 3-kinase and mitogen-activated protein kinase signaling: a mechanism for growth cone collapse." Journal of Neuroscience **23**(20): 7602-7609.
- Aurandt, J., H. G. Vikis, et al. (2002). "The semaphorin receptor plexin-B1 signals through a direct interaction with the Rho-specific nucleotide exchange factor, LARG." Proc Natl Acad Sci U S A **99**(19): 12085-12090.
- Avila, J., J. Dominguez, et al. (1994). "Regulation of microtubule dynamics by microtubule-associated protein expression and phosphorylation during neuronal development." Int J Dev Biol **38**(1): 13-25.
- Backer, J. M. (2010). "The regulation of class IA PI 3-kinases by inter-subunit interactions." Curr Top Microbiol Immunol **346**: 87-114.
- Bagnard, D., M. Lohrum, et al. (1998). "Semaphorins act as attractive and repulsive guidance signals during the development of cortical projections." Development **125**(24): 5043-5053.
- Beck, K., I. Hunter, et al. (1990). "Structure and function of laminin: anatomy of a multidomain glycoprotein." FASEB J **4**(2): 148-160.
- Beffert, U., G. Morfini, et al. (2002). "Reelin-mediated signaling locally regulates protein kinase B/Akt and glycogen synthase kinase 3beta." J Biol Chem **277**(51): 49958-49964.
- Behar, O., K. Mizuno, et al. (1999). "Semaphorin 3A growth cone collapse requires a sequence homologous to tarantula hanatoxin." Proc Natl Acad Sci U S A **96**(23): 13501-13505.



- Bouquet, C., M. Ravaille-Veron, et al. (2007). "MAP1B coordinates microtubule and actin filament remodeling in adult mouse Schwann cell tips and DRG neuron growth cones." Mol Cell Neurosci **36**(2): 235-247.
- Brown, J. A., R. B. Wysolmerski, et al. (2009). "Dorsal root ganglion neurons react to semaphorin 3A application through a biphasic response that requires multiple myosin II isoforms." Mol Biol Cell **20**(4): 1167-1179.
- Brown, M., T. Jacobs, et al. (2004). "Alpha2-chimaerin, cyclin-dependent Kinase 5/p35, and its target collapsin response mediator protein-2 are essential components in semaphorin 3A-induced growth-cone collapse." J Neurosci **24**(41): 8994-9004.
- Bryan, N. S., K. Bian, et al. (2009). "Discovery of the nitric oxide signaling pathway and targets for drug development." Front Biosci (Landmark Ed) **14**: 1-18.
- Buck, K. B. and J. Q. Zheng (2002). "Growth cone turning induced by direct local modification of microtubule dynamics." J Neurosci **22**(21): 9358-9367.
- Burnette, D. T., A. W. Schaefer, et al. (2007). "Filopodial actin bundles are not necessary for microtubule advance into the peripheral domain of Aplysia neuronal growth cones." Nat Cell Biol **9**(12): 1360-1369.
- Castellani, V., E. De Angelis, et al. (2002). "Cis and trans interactions of L1 with neuropilin-1 control axonal responses to semaphorin 3A." EMBO J **21**(23): 6348-6357.
- Chadborn, N. H., A. I. Ahmed, et al. (2006). "PTEN couples Sema3A signalling to growth cone collapse." J Cell Sci **119**(Pt 5): 951-957.
- Challacombe, J. F., D. M. Snow, et al. (1997). "Dynamic microtubule ends are required for growth cone turning to avoid an inhibitory guidance cue." J. Neurosci. **17**: 3085-3095.

- Cook, D., M. J. Fry, et al. (1996). "Wingless inactivates glycogen synthase kinase-3 via an intracellular signalling pathway which involves a protein kinase C." *e* **15**: 4526-4536.
- Cosker, K. E. and B. J. Eickholt (2007). "Phosphoinositide 3-kinase signalling events controlling axonal morphogenesis." *Biochem Soc Trans* **35**(Pt 2): 207-210.
- Cramer, K. S., A. Angelucci, et al. (1996). "A role for nitric oxide in the development of the ferret retinogeniculate projection." *J Neurosci* **16**(24): 7995-8004.
- Cross, D. A., D. R. Alessi, et al. (1995). "Inhibition of glycogen synthase kinase-3 by insulin mediated by protein kinase B." *Nature* **378**(6559): 785-789.
- Culotti, J. G. and D. C. Merz (1998). "DCC and netrins." *Curr Opin Cell Biol* **10**(5): 609-613.
- Dajani, R., E. Fraser, et al. (2001). "Crystal structure of glycogen synthase kinase 3 beta: structural basis for phosphate-primed substrate specificity and autoinhibition." *Cell* **105**(6): 721-732.
- Davies, S. P., H. Reddy, et al. (2000). "Specificity and mechanism of action of some commonly used protein kinase inhibitors." *Biochem J* **351**(Pt 1): 95-105.
- de la Torre, J. R., V. H. Hopker, et al. (1997). "Turning of retinal growth cones in a netrin-1 gradient mediated by the netrin receptor DCC." *Neuron* **19**(6): 1211-1224.
- Del Rio, J. A., C. Gonzalez-Billault, et al. (2004). "MAP1B is required for Netrin 1 signaling in neuronal migration and axonal guidance." *Curr Biol* **14**(10): 840-850.
- Diaz-Nido, J., L. Serrano, et al. (1988). "A casein kinase II-related activity is involved in phosphorylation of microtubule-associated protein MAP-1B during neuroblastoma cell differentiation." *J Cell Biol* **106**(6): 2057-2065.
- Dickson, B. J. (2002). "Molecular mechanisms of axon guidance." *Science* **298**(5600): 1959-1964.

- Dickson, B. J. and G. F. Gilestro (2006). "Regulation of commissural axon pathfinding by slit and its Robo receptors." Annu Rev Cell Dev Biol **22**: 651-675.
- Ding, V. W., R. H. Chen, et al. (2000). "Differential regulation of glycogen synthase kinase 3beta by insulin and Wnt signaling." J Biol Chem **275**(42): 32475-32481.
- Edelmann, W., M. Zervas, et al. (1996). "Neuronal abnormalities in microtubule-associated protein 1B mutant mice." pnas **93**: 1270-1275.
- Edstrom, A. and P. A. Ekstrom (2003). "Role of phosphatidylinositol 3-kinase in neuronal survival and axonal outgrowth of adult mouse dorsal root ganglia explants." J Neurosci Res **74**(5): 726-735.
- Eickholt, B. J., F. S. Walsh, et al. (2002). "An inactive pool of GSK-3 at the leading edge of growth cones is implicated in Semaphorin 3A signaling." J Cell Biol **157**(2): 211-217.
- Eldar-Finkelman, H., R. Seger, et al. (1995). "Inactivation of glycogen synthase kinase-3 by epidermal growth factor is mediated by mitogen-activated protein kinase/p90 ribosomal protein S6 kinase signaling pathway in NIH/3T3 cells." J Biol Chem **270**(3): 987-990.
- Engelman, J. A., J. Luo, et al. (2006). "The evolution of phosphatidylinositol 3-kinases as regulators of growth and metabolism." Nat Rev Genet **7**(8): 606-619.
- Ernst, A. F., H. H. Wu, et al. (1999). "NMDA receptor-mediated refinement of a transient retinotectal projection during development requires nitric oxide." J Neurosci **19**(1): 229-235.
- Etienne-Manneville, S. and A. Hall (2002). "Rho GTPases in cell biology." Nature **420**(6916): 629-635.
- Fazeli, A., S. L. Dickinson, et al. (1997). "Phenotype of mice lacking functional Deleted in colorectal cancer (Dcc) gene." Nature **386**(6627): 796-804.

- Fischer, I., J. Konola, et al. (1990). "Microtubule associated protein (MAP1B) is present in cultured oligodendrocytes and co-localizes with tubulin." J Neurosci Res **27**(1): 112-124.
- Fukata, Y., T. J. Itoh, et al. (2002). "CRMP-2 binds to tubulin heterodimers to promote microtubule assembly." Nat Cell Biol **4**(8): 583-591.
- Gallo, G. (2006). "RhoA-kinase coordinates F-actin organization and myosin II activity during semaphorin-3A-induced axon retraction." J Cell Sci **119**(Pt 16): 3413-3423.
- Gonzalez-Billault, C., J. A. Del Rio, et al. (2005). "A role of MAP1B in Reelin-dependent Neuronal Migration." Cereb Cortex **15**(8): 1134-1145.
- Gonzalez-Billault, C., E. Demandt, et al. (2000). "Perinatal lethality of microtubule-associated protein 1B-deficient mice expressing alternative isoforms of the protein at low levels." Mol Cell Neurosci **16**(4): 408-421.
- Gonzalez-Billault, C., E. Demandt, et al. (2000). "Perinatal lethality of microtubule-associated protein 1B-deficient mice expressing alternative isoforms of the protein at low levels." Mol Cell Neurosci **16**(4): 408-421.
- Goold, R. G. and P. R. Gordon-Weeks (2004). "Glycogen synthase kinase 3beta and the regulation of axon growth." Biochem Soc Trans **32**(Pt 5): 809-811.
- Goold, R. G., R. Owen, et al. (1999). "Glycogen synthase kinase 3b phosphorylation of microtubule-associated protein 1B regulates the stability of microtubules in growth cones." J Cell Sci **112**(Pt 19): 3373-3384.
- Hall, A. (2005). "Rho GTPases and the control of cell behaviour." Biochem Soc Trans **33**(Pt 5): 891-895.

- Hanks, S. K. and T. Hunter (1995). "Protein kinases 6. The eukaryotic protein kinase superfamily: kinase (catalytic) domain structure and classification." FASEB J **9**(8): 576-596.
- He, Y., W. Yu, et al. (2002). "Microtubule reconfiguration during axonal retraction induced by nitric oxide." J Neurosci **22**(14): 5982-5991.
- Henle, S. J., L. P. Carlstrom, et al. (2013). "Differential Role of PTEN Phosphatase in Chemotactic Growth Cone Guidance." Journal of Biological Chemistry **288**(29): 20837-20842.
- Hess, D. T., S. I. Patterson, et al. (1993). "Neuronal growth cone collapse and inhibition of protein fatty acylation by nitric oxide." Nature **366**(6455): 562-565.
- Hong, K., L. Hinck, et al. (1999). "A ligand-gated association between cytoplasmic domains of UNC5 and DCC family receptors converts netrin-induced growth cone attraction to repulsion." Cell **97**(7): 927-941.
- Hur, E. M., Saijilafu, et al. (2011). "GSK3 controls axon growth via CLASP-mediated regulation of growth cone microtubules." Genes & Development **25**(18): 1968-1981.
- Ishizaki, T., M. Maekawa, et al. (1996). "The small GTP-binding protein Rho binds to and activates a 160 kDa Ser/Thr protein kinase homologous to myotonic dystrophy kinase." EMBO J **15**(8): 1885-1893.
- Islam, S. M., Y. Shinmyo, et al. (2009). "Draxin, a repulsive guidance protein for spinal cord and forebrain commissures." Science **323**(5912): 388-393.
- Johnstone, M., R. G. Goold, et al. (1997). "Localisation of microtubule-associated protein 1B phosphorylation sites recognised by monoclonal antibody SMI-31." in **69**: 1417-1424.

- Jope, R. S. and G. V. Johnson (2004). "The glamour and gloom of glycogen synthase kinase-3." Trends Biochem Sci **29**(2): 95-102.
- Kalil, K., L. Li, et al. (2011). "Signaling mechanisms in cortical axon growth, guidance, and branching." Front Neuroanat **5**: 62.
- Kapfhammer, J. P., H. Xu, et al. (2007). "The detection and quantification of growth cone collapsing activities." Nature Protocols **2**(8): 2005-2011.
- Kawano, Y., Y. Fukata, et al. (1999). "Phosphorylation of myosin-binding subunit (MBS) of myosin phosphatase by Rho-kinase in vivo." J Cell Biol **147**(5): 1023-1038.
- Kawauchi, T., K. Chihama, et al. (2003). "The in vivo roles of STEF/Tiam1, Rac1 and JNK in cortical neuronal migration." Embo J **22**(16): 4190-4201.
- Kennedy, T. E., H. Wang, et al. (2006). "Axon guidance by diffusible chemoattractants: a gradient of netrin protein in the developing spinal cord." J Neurosci **26**(34): 8866-8874.
- Kolodkin, A. L., D. J. Matthes, et al. (1992). "Fasciclin IV: sequence, expression, and function during growth cone guidance in the grasshopper embryo." Neuron **9**(5): 831-845.
- Kölsch, V., P. G. Charest, et al. (2008). "The regulation of cell motility and chemotaxis by phospholipid signaling." Journal of Cell Science **121**(Pt 5): 551-559.
- Koppel, A. M., L. Feiner, et al. (1997). "A 70 amino acid region within the semaphorin domain activates specific cellular response of semaphorin family members." Neuron **19**(3): 531-537.
- Kruger, R. P., J. Aurandt, et al. (2005). "Semaphorins command cells to move." Nat Rev Mol Cell Biol **6**(10): 789-800.

- Kureishi, Y., S. Kobayashi, et al. (1997). "Rho-associated kinase directly induces smooth muscle contraction through myosin light chain phosphorylation." J Biol Chem **272**(19): 12257-12260.
- Kusy, S., L. Funkelstein, et al. (2003). "Redundant functions but temporal and regional regulation of two alternatively spliced isoforms of semaphorin 3F in the nervous system." Mol Cell Neurosci **24**(2): 409-418.
- Lamas, S., P. A. Marsden, et al. (1992). "Endothelial nitric oxide synthase: molecular cloning and characterization of a distinct constitutive enzyme isoform." Proc Natl Acad Sci U S A **89**(14): 6348-6352.
- Lee, A. C. and D. M. Suter (2008). "Quantitative analysis of microtubule dynamics during adhesion-mediated growth cone guidance." Dev Neurobiol **68**(12): 1363-1377.
- Leung, T., X. Q. Chen, et al. (1996). "The p160 RhoA-binding kinase ROK alpha is a member of a kinase family and is involved in the reorganization of the cytoskeleton." Mol Cell Biol **16**(10): 5313-5327.
- Leung, T., E. Manser, et al. (1995). "A novel serine/threonine kinase binding the Ras-related RhoA GTPase which translocates the kinase to peripheral membranes." J Biol Chem **270**(49): 29051-29054.
- Lock, F. E. and N. A. Hotchin (2009). "Distinct roles for ROCK1 and ROCK2 in the regulation of keratinocyte differentiation." PLoS One **4**(12): e8190.
- Lowery, L. A. and D. Van Vactor (2009). "The trip of the tip: understanding the growth cone machinery." Nat Rev Mol Cell Biol **10**(5): 332-343.
- Lucas, F. R., R. G. Goold, et al. (1998). "Inhibition of GSK-3b leading to the loss of phosphorylated MAP-1B is an early event in axonal remodelling induced by WNT-7a or lithium." J Cell Sci **111**(Pt 10): 1351-1361.

- Luduena, R. F. (1998). "Multiple forms of tubulin: different gene products and covalent modifications." Int Rev Cytol **178**: 207-275.
- Luo, Y., D. Raible, et al. (1993). "Collapsin: a protein in brain that induces the collapse and paralysis of neuronal growth cones." Cell **75**(2): 217-227.
- Ma, D., S. Chow, et al. (1999). "Induction of microtubule-associated protein 1B expression in Schwann cells during nerve regeneration." Brain Res **823**(1-2): 141-153.
- Maccioni, R. B. and V. Cambiazo (1995). "Role of microtubule-associated proteins in the control of microtubule assembly." Physiol Rev **75**(4): 835-864.
- Maehama, T. and J. E. Dixon (1999). "PTEN: a tumour suppressor that functions as a phospholipid phosphatase." Trends Cell Biol **9**(4): 125-128.
- Maekawa, M., T. Ishizaki, et al. (1999). "Signaling from Rho to the actin cytoskeleton through protein kinases ROCK and LIM-kinase." Science **285**(5429): 895-898.
- Mann, F., W. A. Harris, et al. (2004). "New views on retinal axon development: a navigation guide." Int J Dev Biol **48**(8-9): 957-964.
- Manning, B. D. and L. C. Cantley (2007). "AKT/PKB signaling: navigating downstream." Cell **129**(7): 1261-1274.
- Matsui, T., M. Amano, et al. (1996). "Rho-associated kinase, a novel serine/threonine kinase, as a putative target for small GTP binding protein Rho." EMBO J **15**(9): 2208-2216.
- Medeiros, N. A., D. T. Burnette, et al. (2006). "Myosin II functions in actin-bundle turnover in neuronal growth cones." Nat Cell Biol **8**(3): 215-226.
- Mehlen, P. (2003). "The dependence receptors DCC and UNC5H as a link between neuronal guidance and survival." Biology of the Cell.



- Meixner, A., S. Haverkamp, et al. (2000). "MAP1B is required for axon guidance and is involved in the development of the central and peripheral nervous system." J Cell Biol **151**(6): 1169-1178.
- Meixner, A., S. Haverkamp, et al. (2000). "MAP1B is required for axon guidance and is involved in the development of the central and peripheral nervous system." jcb **151**: 1169-1178.
- Ming, G., H. Song, et al. (1999). "Phospholipase C-gamma and phosphoinositide 3-kinase mediate cytoplasmic signaling in nerve growth cone guidance." Neuron **23**(1): 139-148.
- Mitchison, T. and M. Kirschner (1984). "Dynamic instability of microtubule growth." Nature **312**(5991): 237-242.
- Mize, R. R., H. H. Wu, et al. (1998). "The role of nitric oxide in development of the patch-cluster system and retinocollicular pathways in the rodent superior colliculus." Prog Brain Res **118**: 133-152.
- Mohamed, A. M. and I. D. Chin-Sang (2006). "Characterization of loss-of-function and gain-of-function Eph receptor tyrosine kinase signaling in *C. elegans* axon targeting and cell migration." Dev Biol **290**(1): 164-176.
- Nakagawa, O., K. Fujisawa, et al. (1996). "ROCK-I and ROCK-II, two isoforms of Rho-associated coiled-coil forming protein serine/threonine kinase in mice." FEBS Lett **392**(2): 189-193.
- Narumiya, S., T. Ishizaki, et al. (2000). "Use and properties of ROCK-specific inhibitor Y-27632." Methods Enzymol **325**: 273-284.
- Naser, I. B., Y. Su, et al. (2009). "Analysis of a repulsive axon guidance molecule, draxin, on ventrally directed axon projection in chick early embryonic midbrain." Dev Biol **332**(2): 351-359.

- Nishiyama, M., A. Hoshino, et al. (2003). "Cyclic AMP/GMP-dependent modulation of Ca<sup>2+</sup> channels sets the polarity of nerve growth-cone turning." Nature **423**(6943): 990-995.
- Oinuma, I., Y. Ito, et al. (2010). "Semaphorin 4D/Plexin-B1 stimulates PTEN activity through R-Ras GTPase-activating protein activity, inducing growth cone collapse in hippocampal neurons." J Biol Chem **285**(36): 28200-28209.
- Oinuma, I., Y. Ito, et al. (2010). "Semaphorin 4D/Plexin-B1 stimulates PTEN activity through R-Ras GTPase-activating protein activity, inducing growth cone collapse in hippocampal neurons." Journal of Biological Chemistry **285**(36): 28200-28209.
- Owen, R. and P. R. Gordon-Weeks (2003). "Inhibition of glycogen synthase kinase 3beta in sensory neurons in culture alters filopodia dynamics and microtubule distribution in growth cones." Mol Cell Neurosci **23**(4): 626-637.
- Polleux, F. and W. Snider (2010). "Initiating and growing an axon." Cold Spring Harb Perspect Biol **2**(4): a001925.
- Quinn, C. C. and W. G. Wadsworth (2006). "Axon guidance: ephrins at WRK on the midline." Curr Biol **16**(22): R954-955.
- Renteria, R. C. and M. Constantine-Paton (1996). "Exogenous nitric oxide causes collapse of retinal ganglion cell axonal growth cones in vitro." J Neurobiol **29**(4): 415-428.
- Richards, L. J., C. Plachez, et al. (2004). "Mechanisms regulating the development of the corpus callosum and its agenesis in mouse and human." Clin Genet **66**(4): 276-289.
- Riederer, B. M. (2007). "Microtubule-associated protein 1B, a growth-associated and phosphorylated scaffold protein." Brain Res Bull **71**(6): 541-558.

- Riento, K. and A. J. Ridley (2003). "Rocks: multifunctional kinases in cell behaviour." Nat Rev Mol Cell Biol **4**(6): 446-456.
- Rothberg, J. M., D. A. Hartley, et al. (1988). "slit: an EGF-homologous locus of *D. melanogaster* involved in the development of the embryonic central nervous system." Cell **55**(6): 1047-1059.
- Round, J. and E. Stein (2007). "Netrin signaling leading to directed growth cone steering." Curr Opin Neurobiol **17**(1): 15-21.
- Sabry, J. H., T. P. O'Connor, et al. (1991). "Microtubule behavior during guidance of pioneer neuron growth cones in situ." J Cell Biol **115**(2): 381-395.
- Saito, S., G. J. Kidd, et al. (1994). "Rat spinal cord neurons contain nitric oxide synthase." Neuroscience **59**(2): 447-456.
- Saito, Y., J. R. Vandenheede, et al. (1994). "The mechanism by which epidermal growth factor inhibits glycogen synthase kinase 3 in A431 cells." Biochem J **303 ( Pt 1)**: 27-31.
- Sanchez, S., C. L. Sayas, et al. (2001). "The inhibition of phosphatidylinositol-3-kinase induces neurite retraction and activates GSK3." J Neurochem **78**(3): 468-481.
- Schaefer, A. W., V. T. Schoonderwoert, et al. (2008). "Coordination of actin filament and microtubule dynamics during neurite outgrowth." Dev Cell **15**(1): 146-162.
- Schoenfeld, T. A., Obar, R. A. (1994). "Diverse distribution and function of fibrous microtubule-associated proteins in the nervous system." Int Rev Cytol **151**: 67-137.
- Segal, R. A. (2003). "Selectivity in neurotrophin signaling: theme and variations." Annual Reviews in Neuroscience **26**: 299-330.
- Serafini, T., S. A. Colamarino, et al. (1996). "Netrin-1 is required for commissural axon guidance in the developing vertebrate nervous system." Cell **87**(6): 1001-1014.

- Shelly, M., L. Cancedda, et al. (2011). "Semaphorin3A regulates neuronal polarization by suppressing axon formation and promoting dendrite growth." Neuron **71**(3): 433-446.
- Shu, T. and L. J. Richards (2001). "Cortical axon guidance by the glial wedge during the development of the corpus callosum." J Neurosci **21**(8): 2749-2758.
- Silver, J., S. E. Lorenz, et al. (1982). "Axonal guidance during development of the great cerebral commissures: descriptive and experimental studies, in vivo, on the role of preformed glial pathways." J Comp Neurol **210**(1): 10-29.
- Somlyo, A. P. and A. V. Somlyo (2003). "Ca<sup>2+</sup> sensitivity of smooth muscle and nonmuscle myosin II: modulated by G proteins, kinases, and myosin phosphatase." Physiol Rev **83**(4): 1325-1358.
- Song, H., G. Ming, et al. (1998). "Conversion of neuronal growth cone responses from repulsion to attraction by cyclic nucleotides." Science **281**(5382): 1515-1518.
- Stambolic, V. and J. R. Woodgett (1994). "Mitogen inactivation of glycogen synthase kinase-3 beta in intact cells via serine 9 phosphorylation." Biochem J **303 ( Pt 3)**: 701-704.
- Stroissnigg, H., A. Trancikova, et al. (2007). "S-nitrosylation of microtubule-associated protein 1B mediates nitric-oxide-induced axon retraction." Nat Cell Biol **9**(9): 1035-1045.
- Stroissnigg, H., A. Trančíková, et al. (2007). "S-nitrosylation of microtubule-associated protein 1B mediates nitric oxide induced axon retraction." Nat Cell Biol **9**(9): 1035-1045.
- Sunico, C. R., D. Gonzalez-Forero, et al. (2010). "Nitric oxide induces pathological synapse loss by a protein kinase G-, Rho kinase-dependent mechanism preceded by myosin light chain phosphorylation." Journal of Neuroscience **30**(3): 973-984.

- Swiercz, J. M., R. Kuner, et al. (2002). "Plexin-B1 directly interacts with PDZ-RhoGEF/LARG to regulate RhoA and growth cone morphology." Neuron **35**(1): 51-63.
- Takei, Y., S. Kondo, et al. (1997). "Delayed development of nervous system in mice homozygous for disrupted microtubule-associated protein 1B (MAP1B) gene." J Cell Biol **137**(7): 1615-1626.
- Takei, Y., S. Kondo, et al. (1997). "Delayed development of nervous system in mice homozygous for disrupted microtubule-associated protein 1B (MAP1B) gene." jcb **137**: 1615-1626.
- Tedeschi, A., T. Nguyen, et al. (2009). "The tumor suppressor p53 transcriptionally regulates cGKI expression during neuronal maturation and is required for cGMP-dependent growth cone collapse." Journal of Neuroscience **29**(48): 15155-15160.
- Tessier-Lavigne, M. and C. S. Goodman (1996). "The molecular biology of axon guidance." Science **274**(5290): 1123-1133.
- Togel, M., G. Wiche, et al. (1998). "Novel features of the light chain of microtubule-associated protein MAP1B: microtubule stabilization, self interaction, actin filament binding, and regulation by the heavy chain." J Cell Biol **143**(3): 695-707.
- Tojima, T., R. Itofusa, et al. (2009). "The nitric oxide-cGMP pathway controls the directional polarity of growth cone guidance via modulating cytosolic Ca<sup>2+</sup> signals." J Neurosci **29**(24): 7886-7897.
- Torres, J. and R. Pulido (2001). "The tumor suppressor PTEN is phosphorylated by the protein kinase CK2 at its C terminus. Implications for PTEN stability to proteasome-mediated degradation." J Biol Chem **276**(2): 993-998.

- Trivedi, N., P. Marsh, et al. (2005). "Glycogen synthase kinase-3beta phosphorylation of MAP1B at Ser1260 and Thr1265 is spatially restricted to growing axons." J Cell Sci **118**(Pt 5): 993-1005.
- Tymanskyj, S. R., S. Lin, et al. (2010). "Evolution of the spatial distribution of MAP1B phosphorylation sites in vertebrate neurons." J Anat **216**(6): 692-704.
- Uchida, Y., T. Ohshima, et al. (2005). "Semaphorin3A signalling is mediated via sequential Cdk5 and GSK3beta phosphorylation of CRMP2: implication of common phosphorylating mechanism underlying axon guidance and Alzheimer's disease." Genes Cells **10**(2): 165-179.
- Vanhaesebroeck, B. and D. R. Alessi (2000). "The PI3K-PDK1 connection: more than just a road to PKB." Biochem J **346 Pt 3**: 561-576.
- Vanhaesebroeck, B., S. J. Leever, et al. (2001). "Synthesis and function of 3-phosphorylated inositol lipids." Annu Rev Biochem **70**: 535-602.
- Villarroel-Campos, D. and C. Gonzalez-Billault (2014). "The MAP1B case: An old MAP that is new again." Dev Neurobiol.
- Vivanco, I. and C. L. Sawyers (2002). "The phosphatidylinositol 3-Kinase AKT pathway in human cancer." Nat Rev Cancer **2**(7): 489-501.
- von Philipsborn, A. and M. Bastmeyer (2007). "Mechanisms of gradient detection: a comparison of axon pathfinding with eukaryotic cell migration." Int Rev Cytol **263**: 1-62.
- Wadsworth, W. G. (2002). "Moving around in a worm: netrin UNC-6 and circumferential axon guidance in *C. elegans*." Trends Neurosci **25**(8): 423-429.
- Waite, K. and B. J. Eickholt (2010). "The neurodevelopmental implications of PI3K signaling." Curr Top Microbiol Immunol **346**: 245-265.

- Waltzer, L. and M. Bienz (1999). "The control of beta-catenin and TCF during embryonic development and cancer." Cancer Metastasis Rev **18**(2): 231-246.
- Westermann, S. and K. Weber (2003). "Post-translational modifications regulate microtubule function." Nat Rev Mol Cell Biol **4**(12): 938-947.
- Woodgett, J. R. (1990). "Molecular cloning and expression of glycogen synthase kinase-3/factor A." EMBO J **9**(8): 2431-2438.
- Wu, H. H., C. V. Williams, et al. (1994). "Involvement of nitric oxide in the elimination of a transient retinotectal projection in development." Science **265**(5178): 1593-1596.
- Wymann, M. P., K. Bjorklof, et al. (2003). "Phosphoinositide 3-kinase gamma: a key modulator in inflammation and allergy." Biochem Soc Trans **31**(Pt 1): 275-280.
- Yazdani, U. and J. R. Terman (2006). "The semaphorins." Genome Biol **7**(3): 211.
- Yoneda, A., H. A. Multhaupt, et al. (2005). "The Rho kinases I and II regulate different aspects of myosin II activity." J Cell Biol **170**(3): 443-453.
- Yoshimura, T., Y. Kawano, et al. (2005). "GSK-3beta regulates phosphorylation of CRMP-2 and neuronal polarity." Cell **120**(1): 137-149.
- Zhang, X. F., A. W. Schaefer, et al. (2003). "Rho-dependent contractile responses in the neuronal growth cone are independent of classical peripheral retrograde actin flow." Neuron **40**(5): 931-944.
- Zhou, F. Q., J. Zhou, et al. (2004). "NGF-induced axon growth is mediated by localized inactivation of GSK-3beta and functions of the microtubule plus end binding protein APC." Neuron **42**(6): 897-912.

---

# Curriculum vitae



# Rajeshwari Meli

[rajeshwari.meli@univie.ac.at](mailto:rajeshwari.meli@univie.ac.at)



---

## PERSONAL DETAILS:

Sex	Female.
Date of Birth	11-Nov-1981.
Place of Birth	Haveri, Karnataka, India.
Family status	Married.
Nationality	India.

## EDUCATION

2009-present	<b>PhD</b> , Neuroscience, Max F. Perutz Laboratories, University of Vienna, Department of Biochemistry and Cell Biology, Vienna, Austria. Thesis: <i>Mechanism of draxin signaling in axonal guidance</i> . Supervisor: Prof. Friedrich Propst
2003-2006	<b>Master of Science</b> , Applied Genetics, Karnatak University, Dharwad, India. <b>1<sup>st</sup> class with distinction, 1<sup>nd</sup> Rank</b> . Thesis: <i>Cloning and Purification of Rab 5 protein from Leishmania donovani</i> . Supervisor: Dr. Amitabh Mukhopadhyay
2001-2004	<b>Bachelor of Science</b> , Chemistry, Genetic and Botany. Karnatak University, Dharwad, India. <b>1<sup>st</sup> class with distinction</b> .

## HONOURS

2009	<b>Vienna Biocenter Doctoral Fellowship</b> , Max F. Perutz laboratories, University of Vienna, Austrian Science Fund (FWF), Vienna, Austria.
2009	<b>Junior Research Fellowship</b> , National Center for Biological Sciences, Bangaluru, Karnataka, India.
2007	<b>Research assistantship</b> : Institute of Genomics and Integrative Biology, New Delhi, India.

## RESEARCH EXPERIENCE

2009 (Jan–Jun)

**Junior Research Fellow,**

National Centre for Biological Sciences, Bangaluru, Karnataka, India.

Projects: Genetic and Behavioral analysis of olfaction and olfactory conditioning in *Drosophila*.

Supervisors: Prof. Obaid Siddiqi.

2007-2008

**Research Assistant,**

Institute of Genomics and Integrative Biology, Delhi, India

Projects: FishMap: A Community Resource for Zebrafish Genomics.

The Zebrafish GenomeWiki.

Molecular characterization of a novel gene involved in Zebrafish development.

Supervisors: Dr. Shridhar Sivasubbu and Dr. Vinod Scaria.

2006 (Jan-Jul)

**Summer Internship,**

National Institute of Immunology, Delhi, India.

Projects: Cloning and purification of Rab 5 protein from *Leishmania donovani*.

Supervisors: Prof. Amitabha Mukhopadhyay.

## SKILLS & ACTIVITIES

**SKILLS** Neuronal Cell Cultures (Cerebral cortex, Hippocampus, Dorsal root ganglion), Explant cultures, Cell Biology, Confocal and Spinning disc Microscopy, Biochemical assays. PCR and Cloning, whole mount *in situ* hybridization (in zebrafish) and micro injection (zebrafish embryos).

**Behavioural Science:** Conditioning flies with odors and testing the olfactory memory using trap assays and tracking the adult and larval paths using tools and software's.

**Other experience:** Mouse, Zebrafish and *Drosophila* handling.

**LANGUAGES** English (fluent), Hindi, Kannada (Native)

**SCIENTIFIC MEMBERSHIPS** Society of Neuroscience.

**ORGANIZATIONAL ACTIVITIES** Member of organizing committee Cells don't play Dice, Student symposium, Vienna, Austria.

## PUBLICATIONS

### Publication:

1. **Meli R**, Weisova P and Propst F. Repulsive axon guidance by draxin is mediated by GSK-3 $\beta$  and Microtubule-associated protein MAP1B. (In communication JBC).
2. Krupa E, **Meli R**, Völk T, Nothias F and Propst F. Nitric oxide-induced axon retraction involves simultaneous changes in microtubule and actin networks. (In communication).
3. Singh M, Bhartiya D, Maini J, Sharma M, Singh AR, Kadarkaraisamy S, Rana R, Sabharwal A, Nanda S, Ramachandran A, Mittal A, Kapoor S, Sehgal P, Asad Z, Kaushik K, Vellarikkal SK, Jagga D, Muthuswami M, Chauhan RK, Leonard E, Priyadarshini R, Halimani M, Malhotra S, Patowary A, Vishwakarma H, Joshi P, Bhardwaj V, Bhaumik A, Bhatt B, Jha A, Kumar A, Budakoti P, Lalwani MK, **Meli R**, Jalali S, Joshi K, Pal K, Dhiman H, Laddha SV, Jadhav V, Singh N, Pandey V, Sachidanandan C, Ekker SC, Klee EW, Scaria V, Sivasubbu S The Zebrafish GenomeWiki: a crowdsourcing approach to connect the long tail for zebrafish gene annotation. The Zebrafish GenomeWiki: a crowdsourcing approach to connect the long tail for zebrafish gene annotation. Database (Oxford). 2014 Feb 26; 2014 PMID: 24578356.
4. **Meli R**, Prasad A, Patowary A, Lalwani MK, Maini J, Sharma M, Singh AR, Kumar G, Jadhav V, Scaria V, Sivasubbu S. FishMap: a community resource for zebrafish genomics. *Zebrafish*. 2008 (2):125-30.PMID: 18554176.

## PRESENTATION

- 2013 Society of Neuroscience conference. San Diego, USA. Nov 9-13, 2013.  
**Poster:** Mechanism of draxin signaling in axonal guidance.
- 2011 Society of Neuroscience conference. Washington, USA. Nov. 12-16, 2011  
**Poster:** Mechanism of draxin signaling in axonal guidance.
- 2011 EMBO Workshop. Cell Biology of the Neuron polarity, Plasticity and Regeneration. Heraklion, Greece. May 7-10, 2011.  
**Poster:** Mechanism of draxin signaling in axonal guidance.
- 2008 HUGO's 13th Human Genome Meeting, Sep 27-30, in Hyderabad, INDIA.  
**Poster:** *Community Annotation of the zebrafish genome: A wiki solution.*

July-2014. Wien.